12-2015

# PREVENTING THYMUS INVOLUTION IN K5.CYCLIN D1 TRANSGENIC MICE SUSTAINS THE NAÏVE T CELL COMPARTMENT WITH AGE

Michelle L. Bolner

**PREVENTING THYMUS INVOLUTION IN K5.CYCLIN D1 TRANSGENIC MICE SUSTAINS THE NAÏVE T CELL COMPARTMENT WITH AGE**

**BY**

**Michelle Lynn Bolner, Ph.D. Candidate**

**APPROVED:**

_____

Ellen R. Richie, Ph.D., Supervisory Professor

_____

Shawn B. Bratton, Ph.D.

_____

David G. Johnson, Ph.D.

_____

Kevin M. McBride, Ph.D.

_____

Jagan K. Sastry, Ph.D.

APPROVED:

_____

Dean, The University of Texas
Graduate School of Biomedical Sciences at Houston

# PREVENTING THYMUS INVOLUTION IN K5.CYCLIN D1 TRANSGENIC MICE SUSTAINS THE NAÏVE T CELL COMPARTMENT WITH AGE

A

Dissertation

Presented to the Faculty of

The University of Texas Health Science Center at Houston

And

The University of Texas M.D. Anderson Cancer Center

Graduate School of Biomedical Sciences

in Partial Fulfillment

of the Requirements

for the degree of

DOCTOR OF PHILOSOPHY

By

Michelle Lynn Bolner, Ph.D. Candidate

Houston, Texas

May 2016

**DEDICATION**

**This dissertation is dedicated to my Grammy, who taught me that anything worth wanting is worth working for.**

**ACKNOWLEDGEMENTS**

I am eternally grateful for the love and support of the people who have brought me to this crossroad. My parents have been the bedrock upon which I built my foundation. I thank my father for showing me what hard work is, and how to always keep an eye on the prize (*Git 'Er Done!*). I thank my mother for the years (and years) of love, emotional counseling and encouragement that I would surely be in debt from if I had instead visited a licensed psychologist. I thank my much better half for standing here beside me while I swore to him I could bust a hole through the wall we all call graduate school with only my head and a few pipettes (*Look Fred, I finally did it!*). I am grateful for the love of my best friend Sam, who always says 'Weeeell Chelle, you did this to yourself, buddy..." and then reminds me how far I've come from the schoolgirl he knew. Without the love and ceaseless support of these people, I would not have arrived at Science Park seven years ago.

I am indebted to my mentor, Ellen Richie, for the patience, support, and occasional straightening-outs I've needed over the years, and for providing the space and timeframe for my scientific development. I also thank my committee members, past and present, for their patience and suggestions as I've learned to present my ideas and myself, and found my voice. I would not have survived a day of graduate school without the tireless support and friendship of Becky Brooks, Carla Carter, or Pam Whitney. I am also grateful for the daily conversations with the Richie lab group, including Nandini Singarapu, Ginny Bain, Jia Li, and Kim Cardenas. I would be completely remiss if I didn't point out the other two of the *Three Amigos* Katie Reeh and Matt Yousefzadeh, without whom I would have walked away from this process a long time ago. I do love them more than they know, even if Matt didn't send me the personalized thank you card he promised in lieu of acknowledgement during his dissertation defense. I am so thankful for the support of the entire Mouse House staff over the years, including Meredith Spice and Pam Huskey – they are the unsung heroes of rodent research.

Finally, because it wouldn't be right not to, I thank my favorite guy in the whole wide world, Lucky, who's still here, every step of the way.

I am one unbelievably blessed person, and can never repay the kindness that has been shown to me during my time at Science Park, both on and beyond its campus. But I will always share my Goldfish crackers with the people here.

**PREVENTING THYMUS INVOLUTION IN K5.Cyclin D1 TRANSGENIC MICE SUSTAINS THE NAÏVE T CELL COMPARTMENT WITH AGE**

Michelle Lynn Bolner, Ph.D. Candidate

Supervisory Professor: Ellen R. Richie, Ph.D.

The thymus maintains T cell receptor (TCR) repertoire diversity through perpetual release of self-MHC restricted naive T cells. However, thymus involution during the aging process reduces naïve T cell output, leading to defective immune responsiveness to newly encountered antigens. We have found that early thymus involution precipitates the age-associated shift favoring memory T cell dominancy in young control mice. Furthermore, we have shown that age-related thymus involution is prevented in mice expressing a keratin 5 promoter-driven Cyclin D1 (K5.D1) transgene in thymic epithelial cells (TECs). Thymopoiesis occurs normally in K5.D1 transgenic thymi and sustains T cell output to prevent the age-associated decline of naïve T cells in the periphery. We find that K5.D1 recent thymic emigrants (RTEs) undergo typical phenotypic maturation. In addition, functional studies show that K5.D1 peripheral T cells are responsive to anti-CD3 and anti-CD28 stimulation *in vitro*. Competitive adoptive transfer studies with K5.D1 and nontransgenic RTEs indicate that K5.D1 RTEs are incorporated into the peripheral T cell pool comparably to nontransgenic controls. However, K5.D1 mature naïve (MN) T cells out-persist control counterparts, which likely occurs, in part, to increased expression of the cytokine receptor IL-7Rα. Collectively, these data show that preventing thymus

involution not only sustains T cell output to maintain naïve T cell numbers, but also provides functionally competent MN T cells during aging.

## TABLE OF CONTENTS

## LIST OF FIGURES

## LIST OF ABBREVIATIONS

Aire – autoimmune regulator

APC – antigen presenting cell

BrdU - bromodeoxyuridine

CCR – chemokine receptor

CFSE – Carboxyfluorescein succinimidyl ester

CM – central memory

CMJ – corticomedullary junction

cTEC – cortical TECs

DCs – dendritic cells

DLL4 – delta-like 4

DN – double negative subset

DP – double positive subset

EDTA - Ethylenediaminetetraacetic acid

EM – effector memory

EMT – epithelial to mesenchymal transition

ETP – early thymocyte progenitor

FACS – fluorescence activated cell sorting

FCS – fetal calf serum

FITC – fluorescein isothiocyanate

Foxn1 – forkhead box 1

GALT – gut-associated lymphoid tissues

H&E – hematoxylin and eosin

IFNγ – interferon gamma

IHC - immunohistochemistry

IL - interleukin

KGF – keratinocyte growth factor

KLF2 – kruppel like factor 2

MFI – mean fluorescent intensity

MHCII – major histocompatibility complex II

MN – mature naïve T cell

mTEC – medullary TECs

PBS – phosphate buffered saline

pTα – pre-TCR alpha

qRT-PCR – quantitative real time polymerase chain reaction

RAG – recombinase activating gene

RANK - Receptor activator of nuclear factor kappa-B ligand

Rb - retinoblastoma

RTE – recent thymic emigrant

S1P – sphingosine 1 phosphate

S1P1R – sphingosine 1 phosphate 1 receptor

SLO – secondary lymphoid organ

SP – single positive subset

SSA – sex steroid ablation

TCR – T cell receptor

TCRα – T cell receptor alpha chain

TCRβ – T cell receptor beta chain

TECs – thymic epithelial cells

TEPC – thymic epithelial progenitor cell

TNFα – tumor necrosis factor alpha

TRA – tissue restricted antigens

TREC – TCR excision circle

Treg – regulatory T cell

UEA1- ulex europaeus agglutinin

VM – virtual memory

# CHAPTER ONE

## INTRODUCTION & BACKGROUND

T cells mediate protective immune responses against infectious diseases and cancer. T cells develop in the unique microenvironment of the thymus, where thymic epithelial cells (TECs) provide essential cues for thymocyte differentiation and selection to generate naïve T cells that are both self-MHC restricted and self-tolerant. A highly diverse T cell receptor (TCR) repertoire in the peripheral T cell pool is essential to generate immune responses against a vast array of antigens. To maintain TCR diversity, the thymus continually produces and exports naive T cells to the T cell pool. However, the thymus undergoes involution naturally with age and during severe stress. This process is primarily due to degeneration of the TEC compartment. Reduced thymopoiesis in the involuted thymus decreases the number of recent thymic emigrants (RTEs) released to the peripheral T cell pool, which in turn restricts TCR diversity. Contraction of the TCR repertoire increases susceptibility to infectious disease and cancer (1). Furthermore, increased autoimmunity incidences during aging have been linked to thymus involution, as degradation of the TEC compartment may allow self-reactive T cells to escape negative selection and compromise central tolerance (2).

While many groups have demonstrated that the extreme involution of the aged thymus has severe consequences on thymocyte and peripheral T cell cellularity and function, the potential consequences of early thymus involution have a been mostly overlooked. Thymus cellularity in mice declines as early as 7 weeks of age. Previous studies comparing thymocyte and peripheral T cells from young and old mice considered mice young even if they were 3 or more months of age and therefore had already undergone significant decline in thymus size (3-5). Hence, there is a gap in

knowledge regarding whether early thymus involution impacts the cellular composition of the peripheral T cell pool in young adult mice. Therefore, the focus of this thesis is to identify how early thymus involution influences the dynamics of peripheral T cell pool subsets, and to determine whether preventing thymus involution may alter the presence of these T cell populations.

## 1.1 The Thymus

The thymus is structurally complex. Anatomically, the thymus is composed of two separate lobes that lie on either side of the body midline above the heart. Each lobe contains functionally distinct outer cortex and inner medullary zones. Hematoxylin and eosin (H&E) stained thymus sections show that the thymus is organized into outer cortical and inner medullary regions (Figure 1A). The cortex, which is densely packed with immature thymocytes, is stained dark blue by DNA-binding hematoxylin. The medulla, however, contains fewer cells that take up less hematoxylin stain, allowing the pink cytoplasmic eosin stain to be visible. Though the thymus is highly vascularized, large vessels are present at the corticomedullary junction (CMJ) and serve as the site of hematopoietic progenitor entry and emigration of mature T cells (6). The thymus also contains a complex stromal microenvironment not visible by H&E stain consisting of fibroblasts, endothelial cells, dendritic cells, macrophages and TECs. Stroma present throughout the thymus provide essential instruction for developing thymocytes (Reviewed in (7)).

### *1.1.1 Thymopoiesis*

The production of T cells via thymopoiesis is a stringent process that is essential for the maintenance of a broad TCR repertoire (For a schematic overview of

**A.**

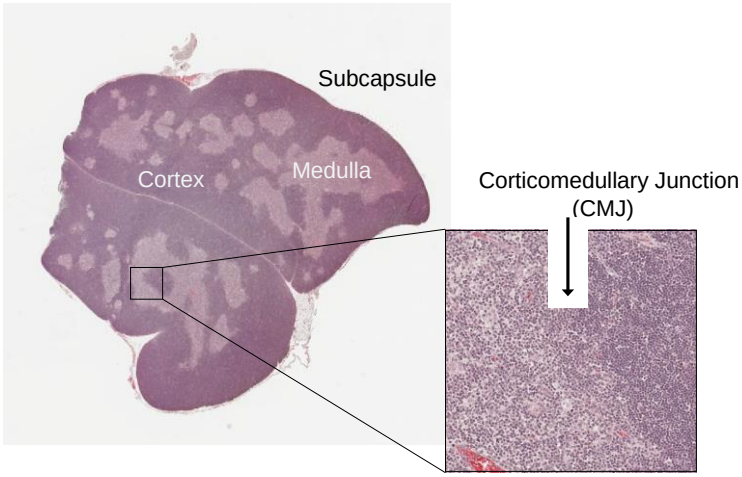


**B.**

Critical Checkpoints: β-Selection; Positive Selection; Negative Selection

Thymopoiesis and Migration:

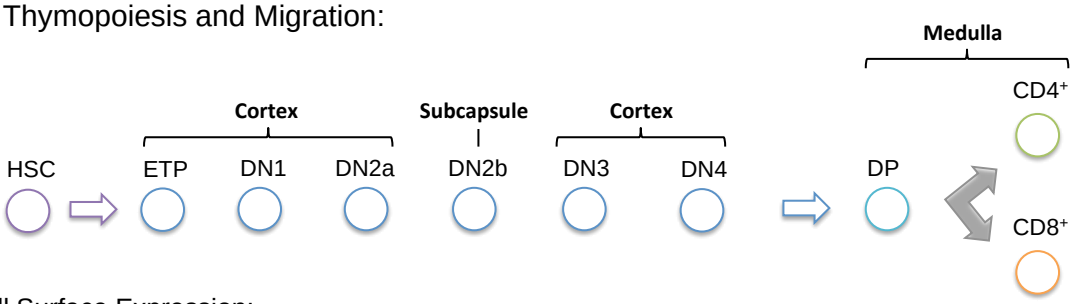


Cell Surface Expression:

| | ETP | DN1 | DN2a | DN2b | DN3 | DN4 | DP | CD4 or CD8 SP only |
|---|---|---|---|---|---|---|---|---|
| CD25 | | | | | | | | |
| CD44 | | | | | | | | |
| CD117 | | | | | | | | |
| TCRβ | | | | | | | | |
| TCRα | | | | | | | | |
| CD4 | | | | | | | | |
| CD8 | | | | | | | | |

**Figure 1. Overview of thymus architecture and thymopoiesis.**

(**A**) Overview of thymus organization, including cortex (dark stain), medulla (light stain), subcapsule and corticomedullary junction (CMJ, magnification). (**B**) Schematic representation of the stage of thymocyte development.

thymopoiesis – see Figure 1B). Hematopoietic progenitors in adult bone marrow are attracted to the thymus by chemokine gradients including CCL19, CCL21 and CCL25 expressed by TECs (8-10). Thymus-seeding progenitors continually migrate into the thymic microenvironment and are thought to fill any available intrathymic niches to sustain thymopoiesis (11). The most immature thymocytes lack the expression of CD4 and CD8 cell surface molecules and thus are referred to as double negative (DN) thymocytes. DN thymocytes are further subdivided by the expression of the CD117, CD44 and CD25 molecules to distinguish the first stages of T cell development (12).

The earliest DN thymocytes are not yet committed to the T cell lineage. In fact, the primitive $CD117^{+}CD44^{+}CD25^{-}$ DN1 thymocytes retain the potential to differentiate into multiple cell types, including the myeloid, NK and DC lineages (13). Therefore, very specific signaling must occur in the cortex to support commitment to the T cell lineage (14). To this end, deep cortical TECs express the Notch ligand Delta-like 4 (DLL4) that promotes T lineage commitment (15, 16). The Dll4/Notch signaling pathway is crucial to drive early thymocyte differentiation, and is thought to induce the maturation program by gradually persuading T cell fate decisions through the activation of multiple transcription factors (10, 17). In this way, *Notch* inhibits other cell fate potentials including B cell, DC, lymphoid and myeloid lineages (18, 19). Disruption of Dll4/Notch signaling during the ETP/DN1 stages drives cells instead toward a B cell lineage (20). Thus the Notch signaling pathway, mediated by cTECs, critically influences cells towards early T cell lineage commitment.

Thymocytes commit to the T cell lineage and initiate TCRβ gene rearrangement during the DN2 ($CD117^{+}CD44^{+}CD25^{+}$) developmental stage. While early DN2 cells that express high levels of CD117 can be still diverted to the DC and NK lineages, this cell fate potential narrows dramatically as cells initiate gene rearrangement of the β, γ and

δ chains of the TCR. Rearrangement of germ line DNA encoding each chain is driven by the recombinase-activating (RAG) genes, and produces unique receptor sequences to promote TCR diversity in thymocyte pool (RAG-mediated gene recombination is outlined in (21)). Furthermore, the development of conventional αβ and rare γδ T cell lineages bifurcate the DN2 stage ((22), reviewed in reference (23)), but for the purposes of this thesis, we will focus on αβ T cell development. Upon completing the DN2 stage by initiating β chain rearrangement, αβ thymocytes are subjected to multiple stringent tests to become peripheral αβ T cells.

Successful rearrangement of the TCRβ chain is assessed during the DN3 ($CD117^{-}CD44^{-}CD25^{+}$) developmental stage. TCRβ polypeptides are paired with the invariant pre-TCRα (pTα) chain to form a pre-TCR. Successful extracellular expression of this complex rescues thymocytes from programmed cell death via Lck/Fyn mediated signaling (24, 25). Additionally, intracellular pre-TCR signaling permits continued maturation to the short-lived DN4 ($CD117^{-}CD44^{-}CD25^{-}$) stage, during which cells undergo 8-9 rounds of proliferation, and initiate CD4 and CD8 expression to become $CD4^{+}CD8^{+}$ double positive (DP) thymocytes (26).

Thymocytes that mature to the DP stage initiate TCRα gene rearrangement to produce a functional TCR and receive positive selection signaling. In order for this to occur, a second wave of RAG expression is initiated to drive TCRα gene rearrangement, which continues until either positive selection signals extinguish recombination or α chain rearrangement is exhausted. Polypeptide chains produced from TCRα gene rearrangement displace the preTα chain to form αβTCRs. DP thymocytes that do not generate functional TCRα gene rearrangements fail to express αβTCRs and undergo apoptosis (death by neglect). However, those DP thymocytes that do express αβTCRs are subject to positive selection, a process by which

thymocytes are tested for recognition of self-peptide in the context of MHC molecules. Interactions between self-peptide MHC and TCRs on thymocytes provoke a goldilocks-like scenario, such that thymocytes that react too strongly to self-peptide receive TCR-mediated apoptosis signaling, while cells bearing nonresponsive TCRs undergo programmed cell death (27). Only thymocytes with low to moderate binding affinity to self-peptide in the context of MHC receive low, sustained TCR engagement that drives RAS signaling to promote survival (Reviewed in (28)). Therefore, positive selection ensures that thymocytes bear TCRs that are self-restricted. Because most DP thymocytes express useless TCRs, only a small fraction (~10%) are positively selected to upregulate the chemokine CCR7 to migrate into the medulla to become $CD4^+$ or $CD8^+$ single positive (SP) thymocytes (29, 30).

Many different genes influence the SP thymocyte identity decision. For example, the presence of ThPOK in the developing thymocytes helps direct T cell fate toward the $CD4^+$ lineage, whereas the absence of ThPOK redirects T cells to the CD8 lineage (31). Recently, IL-7 and IL-15 signaling have also been implicated in specifying CD8 T cell fate, as loss of these or the common cytokine receptor chain γ results in the absence of SP $CD8^+$ SP thymocytes *in vivo* (32). These results are consistent with the kinetic signaling model proposed by the Singer group, in which the $\gamma_c$ cytokines detect the duration of TCR signaling that directs cell fate (33, 34). While there are still many aspects of the cell fate choice to become CD4 or CD8 that remain unclear, positively selected thymocytes do transition to the SP stage after down regulation of either CD4 or CD8 (34).

The last major hurdle of thymocyte development is necessary to impose central tolerance by deleting auto-reactive cells from the repertoire that may promote autoimmunity. Negative selection occurs primarily in the medulla and serves to delete

thymocytes bearing TCRs that strongly bind to self-antigen. Medullary thymic epithelial cells (mTECs) promiscuously express tissue-restricted antigens (TRAs) that are otherwise expressed elsewhere throughout the body, and both mTECs and DCs present these self-antigens to SP thymocytes for sampling (35, 36). Thymocytes that strongly recognize self-peptide are signaled through the TCR to undergo apoptosis, thereby culling the population of potentially autoreactive clones (27). This negative selection process is essential for establishing central tolerance, as systemic autoimmunity occurs in mouse models where negative selection is averted (37, 38). Importantly, CD4 thymocytes that have strong affinity for self-ligand can be diverted to the regulatory T cell (Treg) lineage during negative selection, and serve to dampen the peripheral immune response in particular contexts (39). Cells that survive β, positive and negative selection may prepare for T cell exit from the thymus. However, these essential checkpoints delete nearly 95% of cells before thymocyte development is complete in order to ensure the production of only self-tolerant, self-restricted T cells.

The process of thymocyte selection and preparation for thymus exit can be defined as multiple stages in CD4 SP thymocytes. Four subsets (SP1-4) identify the transition from early stage TCR-auditioning thymocyte to the mature T cell poised for thymic emigration. Early SP1 CD4 thymocytes mature from the DP subset and express high levels of heat stable antigen (CD24) and C-type lectin CD69, indicative of TCR engagement during positive selection (40). Positively selected cells then express the CCR7 to migrate into the medulla to become SP2 CD4 thymocytes. During medullary residency, thymocytes lose CD69 expression after completing negative selection, identifying transition to the SP3 subset. Once CD69 expression is lost, transcription of the sphingosine 1 phosphate receptor 1 (S1P1R) is initiated. This, along with Qa-2 and

the re-expression of CCR7, identifies the late stage CD4 SP4 thymocytes prepared for thymus emigration.

Exit from the thymus is the final step necessary to become a peripheral naïve T cell. For the $CD4^+$ and $CD8^+$ SP cells that survive development, emigration is initiated by the expression of genes under control of the transcription factor Kruppel-like factor 2 (KLF2) (41). KLF2 binds directly to the promoter of the G protein-coupled sphingosine 1 phosphate (S1P) receptor 1 (*S1p1r*) to drive expression. While all cells are believed to produce S1P, pericytes lining the thymic vasculature create a S1P chemotactic gradient that is strongest at the vasculature (42). Thymocytes bearing S1P1R follow this increasing S1P gradient to the vessels to emigrate from the thymus (43, 44). Interestingly, TCR engagement may act as a braking mechanism on thymus emigration. Using a transgenic mouse model to drive expression of the C-type lectin CD69, which is upregulated upon TCR signaling and binds to and induces S1P1R internalization and retention of SP thymocytes in the thymus (45). Other studies have shown that PI3K signaling exerts some control on thymus emigration, since SP thymocytes are retained in the thymus during constitutive PI3K signaling (46). Therefore, even the process of thymus emigration is regulated to ensure that thymocytes undergo final maturation before being released to the periphery. Upon successful exit through the perivascular spaces, emigrants escape the thymus through the circulatory system and enter the peripheral T cell pool.

### *1.1.2 Thymus Stroma Overview*

Though thymocytes constitute the major cell population within the thymus, thymopoiesis relies upon interactions between thymocytes and the resident stroma to produce functional, self-tolerant T cells. The thymic stromal cell compartment

encompasses a variety of cell types, including mesenchymal fibroblasts, endothelial cells, TECs and hematopoietic-derived professional antigen presenting cells (APCs) such as dendritic cells (DCs), macrophages and B cells (6). Each of these stromal cell types provides an important component of the microenvironment. Thymic fibroblasts, for example, create scaffolding for the organ by producing extracellular matrix (47). Endothelial cells line the vasculature penetrating the lobes to regulate HSC entry and naïve T cell emigration. DCs and TECs are indispensible for thymocyte development, by providing thymocytes with essential microenvironmental niches that support survival and T-lineage commitment as well as by presenting peptide/MHC complexes that impose stringent TCR testing during positive and negative selection.

### *1.1.3 Thymic Epithelial Cells*

Thymopoiesis depends on indispensable signals from the TEC-derived microenvironment located throughout the thymus. TECs are present in a three-dimensional network that is atypical compared to the stratified epithelium lining the lumen of most organs. This unique epithelial orientation maximizes interactions between thymocytes and TECs to promote cellular ‘crosstalk’ that sustains survival and differentiation of both cell types. Additionally, the number and fitness of TECs directly influences thymus size and the capacity for thymopoiesis through the availability of niches promoting fate specification and survival signaling for developing thymocytes. Thus, the capacity for thymopoiesis is unarguably linked to the condition of TECs present in the thymus.

Distinct TEC subsets throughout the thymus promote specific stages of thymocyte development. The cTEC subset, for instance, recruits bone marrow-derived progenitors to seed the thymus by concerted expression of CCL19, CCL21 and CCL25,

and promotes early thymopoiesis by expressing IL-7 and Dll4 ligands for thymocyte survival and T cell lineage commitment (15, 48, 49). Additionally, cTECs express the unique proteosomal subunit β5t that permits self-antigen processing for positive selection (50). Deletion of β5t results in the loss of CD8 SP thymocytes and reflects the importance of this subunit for self-peptide processing for MHC class I loading during positive selection (51). The mTEC subset, on the other hand, plays a central role in negative selection of developing thymocytes. Mature mTECs express the transcription factor *Aire* (Autoimmune regulator), which drives promiscuous expression of TRAs normally found throughout the body. TRAs then are loaded onto MHC molecules and presented on the cell surface for thymocyte sampling. Thymocytes that recognize TRAs are either deleted from the thymocyte population or redirected towards the Treg lineage. Without Aire expression, autoreactive thymocytes avoid cell death and promote multiorgan autoimmunity (52). It is therefore imperative to maintain diverse cortical and medullary TEC subsets for self-tolerant and self-restricted T cell generation.

The TEC compartment originates from the endoderm of the 3$^{rd}$ pharyngeal pouch during embryogenesis. The expression of transcription factor *Foxn1* identifies cells fated to become TECs in the pouch by mouse embryonic day 11.5 (6). Though *Foxn1* does not determine cell fate, expression is essential for differentiation and maintenance of both embryonic and adult TECs, as evidenced by the arrest of TEC development at the MTS24$^{+}$ progenitor stage in *Foxn1*$^{nu/nu}$ mice (6, 53, 54). Furthermore, embryonic TECs are the bipotent progenitors of both mTEC and cTEC lineages during development (55, 56). Through complex interactions with the surrounding mesenchyme and incoming lymphoid progenitors, the thymic anlage develops cortical and medullary regions by late gestation that loosely resemble the

postnatal thymus. Many speculate that some TEC progenitor cells (TEPCs) may persist past embryogenesis to maintain the postnatal TEC population.

In the adult thymus, the TEC population is far from quiescent. In fact, the half-life of post-natal TECs is approximately 10-14 days, even in the involuting thymus (57). There has long been speculation that a bipotent TEC progenitor cell (TEPC) must exist to support such rapid cell replacement, and may reside at the corticomedullary junction (58). Recently, two groups have independently identified progenitors in the thymus that give rise to both cTECs and mTECs. The Chidgey group identified a Foxn1$^{+}$ cTEC subset that was capable of producing differentiated mTECs and cTECs *in vivo* (59). The Kyewski group also identified a self-renewing, bipotent TEC progenitor (60). These reports strongly suggest the existence of an adult thymic TEPC capable of producing differentiated TECs. Furthermore, these studies suggest that sustaining functional TEPCs may maintain the differentiated TEC environment to support continued thymopoiesis beyond the normal involution timeframe.

TECs mature into multiple subsets that provide indispensible interactions with developing thymocytes. Cortical and medullary TEC maturation stages may be identified by the expression of multiple cell surface molecules (For overview, see Figure 2). Generally, maturation of both cTECs and mTECs is loosely defined by MHCII expression, which increases as TECs mature from undifferentiated precursors to mature, terminally differentiated TECs (61). Maturing cTECs also express the apoptotic recognition receptor CD205 (61) and the glutamyl aminopepsidase marker Ly51. Additionally, cTECs are the only known cell type that expresses thymoproteosomal subunit β5t (51, 62). In mTECs, increased expression of the co-stimulatory molecule CD80 is indicative of maturation (61, 63). Some MHCII$^{hi}$ CD80$^{+}$ mTECs further differentiate to express *AIRE* for negative selection. Additionally, a maturation stage

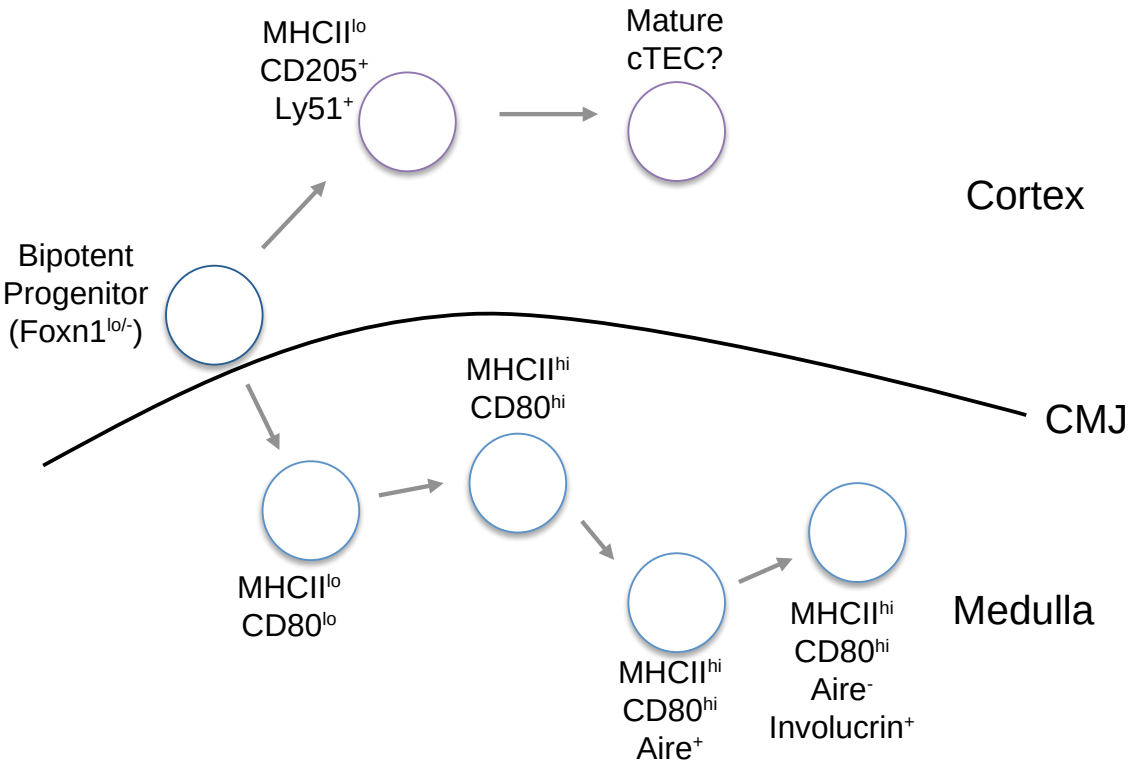
MHCII$^{lo}$
CD205$^{+}$
Ly51$^{+}$
Mature
cTEC?
Cortex
Bipotent
Progenitor
(Foxn1$^{lo/-}$)
CMJ
MHCII$^{hi}$
CD80$^{hi}$
MHCII$^{lo}$
CD80$^{lo}$
MHCII$^{hi}$
CD80$^{hi}$
Aire$^{+}$
MHCII$^{hi}$
CD80$^{hi}$
Aire$^{-}$
Involucrin$^{+}$
Medulla

**Figure 2. TEC Maturation in the post-natal thymus.**

Both TEC lineages develop from a common bipotent progenitor. cTEC maturation is not well defined, but cTECs can be identified by the expression of MHCII, CD205 and Ly51. mTEC maturation progresses through an $MHCII^{lo}CD80^{lo}$ expression stage to an $MHCII^{hi}CD80^{hi}$ expression stage. Some mTECs further mature to the $Aire^{+}$ stage, and finally an $Aire^{-}Involucrin^{+}$ terminally differentiated stage.

past Aire$^{+}$ occurs, in which some TECs express the terminal indicator involucrin that is expressed in mature skin epithelium. Skewing of any stages of TEC maturation significantly impairs the quantity and quality of niches available for T cell development, which reemphasizes the importance of maintaining the diverse TEC microenvironments.

TECs and thymocytes engage in active bidirectional crosstalk that promotes survival of both cell types. While it is understood that TEC subsets must be present for thymocyte development to occur, the presence of thymocytes also promotes TEC survival and differentiation. Perturbations of thymocyte development can critically influence and even prevent the differentiation of TEC subsets. For instance, blocking IL-7 signaling and TCRβ gene rearrangement through the use of RAG2/$\gamma_c$ double deficient mice arrests thymocyte development at or prior to the DN1 stage and results in the blockade of TEC differentiation at a primitive K5$^{+}$K8$^{+}$ precursor stage (64). Furthermore, the presence of DP thymocytes drives a cellular feedback mechanism to regulate the amount of Dll4 expressed by CD40$^{+}$MHCII$^{+}$ cTECs to support ETPs (65). Thymocyte-derived signals also directly influence mTEC differentiation. Arresting thymocyte development at the DN3 stage by knocking out RAG expression impairs mTEC differentiation and expansion (66). Deleting the TCRα locus or the downstream signal transducer Zap-70 blocks thymocyte maturation at the DP thymocyte stage, and the failure to generate SP thymocytes severely reduces mTEC numbers (67, 68). The RANK signaling pathway also plays an important role in TEC proliferation. RANKL is expressed by positively selected thymocytes and the receptor RANK is present on medullary TECs. Mice harboring a mutation in either RANK or RANKL have fewer mTECs and exhibit defective Aire$^{+}$ mTEC development, whereas forced RANKL expression restores the mTEC compartment in *Tcra*$^{-/-}$ mice (69, 70). Therefore,

interactions with SP thymocytes are necessary for shaping the mTEC microenvironment. Together, these studies demonstrate that blocking thymocyte maturation at various stages affects TEC subset differentiation and reaffirms the extent of interdependence between thymocytes and TECs.

## 1.2 Thymus Involution

The thymus is maximal in size and cellularity in young individuals, but undergoes gradual and progressive involution with age. Declining thymus size is evident after just one year of age in humans (71). In mice, reduced thymus cellularity and T cell output occurs by 6-7 weeks of age (6, 72). While the exact driving forces behind thymus involution are still a matter of debate, involution accelerates after puberty and drives disorganization of the thymic architecture (Reviewed in (6, 73)). Severe thymic involution is evident in both aged mice and elderly patients, which significantly restricts thymopoiesis necessary for supporting peripheral naïve TCR diversity (1, 74). Naïve T cell numbers decline and promote the homeostatic proliferation of existing peripheral T cells as a consequence of involution. These peripheral T cell pool dynamics lead to increased susceptibility to disease and poor viral clearance (75). Additionally, poor memory formation occurs after vaccination of aged individuals and stems from diminished naïve TCR repertoire diversity, rendering them vulnerable to preventable infectious diseases (76). Thus, deterioration of the thymic microenvironment spurs immune dysfunction in the peripheral T cell pool.

### *1.2.1 Stromal changes during thymic involution*

Thymus involution profoundly impacts the cortical and medullary microenvironments. Declining cellularity and cortical thinning are initiated during early

involution, whereas disorganization of the thymic architecture and the accumulation of adipocytes in and around the thymus are present in advanced involution (6). Furthermore, the representation of stromal cell subsets is altered as a consequence of involution: TEC numbers from one-year-old mice are half that found in one-month-old mice (57). Additionally, the mTEC:cTEC ratio declines substantially during involution, whereas the frequency of other stromal components including fibroblasts significantly increases from one month to one year of age (57, 77). Thus, involution disrupts the balance of essential infrastructure components in the thymic microenvironment.

Degeneration of the TEC compartment is the major physiological alteration that drives declined size and thymopoiesis in involuting thymi. Transferring ETPs from young mice into aged mice cannot restore thymopoiesis or thymic size (78). However, fetal thymi implanted under the kidney capsule of old recipients are efficiently colonized by aged bone marrow progenitors (79). These reports suggest that the impaired ability of aged thymi to support thymopoiesis stems primarily from stromal defects and not from thymus-seeding progenitors. Furthermore, TEC cellularity in aged (1yr old) mice reflects only a third of the cellularity present in one-month-old mice (57). This cellular loss drastically reduces the quantity of niches available to support thymopoiesis. Moreover, the complexity of the remaining microenvironments are compromised with involution: TECs expressing high levels of MHCII are lost as the organ atrophies and skews the TEC subsets present in aged thymi (57). These results, coupled with athymia of the Foxn1 nude mouse strongly suggest that the impairment of thymopoiesis occurs from degenerating TEC populations.

Maintenance of the TEC compartment is dysregulated during the involution process and is thought to stem from downregulation of *Foxn1* (80, 81). Studies using a hypo-allelic scheme for Foxn1 expression show that it is required for the maintenance

of TEC subsets supporting T cell development (81). To this end, over-expressing Foxn1 does maintain TEC numbers and slows the progression of involution, though it does not cease it completely (82). This suggests other factors must circumvent *Foxn1* to drive thymus involution. However, re-expression of *Foxn1* after thymus involution can promote thymus maintenance and regeneration in a TEC-mediated manner. In fact, studies in which *Foxn1* expression was maintained or re-expressed in severely involuted thymi showed both an increase in proliferation and differentiation of TECs (83, 84). Therefore, the aged TEC population retains some regenerative potential in the involuted thymus, through the expression of Foxn1.

The thymic microenvironment is not only altered by the loss of TECs but also by the presence of adipocytes. While the origin of these cells has not been defined, speculation in the literature suggests that adipocytes may be derived from epithelial-to-mesenchymal transition (EMT) (6, 85). Adipocytes appear and increase with the progression of thymus involution, and may alter the cytokine milieu for thymopoiesis. Many cytokines, including leukemia inhibitory factor, stem cell factor, IL-15 and IL-6, can induce thymic atrophy, and are elevated in naturally involuted thymi (86). Interestingly, adipocytes present in involuted thymi have been shown to express these same cytokines, suggesting that adipocyte presence may influence the cytokine milieu and promote involution (86). Furthermore, reports have correlated obesity and calorie restriction to thymic function, in such a manner that obesity promotes thymus involution, whereas calorie restriction improves T cell output and maintenance of thymic architecture (87, 88). Therefore, alterations in the composition of the microenvironment itself may alter the cytokine profile that impairs thymopoiesis.

### *1.2.2 Thymus regeneration*

It is well understood that thymus size is plastic, even after involution. In fact, as early as the turn of the early 20th century castration in cattle was known to increase thymus size (89). Because severe infection, stress and lymphoablative therapy damage the immune system and cause severe thymus involution, thymus regeneration has been looked to as a potential therapy for rebuilding the T cell pool. Thymus cellularity and T cell output are readily rebounded by treatments such as sex steroid ablation (SSA) and administration of keratinocyte growth factor (KGF), both of which drive TEC proliferation. Additionally, these treatments can increase T cell output in both rodents and humans with severely involuted thymi. SSA has been shown to enhance cytotoxic T lymphocyte-mediated viral clearance by increasing naïve CD8 T cell numbers in the periphery (90). Much like SSA, KGF has also proven to be a reliable tool for thymic rebound and increased T cell production. Administration of KGF in mice leads to increased proliferation and higher total TEC numbers (91, 92). Furthermore, the KGF receptor fibroblast growth factor receptor 2 IIIb (FGFR2IIIb) is expressed on TECs and promotes expansion of the microenvironmental niches that support ETPs and thymocyte development (93). These therapies hold potential for rebuilding the peripheral T cell pool after episodes of severe damage.

While SSA and KGF treatments increase TEC number and improve the volume of T cell production, the effects are temporary and thymus involution will reoccur after withdrawal. Additionally, strategies to rebound thymus size may improve T cell production but do not yield complex thymic microenvironments necessary for appropriate T cell selection. Recently, the Petrie group showed that medullary complexity and the expression of tissue-restricted antigens (TRA) are negatively altered with age (94). Global gene expression analysis from stromal cells of castrated

12 month old mice and young mice showed that while the size and T cell output increases after castration, the expression of many TRA remain similar to aged, non-castrated sham mice. In fact, no statistical differences were found between TRA expression in castrated versus sham treated mice at 12 months of age, indicating that thymus regeneration may increase cell numbers but cannot rescue the degenerative TEC function that is driven by involution (94). These data also suggests that thymus regeneration may produce T cells capable of skewed, potentially autoreactive responses. Thus, an aged thymus regenerated by various means is not functionally equivalent to a young, non-involuted thymus with regards to producing self-tolerant T cells.

### 1.3 Peripheral T cells

The peripheral T pool contains functionally and phenotypically distinct T cell subsets, each expressing a diverse TCR repertoire. Such diversity promotes the generation of effective immune responses to a vast array of antigens. Each T cell clone expresses a unique TCR resulting from TCRα and TCRβ gene rearrangements during thymocyte development. In fact, there are up to $10^{11}$ unique clones in young adult humans and nearly $10^{8}$ unique TCR clones in mice (95). However, this diversity declines with age and continued antigen experience, reducing the diversity of peripheral T cells and allowing holes to develop in the TCR repertoire. Therefore investigations focused on rebuilding or sustaining TCR diversity are an important avenue for maintaining a diverse peripheral TCR population.

The T cell pool is comprised of both $CD8^+$ cytotoxic and $CD4^+$ T helper cells. $CD8^+$ cytotoxic T cells serve as the infantry of the T cell response by mediating cell death of infected cells while sparing ‘innocent bystander’ cells. All $CD8^+$ T cells

differentiate to an effector status after activation, and can transfer cytolytic granules to target cells after TCR activation or induce Fas signaling to prompt apoptosis. Furthermore, $CD8^+$ T cells release cytokines such as TNFα and IFNγ to promote antimicrobial defenses and additional immune cell recruitment. In contrast, $CD4^+$ T helper cells constitute a heterogeneous collection of cells that provide help against particular types of pathogens. A single $CD4^+$ T helper clone can produce daughter cells that may be polarized toward different lineages including the $Th_1$, $Th_2$, $Th_3$, $Th_{17}$, $Th_{FH}$ and $T_{reg}$ lineages (Reviewed in (96)). The $Th_1$ subset promotes anti-bacterial responses in infected macrophages by producing IFNγ for macrophage activation, whereas the $Th_2$ subset primarily secretes cytokines to recruit mast cells, eosinophils and plasma cells that combat parasitic infections (97). $Th_{17}$ T cells play an important role during early stages of the adaptive immune response against bacteria and fungal infections by promoting neutrophil responses (98). Recently, the $Th_{FH}$ T cell subset was identified and shown to help activate B cells in the follicular zone of the lymph nodes (99). In contrast to the other subsets of T helper cells, $T_{reg}$ cells perform the important role of suppressing the activation and proliferation of nearby T cells to prevent an autoimmune response (100). Many $T_{reg}$ are derived from thymocyte clones that react strongly to self-antigen during the positive selection stage of thymocyte development, therefore rendering them prime candidates to recognize T cells and dampen the immune response (101). Impressively, the polarization of $CD4^+$ T helper cells is heavily influenced by the cytokine milieu in the infection area. For instance, $Th_1$ T cells secrete IFNγ that promotes the polarization of surrounding T cells toward the $Th_1$ lineage, whereas $Th_2$ T cells produce IL-4 to support differentiation of other T cells to the $Th_2$ subset. In this manner, first-responding cells can dictate the type of immune response necessary to clear the infection.

Within each T cell subset, cells are loosely defined by experience: those that have not yet encountered cognate antigen are considered naïve, whereas T cells that persist after responding to antigen are referred to as memory T cells. Naïve and memory T cells produce distinct responses to infection that play equally important roles in the immune response. Naïve T cells are activated and generate effector cells over the course of a few weeks in response to new antigens presented by APCs. Memory T cells, on the other hand, rapidly clear reinfection in a matter of days. Naïve and memory T cells are identified by the expression of molecules necessary for migration and activation. Naïve T cells circulate through the vasculature and enter lymph nodes to interact with APCs. To permit this movement, naïve T cells express L-selectin (CD62L) to promote diapedesis, as well as the chemokine receptor CCR7 that recognizes the chemokine gradient directing cells towards the lymph nodes (102, 103). Expression of the early activation marker CD69 and the adhesion marker CD44 occur as naïve T cells are activated by APCs to initiate an immune response. Once the immune response is resolved, the majority of activated T cells die, leaving $CD69^{-}CD44^{+}$ memory T cells behind to serve guard to potential reinfection (104).

### *1.3.1 T cell homeostasis and the influence of thymus involution*

The peripheral T cell pool is maintained at a relatively constant number by RTE contribution from the thymus as well as homeostatic proliferation of existing peripheral T cells. All cells in the periphery require interaction with survival factors in order to persist. Naïve T cells require signaling via IL-7 and MHCII, whereas memory T cells require IL-7 and IL-15 signaling to permit homeostasis (105-108). In steady state conditions homeostatic signaling promotes survival, whereas in times of lymphopenia the same signaling promotes clonal proliferation (Reviewed in (109, 110)). In this way,

peripheral T cell numbers remain relatively stable throughout life. However, the frequency of naïve and memory T cells does change significantly during normal aging or after various stresses including viral infection, cytoablative therapy and pregnancy. In normal, healthy individuals, progressive thymus involution slowly restricts T cell production. As decreasing RTE numbers fail to sustain the size of the naïve T cell pool, the naïve T cell numbers decline, resulting in slight lymphopenia. The T cell pool compensates for this cellular loss by promoting proliferation of all cells until total cellularity is restored. Consequently, the ratio of naïve and memory T cells shift in such a way that naïve T cell frequency is diminished while memory T cell frequency becomes predominant, and grows more severe with age to restrict TCR repertoire diversity. Furthermore, 'holes' develop in the TCR repertoire that can be exploited by infection. Therefore, severe thymus involution precipitates the age-associated changes affecting immune responses of the peripheral T cell pool (109).

The function of the T cell pool as a whole declines as a result of aging. While thymus involution diminishes the rate of peripheral T cell replacement, it permits the accumulation of long-lived naïve T cells. Additionally, naïve T cell proliferation increases to maintain cell numbers, and drives exhaustion of the existing cells that promotes sub-optimal IFNγ production upon activation and inadequate helper T cell functions (111). Many aging $CD8^+$ naïve T cells transition to the $CD44^+CD62L^+$ virtual memory (VM) phenotype, further skewing the frequency of T cell populations. While VM cells are more responsive to cognate antigen, these cells proliferate less upon TCR stimulation compared to new naïve T cells, which correlates with higher levels of apoptosis upon encountering peptide (112). Ultimately, with functional defects and declining TCR repertoire diversity, holes develop in the immune response for antigens the T cell pool can no longer recognize (1). Therefore, losing recent thymic emigrants

via thymic involution is likely the catalyst behind T cell population dynamics and diminished immune responses with age.

*1.3.2 Recent thymic emigrants are phenotypically and functionally distinct naïve T cells*

It is no surprise that the T cell pool relies heavily on RTEs. Not only do RTEs maintain the diversity of the adult naïve T cell pool, they also establish the peripheral T cell pool in neonates and play a fundamental role rebounding naïve T cell numbers after infection- and stress-induced lymphopenia (113). The rate of RTE release is relatively constant throughout life and calculated at 1-2% of thymocytes per day, yet the reduction in thymopoiesis from thymus involution severely restricts the number of RTEs produced with age (72, 114). Declining RTE contribution to the peripheral T cell pool drives TCR diversity restriction, increases susceptibility to infectious diseases and reduces vaccination efficacy. Therefore, it has been suggested that maintaining the number of RTE in the peripheral T cell pool is vital to sustaining a naïve T cell population that generates robust immune responses.

RTEs are both phenotypically and functionally distinct from the mature naive (MN) T cells that they mature into during the first few weeks of peripheral residency. During this transition period, RTEs alter expression of cell surface molecules respond to survival factors and cognate antigens ((115), Reviewed in (116, 117)). RTEs do not compete as well as MN T cells for homeostatic signaling in a lymphoreplete environment due to low-level expression of IL-7Rα and must overcome this expression deficit in order to persist in the peripheral T cell pool (118). Additionally, RTEs that are subjected to TCR-stimulation exhibit diminished activation (Discussed in section 1.3.4). While the molecular basis for extra-thymic maturation is not yet fully elucidated, some evidence suggests that promoter methylation of interleukin genes and the tuning of cell

surface molecules does not occur until after thymocytes complete thymus emigration (115, 119). Furthermore, RTEs must immigrate into secondary lymphoid organs in order for the RTEs to transition to MN T cells, supporting the hypothesis that cell extrinsic factors drive RTE maturation (120). TCR repertoire changes from the RTE to MN T cell stage suggests that another facet of RTE maturation may involve pruning the TCR repertoire of RTEs before incorporation into the MN T cell population (121). Thus, extra-thymic RTE maturation is critical for new naïve T cells to persist in the naïve subset of the peripheral T cell pool.

### *1.3.3. Advances in RTE identification*

Identification of RTEs in the past was nearly impossible, as no known cell surface molecules exist to differentiate RTEs from MN T cells in mice and humans. Previous methods of identification relied on TCR excision circles (TRECs), which are a product of RAG-mediated TCR gene rearrangement during thymopoiesis (122). However, the number of TRECs in an RTE are finite and are not inherited equally between daughter cells, which can allow some RTEs to be misidentified as MN T cells (116). Furthermore, visualizing TRECs requires cell fixation due to their intracellular nature, and this process is not permissive for functional analyses of RTEs. Another RTE identification method utilized intrathymic FITC injections to label thymocytes. As a result, T cells that emigrate after the FITC injection can be identified in the periphery as $FITC^+$ cells (123). This method is both physically traumatic to the animal and demands short-term analysis, as cells only retain FITC labeling for a few days. Another major drawback to FITC injections is that this method labels all thymic cells including peripheral T cells that recirculate into the thymus and exit again during the experimental timeframe (116).

Recently, another approach has been taken which unambiguously identifies RTE*s,* in a manner that does not impact the health of the animal and allows for downstream manipulation of RTEs and MN T cells. The Nussenzweig lab generated mice expressing a GFP transgene under control of the RAG2 promoter (RAG2-pGFP) as reporters of *Rag2* expression (124). The RAG2 gene is a faithful reporter of VDJ gene rearrangement in both B and T cells. Since TCR gene rearrangement only occurs during thymocyte development and is silenced thereafter, this transgene provides robust GFP labeling of all RTEs that migrate to the periphery. The GFP label half-life is 16-18hrs, which allows GFP expression to be used as a molecular clock to distinguish RTEs that have resided in the periphery for less than a week ($GFP^{hi}$) from RTEs that have resided in the periphery for one to three weeks ($GFP^{lo}$). Importantly, RTEs can be discriminated from the phenotypically and functionally distinct MN T cells that emigrated from the thymus 3 or more weeks prior to the analysis (115).

### *1.3.4 RTE maturation and function*

Maturation in the periphery must occur for RTEs to develop into functionally mature naïve T cells. The transition of RTEs to MN T cell status is characterized by the altered expression pattern of cell surface molecules important for optimal TCR interaction and signaling (116). Changes in expression of surface markers indicative of RTE to MN transition are summarized in Figure 3. TCR expression decreases during RTE maturation to ensure that only high affinity interactions with cognate antigen drive T cell activation (116). The expression of the co-stimulatory molecule CD28 increases during transition to MN T cells promote TCR signaling (115). Also, IL-7 receptor is essential for T cell persistence in the periphery, and is upregulated as RTEs mature (115).Expression of CD45RB, an isoform of the TCR accessory molecule CD45, is

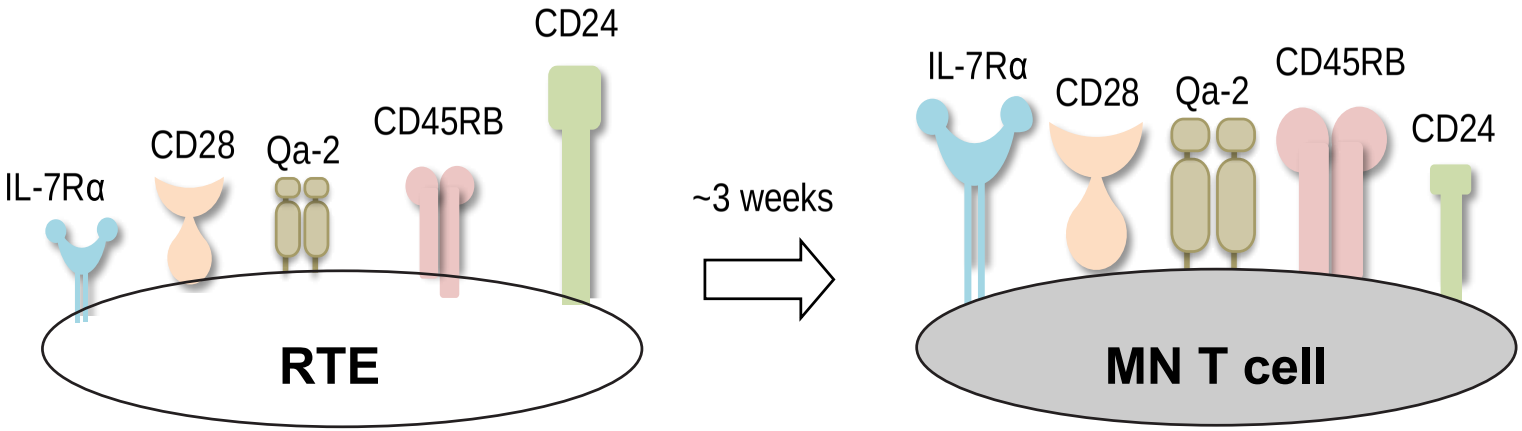
CD24
IL-7Rα
CD28
Qa-2
CD45RB
RTE
~3 weeks
IL-7Rα
CD28
Qa-2
CD45RB
CD24
MN T cell

**Figure 3. RTE maturation is defined by phenotypic changes in cell surface expression.**

Transition from RTE to MN T cell is accompanied by the upregulation of IL-7Rα, CD28, Qa-2, and CD45RB, as well as the downregulation of CD24.

upregulated as RTEs transition to MN T cells (116). Additionally, other molecules are fine tuned during the RTE maturational program. Heat stable antigen (CD24), which is required for optimal homeostatic proliferation of naïve T cells, is downregulated during RTE maturation (116, 125). Qa-2, a non-classical MHC I molecule expressed on most T cells is up regulated during RTE maturation (126). Optimizing the expression of certain molecules during RTE maturation is necessary to persist long term in the peripheral T cell pool and produce robust responses upon activation.

RTE maturation cannot occur without entry into secondary lymphoid organs (SLO), as failure to access lymphoid tissues blocks RTE maturation and causes programmed cell death (120). $CD8^+$ RTEs preferentially home to the gut-associated lymphoid tissues (GALT), which suggests that RTEs play a role in immune responses at mucosal surfaces, which may also promote tolerance to communal bacteria (127). Importantly, the presence of DCs in lymph nodes is necessary to facilitate RTE maturation. While the exact molecular signaling between DCs and RTEs is currently unknown, RTE maturation is stalled when DCs are deleted *in vivo* (128). DCs and the SLO microenvironment provide important homeostatic signals including IL-7 and MHCII expression, which have been investigated as potential means to facilitate RTE maturation. However, neither MHCII nor IL-7 availability is necessary for RTEs to transition to MN T cells. In fact, RTEs can persist without these homeostatic molecules during the first few weeks of peripheral residency (121, 128). Therefore, some unique but unidentified function of DCs and the microenvironment are crucial for RTE maturation.

While RTEs can be activated by TCR signaling during maturation, they are less immunocompetent than MN T cells. RTEs stimulated with anti-CD3 in culture proliferate less than their MN counterparts (115). Furthermore, $CD8^+$ RTEs produce fewer effector

T cells upon activation, and of those effector cells, fewer produce TNFα (129). CD8 RTEs also produce lower amounts of cytokines such as IL-2 and IFNγ and this functional deficiency persists up to 60 days after infection (130). Recently, $CD8^+$ RTEs were reported to produce stronger TCR signaling transduction from low-affinity ligands than MN T cells, and to be more capable of efficiently entering inflamed tissues by expressing high levels of VLA-4 (131). Functional differences between $CD4^+$ RTEs and MN T cells have also been described. TCR signaling during RTE maturation skews $CD4^+$ T cells away from $Th_1$ effector lineage and toward Th2 effector lineage (132). Together, these results suggest that RTEs may respond differently than MN T cells to activation to 1) minimize the impact of activation before being deleted or tolerized to self- or symbiotic- antigen, or 2) supplement existing MN T cell responses during infection.

### *1.3.5 Effects of aging on RTEs*

Age and involution significantly impact the numbers, maturation and function of RTEs. While RTEs are still produced well into old age, RTE numbers in mice decline dramatically by six months of age as a result of thymus involution (72). Furthermore, delayed RTE maturation kinetics can be observed in mice only a year old, such as delayed CD24 downregulation during transition to MN T cell status (72). Mice aged to 16-24 months old have RTEs exhibit significant functional defects, in including less IL-2 secretion, lower proliferation and defective calcium release upon stimulation *in vitro* (72, 133). Both aging ETPs and the degenerating TEC compartment have been implicated as potential sources for delayed RTE maturation and aberrant responsiveness observed in RTEs from older mice (134). These finding suggests that thymus involution not only restricts RTE numbers but may influence extra-thymic

maturation and function of these cells once released from the degenerating thymic microenvironment. More investigation is warranted to determine the extent of influence the thymic microenvironment has on RTE activity in the periphery. How the severe decline in RTEs during the first six months of life impacts the phenotypic and functional changes observed in aged mice is currently unknown. Furthermore, it is not clear if maintaining thymus output can ameliorate the phenotypic differences of older mice. Therefore, we will employ the K5.D1 transgene to investigate how preventing thymus involution impacts RTE output and response to TCR stimulation.

### 1.4 Thymus involution does not occur in K5.Cyclin D1 transgenic mice

Our lab has previously shown that driving overexpression of a Cyclin D1 transgene by a keratin 5 promoter prevents thymus involution (135, 136). While Cyclin D1 is well known for its role as a cell cycle progression protein, it also forms physical associates with more than 30 transcriptional regulators (137). The K5.Cyclin D1 transgenic mouse model exhibits increased thymocyte cellularity with age and does not undergo thymus involution. Pathological studies have found no indication of thymoma or lymphoma. Instead, the K5 Cyclin D1 transgene drives increasing TEC cellularity with age without dysregulating the medullary and cortical architecture (135). Therefore, the microenvironmental niches are expanded in these transgenic mice, making the increase in thymocyte cellularity secondary to the increase in TEC number. Additionally, driving TEC expansion may increase the number of niches available for early thymocytes. The major thymocyte subsets are intact in the K5.Cyclin D1 model, suggesting that normal thymopoiesis occurs, and normal peripheral frequencies of CD4 and CD8 T cells support this data. Therefore, this model serves as a suitable tool for determining how preventing thymus involution affects T cell output with age.

Many have suggested that preventing thymus involution should sustain T cell output and maintain a diverse TCR repertoire for immune responses. However, little investigation has been done to determine how the process of thymus involution affects the peripheral T cell populations of young mice. Therefore, the focus of this thesis is two-fold: first, the impact of thymus involution on the existing T cell pool will be identified, and second, we will determine how preventing thymus involution using the K5.D1 mouse model alters these peripheral changes. Because the K5.D1 mouse model provides an opportunity to study both TEC maintenance and thymopoiesis without the constraint of involution and that influence the peripheral T cell pool, the Results section will be separated into two chapters. First, we will identify the thymic K5.D1 phenotype (**Chapter Three**) followed by its influence in the peripheral T cell pool (**Chapter Four**).

# CHAPTER TWO

# MATERIALS & METHODS

*Mice*

Mice carrying the K5.CyclinD1 (K5.D1) transgenic were originally generated by C. Conti (MD Anderson Cancer Center, Science Park Research Division, Smithville, Texas) and maintained on the C57Bl6/J background in the Richie lab. RAG2p-GFP transgenic mice on the CD45.1 and CD45.2 C57Bl6/J congenic backgrounds were gifted from P. Fink (University of Washington) and crossed to the K5. D1 model to obtain K5.D1;RAG2p-GFP double transgenic mice. PCR was utilized to determine K5.D1 and RAG2p-GFP transgene expression, and GFP expression was confirmed visually in the thymus upon dissection by fluorescence microscope (Olympus Provis AX70). Female Nur77-GFP mice were gifted from L. Ehrlich and crossed to K5.CyclinD1 males for TCR engagement studies. $F_1$ congenic $CD45.1^+;CD45.2^+$ heterozygous C57Bl6/J recipients of adoptive transfer experimental injections were bred in house by crossing C57Bl6/J CD45.2 females to C57Bl6/J CD45.1 males. All mice were maintained in pathogen-free conditions, and experiments were performed in accordance with all MD Anderson Institutional Animal Care and Use Committee policies.

*Tissue preparation for lymphocyte FACS analysis*

Thymus, spleen, axillary and inguinal lymph nodes were removed and placed in cold, sterile 1x PBS (Hyclone). Organs were trimmed of connective tissues and pressed through a 70μm mesh strainer (Fisher) using the plunger from a 3ml syringe (BD Falcon). Strainers containing tissue were washed with FACS Wash Buffer (5mM

EDTA pH8, 2% FCS) and collected in a 50ml conical tube (BD Falcon). Conical tubes were then centrifuged at 1500rpm for 6 minutes to pellet cells. Cells were treated with RBC Lysis Buffer for 5min at room temperature, then diluted with 10ml FACS Wash Buffer and centrifuged at 1500rpm for 6 minutes to pellet cells. Cell pellets were resuspended in 10ml cold FACS Wash Buffer. Single cell tissue preparations were counted using trypan blue viability stain (Life Technologies) by a Countess® automated cell counter (Life Technologies) or by haemocytometer. Cells were distributed at a concentration of 3 million cells per FACS polystyrene tube (BD Falcon) in 300ul of FACS Wash Buffer for antibody staining.

*Tissue preparation for thymic epithelial cell FACS analysis*

Thymic tissue was excised from the thoracic cavity, places in cold, sterile 1x PBS (Hyclone) and trimmed of connective tissues. Lobes were separated, and 4-5 small nicks were made about 2-3mm into each lobe. For some experiments collagenase followed by collagenase/dispase was used to digest lobes as previously described (138), whereas in later experiments liberase was utilized to dissociate TECs as previously described (139). After the final digestion, enzymes were quenched with up to 50ml ice-cold FACS Wash Buffer, centrifuged to pellet cells. Cell pellets were resuspended to 10ml in FACS Wash Buffer, filtered by passing through a 70μm mesh strainer (Fisher) and counted using Trypan Blue (Life Technologies) on an automated cell counter (Life Technologies). Cells were distributed at a concentration of 3 million cells per FACS polystyrene tube (BD Falcon) in 300ul of FACS Wash Buffer for antibody staining.

*Antibodies used for FACS analysis*

Single cell suspensions were stained with combinations of the following antibodies: anti-CD3-BV450, anti-CD4-Alexafluor 780, anti-CD5-Pacific Blue, anti-CD8-PE/Cy7, anti-CD11b-PE/Cy5, anti-CD11c-PE/Cy5, anti-CD24-PerCP/Cy5.5, anti-CD25-A488, anti-CD44-APC, anti-CD45-PerCP/Cy5.5, anti-CD45.1-Pacific Blue, anti-CD45.2-PE, anti-CD45RB-Pacific Blue, anti-CD62L-PE or anti-CD62L-Alexafluor 700, anti-CD69-PE, αβTCR-Alexa 700, anti-ckit-APC/Cy7, anti-γδ-TCR-PE, anti-TER119-PE/Cy5, anti-CD127-Biotin (eBioscience), anti-IA/IE-Pacific Blue (BioLegend), anti-UEA1-FITC (Vector), anti-Ly51-Biotin, anti-Qa-2-Biotin, and anti-Mouse IgG2a,k-Biotin (BD Pharmingen/BD Biosciences). Primary antibodies were added to 3 million cells suspended in 300ul PBS on ice for 15 minutes in the dark, and washed with up to 3ml cold FACS Wash Buffer. Samples were centrifuged at 1500rpm for 3 minutes to form cell pellets. Supernatant was removed and cell pellets were resuspended in 300ul of PBS. The secondary antibody SA-Qdot 605 or SA-Qdot655 (Life Technologies) was used to visualize streptavidin-labeled antibodies by incubating for 15 minutes in the dark on ice. Samples were again centrifuged at 1500rpm for 3 minutes to pellet cells, supernatant was removed and cell pellets were resuspended. For intracellular staining, antibodies including anti-Bcl2-PE and anti-Foxp3-APC were utilized and cells were incubated 30 min in the dark at room temperature. All samples were brought to a volume of 400ul in PBS for FACS analysis using the AriaIIu® or Fusion® cell sorters, or Fortessa® cell analyzer (BD Biosciences). Acquired data was analyzed using the FlowJo (Versions 9.6.10-9.7.4) program by Treestar (Ashland, Oregon).

*BrdU analysis*

BrdU labeling to determine T cell proliferation was performed by a single i.p. injection of 100µl of BrdU (10mg/ml, BD Biosciences) into adult mice, followed by feeding 0.8mg/ml BrdU water with 0.1% sucrose for 8 days. On the eighth day, mice were sacrificed for flow cytometric analysis. BrdU labeling to determine thymocyte proliferation was performed by a single i.p. injection of 100µl of BrdU (10mg/ml, BD Biosciences) into adult mice, which were sacrificed 16 hours later for flow cytometric analysis. For flow cytometry staining, the BrdU staining protocol (BD Biosciences) included in the kit was followed, and either FITC or APC conjugated anti-BrdU was used to visualize intracellular BrdU labeling.

*Foxp3 analysis*

Extracellular staining of single cell suspensions was performed with antibodies described previously. Cells were then fixed using the Foxp3 (eBioscience) kit and stained with Foxp3-APC antibody according to the kit directions, and analyzed on a FACS Fortessa cell analyzer.

*$V_\beta$ TCR Repertoire Analysis*

$V_\beta$ repertoire analysis was performed using the TCR $V_\beta$ Screening Panel (BD Biosciences), in combination with additional fluorochromes mentioned previously. All repertoire analysis was performed on a FACS Fortessa cell analyzer.

*Splenic T cell sorting*

Single cell suspensions of splenic T cells from RAG2p-GFP and K5.CyclinD1;RAG2p-GFP congenically marked mice were enriched for CD4 and CD8 T

cells by MACS separation (Miltenyi Biotec) using the CD4+ enrichment kit II (Miltenyi Biotec, cat # 130-095-248) and the 'depletion protocol'. In other experiments, T cells were enriched by incubating freshly isolated splenocytes with purified antibodies against CD11b, CD11c, B220 and TER119 for 30 minutes on ice, followed by two 10min incubations with Sheep anti-rat IgG Dynal beads (Life Technologies) on a rotator at room temperature, and applied to a magnetic field. Supernatant was removed, then washed and stained as described above. Cells were sorted on a FACSAria IIu® or Fusion® cell sorter for $Lin^-CD8^-CD44^-GFP^+$, $Lin^-$ $CD8^-CD44^-GFP^-$ subsets directly into 5ml polysterene tubes containing FCS or microcentrifuge tubes containing 800ul TriZol. Live cells in FCS were pelleted by centrifugation for 3min at 1500rpm. Supernatants were removed and cell pellets were resuspended in 100ul PBS, counted by using trypan blue viability stain by a Countess® automated cell counter.

*Adoptive transfer of sorted T cells into lymphoreplete recipients*

$CD4^+$ RTEs and MN T cells were sorted from isolated splenocytes as described above. Cells were pelleted by centrifugation at 1500rpm for 3 minutes, supernatant removed and resuspended less than 200ul of PBS. Cells were counted using trypan blue viability stain (Life Technologies) and a Countess® automated cell counter (Life Technologies). To compare the persistence of cells of interest, adoptive transfers of RTEs and MN T cells at a 1:1 ratio was performed by retro orbital sinus injection of anesthetized 10-14wk old $F_1$ $CD45.1^+$;$CD45.2^+$ congenic WT or K5.D1 transgenic recipients. Input ratios were obtained by staining an aliquot of the mixed cell suspension with CD45.1-PE and CD45.2-PacBlue (eBiosciences) and analyzed by flow cytometry.

*Analysis of lymphoreplete adoptive transfer experiments*

Recipient mice were sacrificed at 1, 3 or 6 weeks after adoptive transfer, and spleen, axial and inguinal lymph nodes were dissected and washed in ice-cold PBS. Organs were trimmed of connective tissues and pressed through a 70μm mesh strainer (Fisher) using the plunger from a 3ml syringe (BD Falcon). Strainers containing tissue were washed with FACS Wash Buffer (5mM EDTA pH8, 2% FCS) and collected in a 50ml conical tube (BD Falcon). Conical tubes were then centrifuged at 1500rpm for 6 minutes to pellet cells; cell pellets were resuspended in 10ml cold FACS Wash Buffer. Single cell tissue preparations were counted using trypan blue viability stain (Life Technologies) by a Countess® automated cell counter (Life Technologies) or by haemocytometer. Cells were distributed at a concentration of 3 million cells per FACS polystyrene tube (BD Falcon) in 300ul of FACS Wash Buffer for antibody staining. Cells were stained with appropriate antibodies and analyzed by flow cytometry.

Determination of K5.D1 vs. control T cell recovery was done as previously described (118). Briefly, the number of $CD45.2^+$ and $CD45.1^+$ congenic cells recovered from recipients was determined by data analysis using FlowJo® software (TreeStar, version 9.6.7). The ratio of CD45.2 vs. CD45.1 cells was obtained for each organ from each recipient, and normalized by dividing this post-transfer ratio by the input ratio to determine the change since adoptive transfer. Furthermore, the change since adoptive transfer for K5.D1 vs. control data was normalized to control vs. control data by dividing the former by the latter, to account for potential incorporation discrepancies between congenic backgrounds (140).

*Adoptive transfer of sorted T cells into RAG2$^{-/-}$ recipients*

Bulk CD4$^{+}$ T cells were sorted from isolated splenocytes as described above. Cells were pelleted by centrifugation at 1500rpm for 3 minutes, supernatant removed and resuspended less than 200ul of PBS. Cells were counted using trypan blue viability stain (Life Technologies) and a Countess® automated cell counter (Life Technologies). Control or K5.D1 T cells were injected into recipient mice by retro orbital sinus injection of anesthetized 13-15wk old C57Bl6/J RAG2$^{-/-}$ mice. Animals were weighed every two days for a total of 21 days, and sacrificed for necropsy. Body mass index was calculated as the starting weight of an animal divided by the weight on day X.

*CFSE Labeling*

Carboxyfluorescein succinimidyl ester (CFSE) labeling was used to monitor proliferation *in vitro* and *in vivo*. Sorted T cells were incubated in pre-warmed 5mM CFSE (CellTrace CFSE Cell Proliferation Kit, Life Technologies) for 10min in PBS at 37°C in the dark. Cells were washed twice with 5x volume of complete media (supplemented with 10% FCS) to neutralize CFSE and allowed to rest 10min before stimulating *in vitro*.

*Cell Culture and in vitro Functional Assays*

For *in vitro* activation and proliferation studies, FACS sorted Lin$^{-}$CD8$^{-}$CD44$^{-}$ splenic T cells were stained with CFSE and seeded into 96 well plates at a concentration of 1x10$^{5}$ cells per well in RPMI 1640 supplemented with non-essential amino acids, 2mM Glutamax, 1mM sodium pyruvate, 55mM β-mercaptoethanol, 10% FCS and antibiotics. Sorted T cells were plated along with 5x10$^{5}$ APCs (CD3$^{-}$ irradiated splenocytes subjected to 3000 rad), and cultured in varying amounts of anti-CD3

(1ug/ml, 500ng/ml, 100ng/ml or no anti-CD3 antibody; clone 145-2C11) and 1 ug/ml anti-CD28 (clone 37.51) from eBioscience for 68 hours. Cells were then restimulated with Cell Stimulation Cocktail (eBioscience) for one hour. Protein transport was blocked (Transport Inhibitor Cocktail, eBioscience) for three additional hours and cells were stained for cell surface markers and the intracellular cytokines IL-2, IL-4 and IFNγ.

For *in vitro* IL-7 experiments, FACS sorted $CD8^{-}CD44^{-}GFP^{-}$ splenic T cells were seeded into 96 well plates at a concentration of $1x10^{5}$ cells per well with varying amounts of IL-7 (10ng/ml, 5ng/ml, 2.5ng/ml, 1.25ng/ml or no IL-7) and analyzed at 4, 8, 24, and 48 after plating. Samples were stained with propidium iodide and recorded on a BD Fortessa® and analyzed in FlowJo® (TreeStar, version 9.6.7).

*Haematoxylin and Eosin Staining*

Fresh frozen sections were thawed to room temperature for thirty minutes, and fixed using 10% neutral buffered formaldyhyde. Slides were treated with haematoxylin (Sigma) for 10 minutes and rinsed briefly in tap water. Slides were then treated with 1% eosin (Sigma) for 3-10 minutes and rinsed briefly in tap water. Slides were dehydrated by increasing ethanol concentrations from 70% to 100% and washed in xylene twice for a total of 10 minutes. Finally slides were coverslipped with cytoseal (Thermo Scientific).

*Immunohistochemistry*

Serial sections (5-7□m) from OCT-embedded frozen tissue were air dried and fixed in cold acetone or 4% paraformaldehyde at room temperature. After washing with PBS, sections were incubated with optimal dilutions of anti-mouse Keratin 5 (Covance Research), anti-mouse CD205 (Ly75, Abcam), anti-rat CD8-efluor 660 (eBioscience), anti-rat ERTR7-Alexa 488 (Nova Biologicals), or anti-rat CD31-biotin (eBioscience) in PBST/5% donkey serum at 4 °C overnight. Slides were washed in PBST and treated

with appropriate secondary antibodies for 30min, or treated with the TSA amplification system (Life Technologies), then washed and stained with 1:1500 dilution of DAPI for 5min. Slides were washed after DAPI staining and treated with Prolong Gold Antifade Mountant (Life Technologies) and coverslipped for microscopy.

Additional IHC stains were performed similarly, and include: Keratin 8 (Troma 1 hybridoma, raised in house), Keratin 5 (Covance), Keratin 14 (Covance), and Ulex Europaeus Agglutinin I (Vector Laboratories).

*Autoantibody Staining (Sera Staining)*

Serial sections (5-7□m) from OCT-embedded frozen tissue from RAG2$^{-/-}$ mice were air dried and fixed in cold acetone at room temperature. After washing with PBS, sections were incubated 100ul of sera from 6-8 month old control or K5.D1 mice at 4 °C overnight. Slides were washed in PBS and treated with anti-mouse IgG-TxRed (Vector Laboratories) and then washed and stained with 1:1500 dilution of DAPI for 5min. Slides were washed again after DAPI staining and treated with Prolong Gold Antifade Mountant (Life Technologies) and coverslipped for microscopy.

*Quantitative Real-Time PCR*

For quantitative RT-PCR (qRT-PCR), cells were sorted directly into TRIzol (Life Technologies) and stored at -80°C until isolated for analysis. RNA was isolated according to the TRIzol protocol, andlinear acrylimide was utilized as a carrier where necessary. cDNA was made from isolated RNA using the Superscript III First Strand Synthesis kit (Life Technologies) with oligo(dT) primers, and stored at -20°C. qRT-PCR was achieved using TaqMan primers and master mixes (Life Technologies) on a LightCycler 480 (Roche). All reactions were run at least 3 times in duplicate for

analysis, and the presence of single RT-PCR products were confirmed by melting curve analysis. Reactions were normalized to the appropriate endogenous controls (α-tubulin for TECs and HPRT for T cell analyses). All data was analyzed using the Livak ($-2^{\Delta\Delta CT}$) method of qRT-PCR analysis.

*Statistics*

Statistical difference between two groups was achieved using a paired or unpaired Student *t* Test (GraphPad Prism) as indicated. A *p* value of $<0.05$ was considered statistically significant.

# CHAPTER THREE

# PREVENTING THYMUS INVOLUTION SUSTAINS THYMOPOIESIS

## 3.1 Introduction

Age-associated thymus involution causes a reduction in thymopoiesis and constricts T cell output resulting in a decreased ratio of naïve to memory T cells in the periphery (1, 74, 109). Declining naïve T cell numbers impairs the ability to mount robust immune responses to newly encountered antigens and ultimately increases susceptibility to infectious disease and cancer. Therefore, it has been suggested that preventing thymus involution would sustain a functional immune system throughout life.

Disorganization and disintegration of the TEC compartment is a major factor that underlies the reduced ability of the involuted thymus to support thymocyte maturation (141, 142). In earlier studies we demonstrated that targeting expression of a Cyclin D1 transgene to the TEC compartment prevents the occurrence of age-associated thymus involution (135, 143, 144). However, these investigations utilized mice on FVB or mixed backgrounds, which undergo thymus involution more rapidly than the C57Bl6/J mouse strain commonly used for experimental immunological studies (145-147). To determine if the non-involuting thymic phenotype persisted in the slower-involuting C57Bl6/J background, the K5.CyclinD1 transgene was backcrossed onto the C57Bl6/J background at least 10 generations. Furthermore, our previous studies did not analyze the number or differentiation of TEC subsets. Finally, the identification of discrete thymocyte subsets has progressed significantly since the initial characterization of this mouse model. For these reasons, we reinvestigated thymocyte and TEC phenotypes in K5.CyclinD1 (hereafter referred to as K5.D1) transgenic mice. The following results confirm and expand upon our original observations and support the notion that

sustaining the TEC compartment prevents thymus involution, which in turn, supports continued release of naïve T cells (135, 143, 144).

## 3.2 Results

*K5.D1 expression prevents thymus involution*

The onset of thymus involution in C57Bl6/J mice is evident by two to three months of age and progresses to severe thymus shrinkage observable by one year of age (81, 141). Organ atrophy indicative of thymus involution is readily apparent by gross morphology of 20 week old C57Bl6/J mice (Figure 4A, left side). In stark contrast, the K5.D1 thymus does not undergo involution. Instead, the size of the K5.D1 thymus continues to increase with age (Figure 4A, right side). In fact, thymus size increases to fill the thoracic cavity, causing lung compression and death by 8-12 months of age. H&E stained thymus sections from nontransgenic (hereafter referred to as control) and K5.D1 littermates reveal that cortical and medullary organization is maintained in K5.D1 thymi (Figure 4B, right side). In control mice, aging is associated with progressive disorganization of thymic structure and blurring of the demarcation between cortex and medulla at the CMJ (Figure 4B, left magnification). This aging phenotype is already apparent by 20 weeks in control mice (Figure 4B, left side). In contrast, thymic organization is well maintained in the K5.D1 thymi, as evidenced by the clear demarcation of medullary and cortical regions (Figure 4B, right magnification).

To relate the size differences of control and K5.D1 thymi with age to thymus cellularity, we counted the total number of cells obtained from thymi of mice from 4 to 40 weeks of age. Total cellularity mainly reflects the number of thymocytes since these cells comprise more than 95% of the thymus. Prior to the onset of thymus involution, thymus cellularity of control mice 4-8 weeks of age averaged 1.4 $x10^8$ cells per thymus.

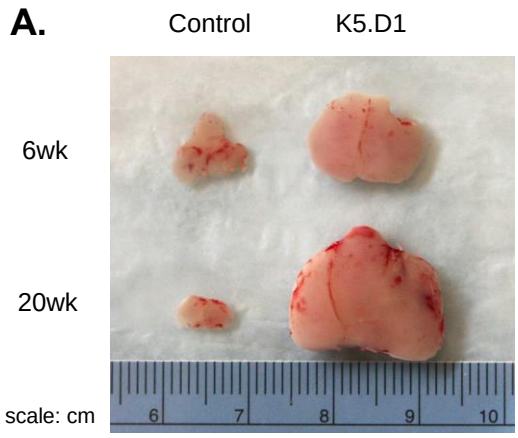
A.
Control
K5.D1
6wk
20wk
scale: cm
6
7
8
9
10

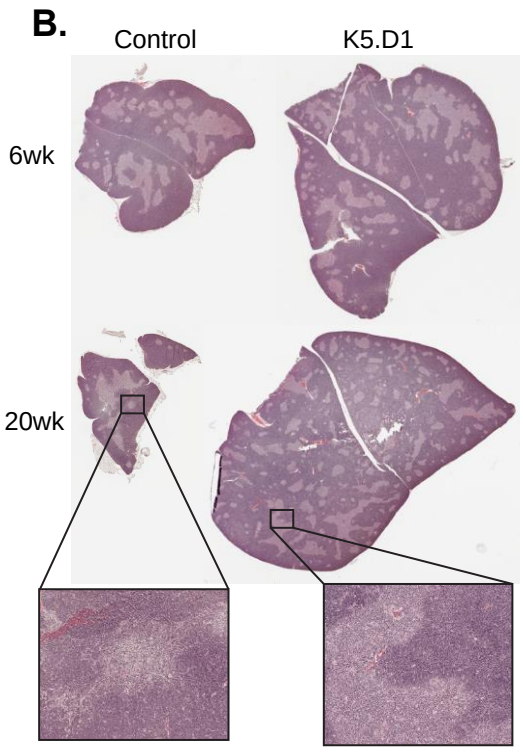
B.
Control
K5.D1
6wk
20wk

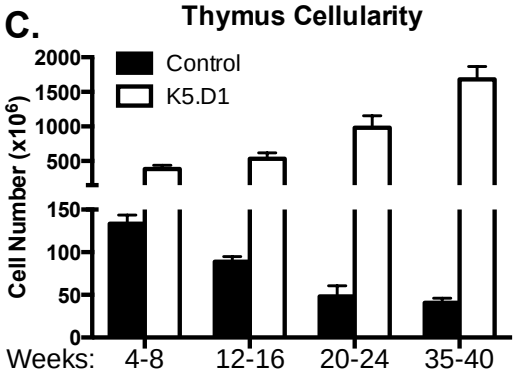
C.
Thymus Cellularity
Control
K5.D1
Cell Number (x10^6)
2000
1500
1000
500
150
100
50
0
Weeks:
4-8
12-16
20-24
35-40

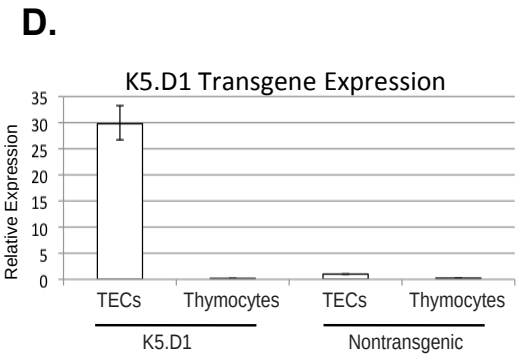
D.
K5.D1 Transgene Expression
Relative Expression
35
30
25
20
15
10
5
0
TECs
Thymocytes
TECs
Thymocytes
K5.D1
Nontransgenic

**Figure 4. Expression of the K5.D1 transgene in TECs prevents age-related thymus involution and maintains thymus organization.**

(**A**) Control and K5.D1 transgenic thymi at 6 and 20 weeks of age. (**B**) Representative H&E images of 6 and 20 week control and K5.D1 littermate thymus sections show darker cortical and lighter medullary regions. Magnification inserts depict the delineation between cortex and medulla. (**C**) Thymus cellularity up to 40 weeks of age in control and K5.D1 mice (Data is presented as mean ±SEM, where each bar represents n≥3). (**D**) Quantitative RT-PCR analysis of Cyclin D1 expression in TECs and thymocytes from control and K5.D1 mice (data is representative of three independent experiments).

By 12-16, 20-24 and 35-40 weeks of age control thymus cellularity declined to 66%, 36% and 30%, respectively, of the pre-involution cell number (Figure 4C, black bars). These observations are in agreement with previous reports of thymus cellularity from C57Bl6/J mice (147, 148). However, thymus involution does not occur in K5.D1 mice. In fact, K5.D1 thymus cellularity increases with age (Figure 4C white bars). Thymus cellularity in K5.D1 animals increases to 42 times the number of cells present in control thymi at 35-40 weeks of age. Histopathological analysis of the K5.D1 thymus confirmed that the increased K5.D1 thymus size is not due to lymphoma or thymoma (data not shown). Furthermore, quantitative RT-PCR analysis of thymocytes and TECs from K5.D1 mice showed that transgene expression is restricted to the TEC subset and is not expressed in thymocytes (Figure 4D, (144)). These latter results suggest that TEC-specific expression of the K5.D1 transgene may drive thymus cellularity by maintaining and expanding the TEC microenvironment that supports thymopoiesis.

*The K5.D1 transgene maintains the TEC microenvironment*

A strong keratin 5 promoter drives expression of the Cyclin D1 transgene exclusively in thymic epithelium. Thus, it is likely that the observed thymus hyperplasia is secondary to expansion of the supporting TEC microenvironment. If so, we would expect to observe an increasing number of TECs to support the number of thymocytes present in the K5.D1 thymi with age. TEC cellularity was quantified in control and K5.D1 thymi. The number of TECs in control thymi declines between 4-8 and 20-24 weeks of age, in agreement with previous reports (Figure 5A, (57)). In contrast, increased TEC cellularity was evident in K5.D1 mice as young as 4 weeks of age and increased 10-fold by 20-24 weeks of age. The transcription factor FOXN1 plays a key role in regulating TEC differentiation and proliferation. *Foxn1* expression has been

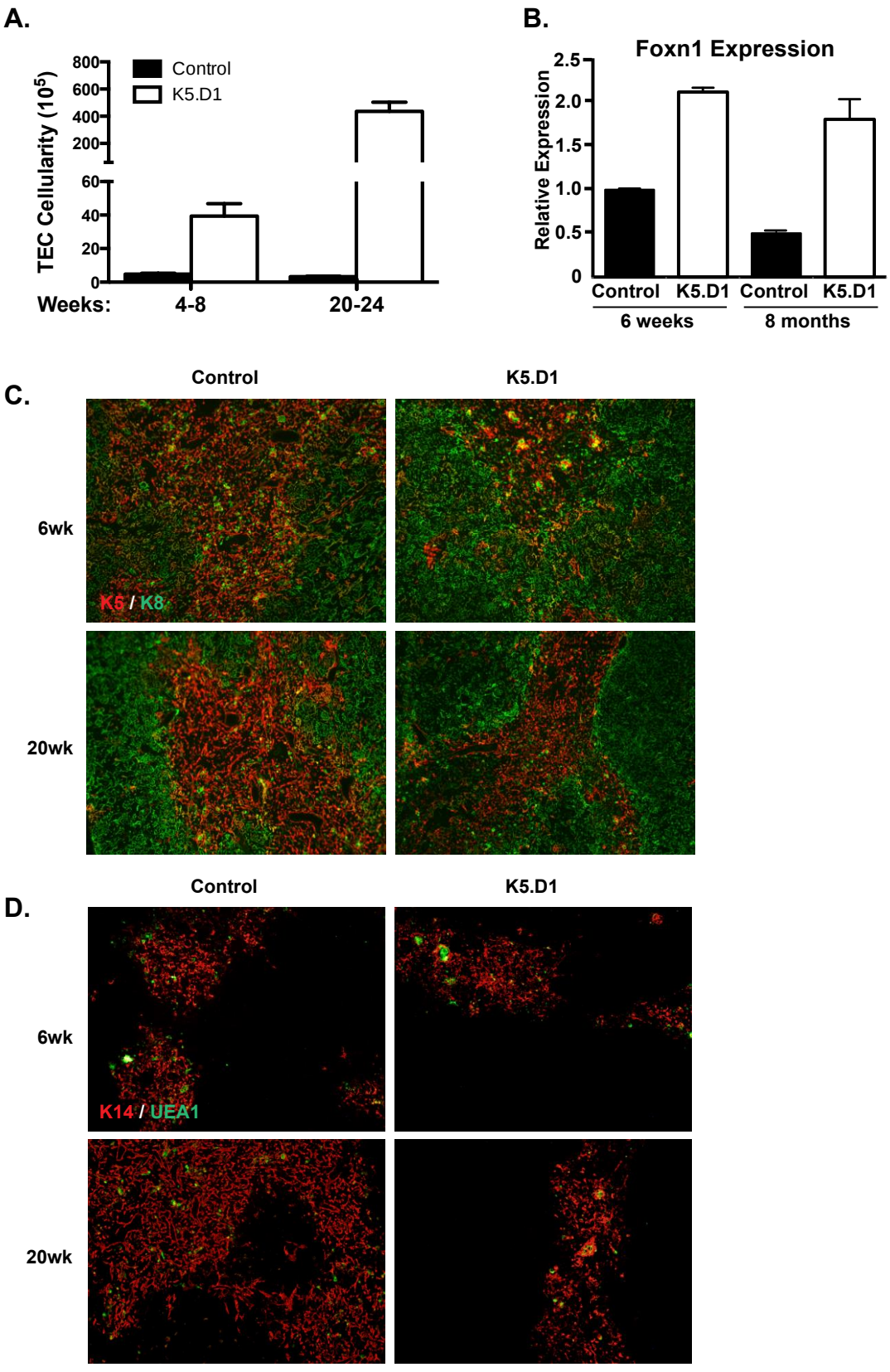
A.
TEC Cellularity ($10^5$)
800
600
400
200
60
40
20
0
Control
K5.D1
Weeks:
4-8
20-24
B.
Foxn1 Expression
Relative Expression
2.5
2.0
1.5
1.0
0.5
0
Control
K5.D1
Control
K5.D1
6 weeks
8 months
C.
Control
K5.D1
6wk
20wk
K5 / K8
D.
Control
K5.D1
6wk
20wk
K14 / UEA1

**Figure 5. Expression of the K5.D1 transgene expands the TEC compartment with age.**

**(A)** Total TEC cell number in control and K5.D1 mice at 4-8 and 20-24 weeks of age (Data is presented as mean ±SEM, where each bar represents n≥6). **(B)** Quantitative RT-PCR analysis of Foxn1 expression in TECs from control and K5.D1 mice at 6 weeks and 8 months of age Data is representative of 3 independent experiments. **(C)** Representative IHC images of Keratin 5+ (K5) mTEC and Keratin 8+ (K8) cTEC staining of 1 and 6 month control and K5.D1 thymic sections. **(C)** Representative IHC images of Keratin 14+ (K5) mTEC and UEA1+ mTEC staining of 1 and 6 month control and K5.D1 thymic sections.

shown to decline during thymus involution (81, 148). Therefore, we asked if the expression of *Foxn1* is maintained with age in K5.D1 TECs. Thymi from control and K5.D1 mice were enzymatically dissociated and TECs were isolated by FACS sorting $MHCII^{+}CD45^{-}$ cells directly into Trizol. Quantitative RT-PCR analysis of *Foxn1* expression in control TECs demonstrated declining expression from 6 weeks to 8 months of age (Figure 5B). However, K5.D1 TECs from 6 week mice exhibited 2-fold greater Foxn1 expression, which was sustained in K5.D1 mice 8 months of age. These data imply that overexpressing Cyclin D1 in TECs directly or indirectly maintains *Foxn1* expression with age, which may be responsible, at least in part, for sustained increase in the number of TECs.

The presence of both the mTEC and cTEC compartment is vital for productive thymopoiesis. Since expression of the K5.D1 transgene drives an increase in both the number of TECs and expression of the FOXN1 transcription factor essential for their maintenance, we asked whether the TEC microenvironment might be altered by K5.D1 transgene expression. Frozen sections from 6 week and 6 month old control and K5.D1 thymi were stained with antibodies recognizing the mTEC marker Keratin 5 and the cTEC marker Keratin 8 (Figure 5C) or Keratin 14 and ulex europaeus agglutinin 1 (UEA1, Figure 5D). Immunofluorescence imaging revealed the distinct organization of mTECs and cTECs in control thymi, which was maintained in K5.D1 thymi. These results suggest that expansion of TEC numbers results in an expansion of both the cTEC and mTEC subsets that support thymopoiesis.

*Thymopoiesis increases with age in K5.D1 thymi*

Our lab has previously shown that the K5.D1 transgene does not alter the frequency of major thymocyte subsets in 4-12 week old mice (135). However, the

distribution of major thymocyte subsets had not been determined in older K5.D1 animals. Therefore, we analyzed the thymocyte population in mice up to 24 weeks of age to determine if thymopoiesis is altered by severe thymic hyperplasia. Thymocyte subsets were defined by expression of CD4 and CD8 as Double Negative (DN, $CD4^-$ $CD8^-$), Double Positive (DP, $CD4^+CD8^+$), and Single Positive (CD4 SP, $CD4^+CD8^-$, and CD8 SP, $CD4^-CD8^+$) subsets (Figure 3A). Control thymi typically contain ~2-3% DN thymocytes, 85-90% DP thymocytes, 6-8% CD4 SP thymocytes, and 2-3% CD8 SP thymocytes at 6 to 24 weeks of age (Figure 6A, left column). The frequency of the major thymocyte subsets was comparable in control and K5.D1 thymi at 4-8 weeks of age (Figure 6B). However, at later ages, the K5.D1 thymi contained a small, but significant, decrease in the percentage of DP thymocytes that was countered by an increased frequency of cells in the CD4 and CD8 SP subsets (Figure 6C and 6D). The increased frequency of SP thymocytes in the K5.D1 thymus could be due to defects in export of this subset or the result of maturation defects in the DP and or SP subsets. Evidence that support or negate these alternative explanations will be discussed below.

Thymocyte cellularity in each subset was increased in the K5.D1 compared to littermate thymi (Figure 6E-G). DN numbers in control 4-8 week thymi averaged 2.5 x $10^6$ cells, DP cell numbers averaged $10^8$ cells, and the CD4 and CD8 SP cellularities averaged 7 x $10^6$ and 2.6 x $10^6$, respectively (Figure 6E). The number of all control thymocyte subsets declined to ~58% at 12-16 weeks, and was further reduced at 20-24 weeks to just 32% of the cellularity at 4-8 weeks. On the other hand, K5.D1 thymocyte cellularity was three times greater than littermate controls at 4-8 weeks, and continued to increase with age. By 12-16 weeks of age, K5.D1 thymi contained ~8 times as many cells in every thymocyte subset as control littermates (Figure 6F). K5.D1 thymocyte cellularity in each subset increased to nearly 50 times that of involuted age-matched

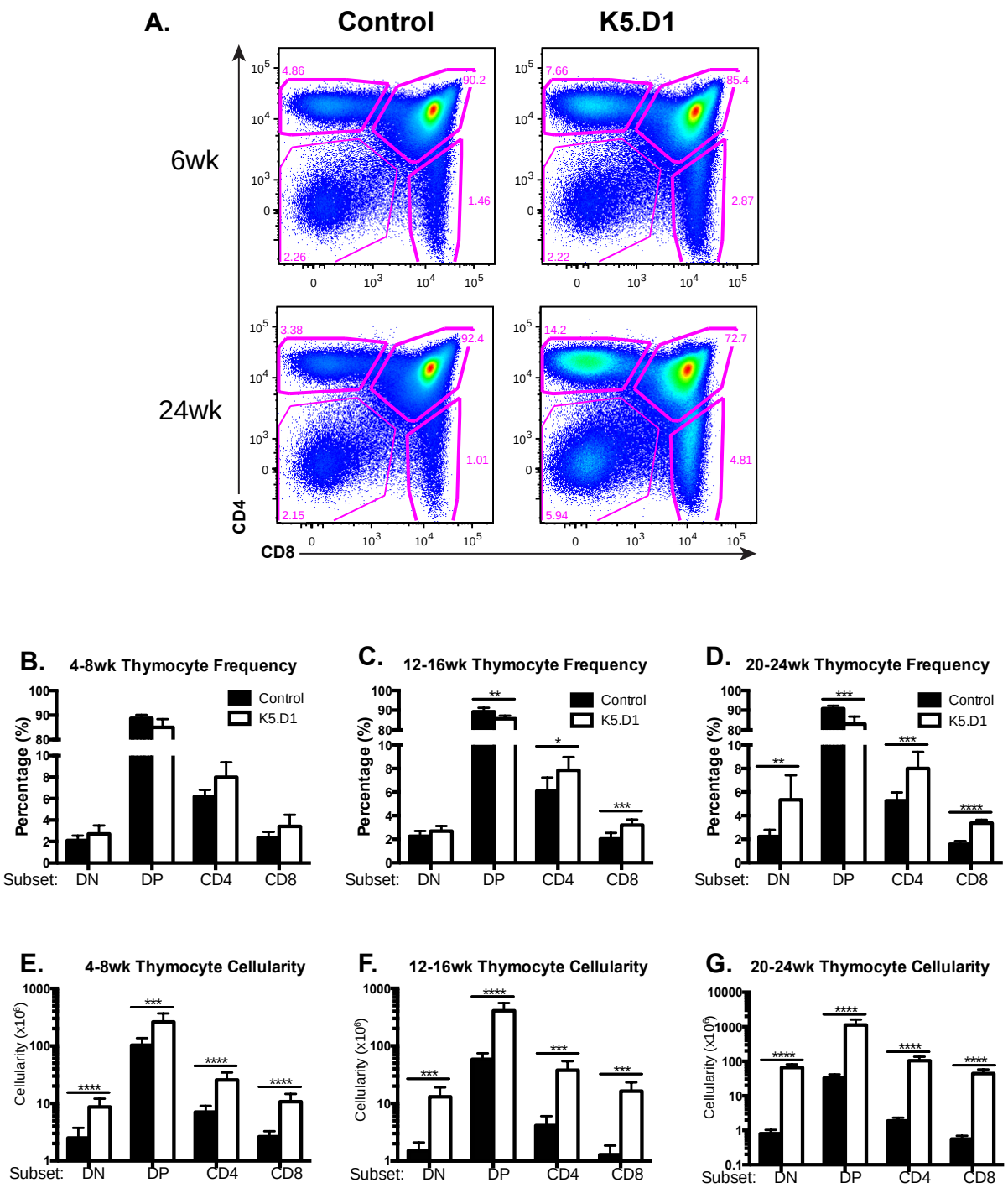
A.
Control
K5.D1
6wk
24wk
CD4
CD8
4.86
90.2
1.46
2.26
7.66
85.4
2.87
2.22
3.38
92.4
1.01
2.15
14.2
72.7
4.81
5.94
B. 4-8wk Thymocyte Frequency
C. 12-16wk Thymocyte Frequency
D. 20-24wk Thymocyte Frequency
Percentage (%)
Control
K5.D1
Subset: DN DP CD4 CD8
E. 4-8wk Thymocyte Cellularity
F. 12-16wk Thymocyte Cellularity
G. 20-24wk Thymocyte Cellularity
Cellularity (x10^6)

**Figure 6. Distribution of major thymocyte subsets in control and K5.D1 thymi.** (**A**) Representative dot plots of major thymocyte subsets defined by CD4 and CD8 expression from control and K5.D1 thymi 6 and 24 weeks of age. (**B**) Percentage of major thymocyte subsets at 4-8 weeks (**C**) 12-16 weeks (**D**) 20-24 weeks of age. (**E**) Total cell number in each major thymocyte subset at 4-8 weeks **(F)** 12-16 weeks (**G**) and 20-24 weeks of age. Data are presented as mean ±SEM and n≥5 for all data. *P<0.05, **P<0.01, ***P< 0.0001, and ****P< 0.00001 using an unpaired two-tailed Student T test.

littermates by 20-24 weeks of age (Figure 6G). Taken together, these data reaffirm that the capacity for thymopoiesis correlates with thymus size, which increases with age in the K5.D1 thymus.

Thymopoiesis depends on continual influx of thymus seeding progenitors from the bone marrow that can undergo T cell lineage commitment in the DN thymocyte compartment. Since all subsequent stages of thymocyte development emanate from DN precursors, we questioned whether the frequency or number of the earliest thymocyte progenitors might be increased in K5.D1 mice to support increased T cell development. Therefore, we analyzed the frequency and number of the four DN subsets by flow cytometry. Thymocytes were gated on $\alpha\beta TCR^-$ $\gamma\delta TCR^-$ DN cells, and DN1-4 subsets were defined by the expression of CD44 and CD25 (Figure 7A). The frequency of DN1-4 thymocyte subsets did not change during the first 6 months of life in either control or K5.D1 thymi (Figures 7B-D). However, the number of each DN subset declined with age in control thymi, whereas the cellularity of each DN subset increased in K5.D1 thymi with age (Figure 7E-G). K5.D1 mice 4-8 weeks of age exhibited roughly three times the DN1-4 cellularity of control littermates, whereas the DN subset cellularity in 12-16 week old K5.D1 thymi increased 5-fold compared to controls. By 20-24 weeks of age, cellularity in the K5.D1 DN subsets expanded to nearly 50 times that of involuted control littermates. Therefore, expanding the TEC microenvironment using the K5.D1 transgene supports a larger pool of immature thymocytes.

The DN1 thymocyte subset is comprised of a heterogeneous mixture of progenitor cell types capable of differentiation to the B, T, NK and DC lineages. Early thymocyte progenitors (ETPs) are most effective at developing towards the T cell lineage but reflect only a small fraction of the DN1 subset of cells and are identified by

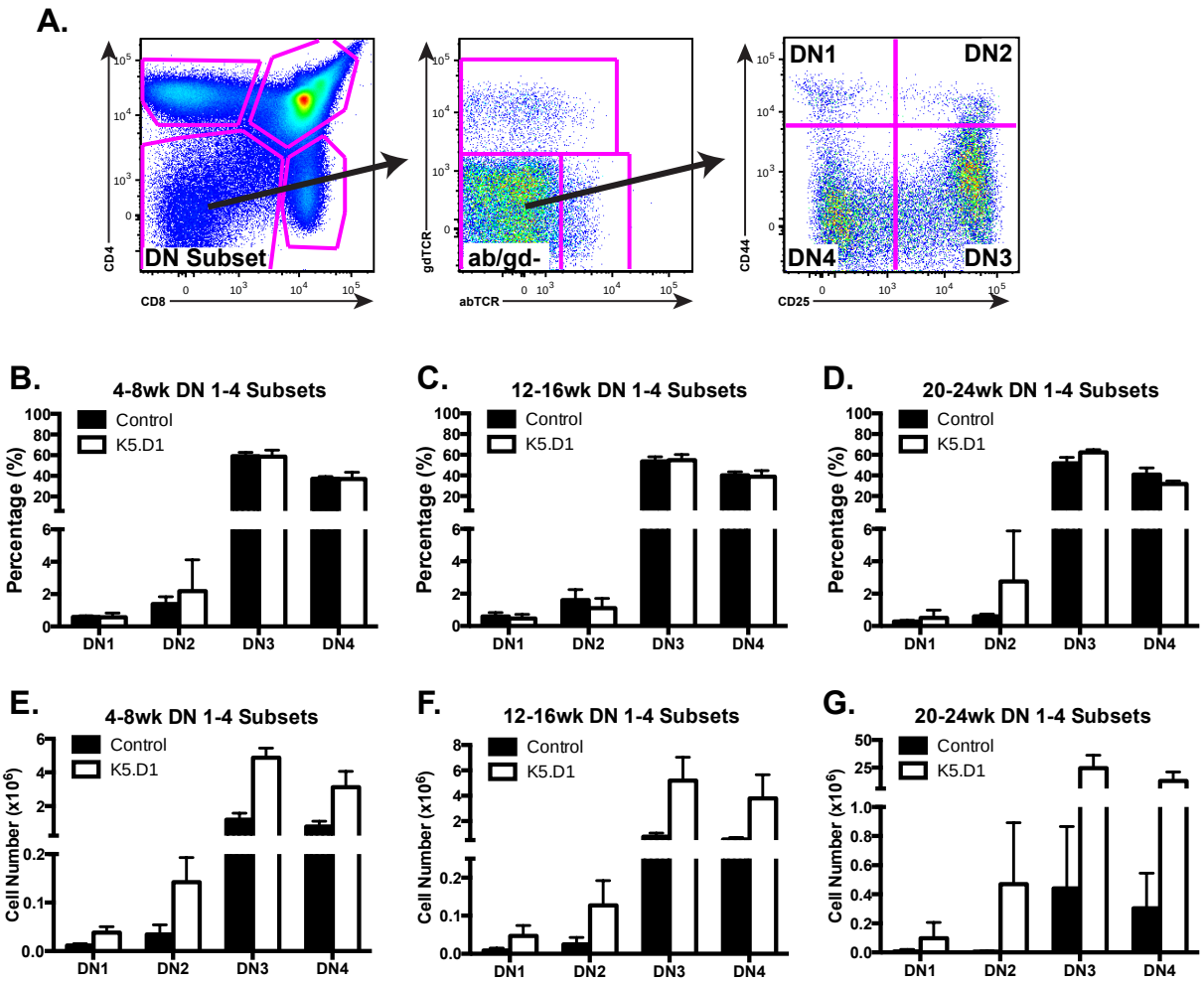
A.
CD4
CD8
DN Subset
gdTCR
abTCR
ab/gd-
CD44
CD25
DN1
DN2
DN4
DN3
B.
4-8wk DN 1-4 Subsets
C.
12-16wk DN 1-4 Subsets
D.
20-24wk DN 1-4 Subsets
E.
4-8wk DN 1-4 Subsets
F.
12-16wk DN 1-4 Subsets
G.
20-24wk DN 1-4 Subsets
Control
K5.D1
Percentage (%)
Cell Number (x10^6)
DN1
DN2
DN3
DN4

**Figure 7. Distribution of DN thymocyte subsets in control and K5.D1 thymi.**

**(A)** Gating scheme and representative dot plots of DN thymocyte subsets. **(B)** Percentage of DN thymocyte subsets at 4-8 weeks **(C)** 12-16 weeks **(D)** 20-24 weeks of age. **(E)** Total cell number of DN thymocyte subsets at 4-8 weeks **(F)** 12-16 weeks **(G)** and 20-24 weeks of age. Data are presented as mean ±SEM and n≥4 for all data.

the dual expression of CD44 and c-kit. Previous work established that the frequency and number of ETPs decline with age in wild type thymi (149). Because the K5.D1 thymus supports increased numbers of developing thymocytes, we questioned whether the size of the ETP population might be increased. To identify ETPs, we gated on αβTCR$^-$ γδTCR$^-$ DN cells that express both CD44 and c-kit, and did not express the DN2 marker CD25 (Figure 8A). In agreement with published reports, both the frequency and number of ETPs declined in control mice with age (Figures 8B-C, (149)). Interestingly, the frequency of ETPs in K5.D1 thymi was not significantly different from controls (Figure 8B). However, the number of ETPs in the K5.D1 thymus was five-fold greater than observed in control mice, and maintained with age (Figure 8C). Therefore, these data support the hypothesis that the increased K5.D1 thymopoiesis stems from an expansion of TEC niches that support ETP survival and differentiation.

*The increased frequency of mature SP thymocytes in K5.D1 thymi is due to accumulation of late maturation stage cells.*

We observed significant increases in CD4 SP and CD8 SP subset frequencies in K5.D1 mice with age (see Figure 6B-D). SP thymocytes are a heterogeneous population consisting of cells at progressive maturation stages that have been defined phenotypically by expression of various surface markers (150). For example, CD69 expression is driven by TCR engagement during positive selection and persists on early, but not late stage SP thymocytes, whereas Qa-2 expression is acquired on late stage SP thymocytes prior to thymic exit. To determine if the increased percentage of SP thymocytes was due to relatively immature or mature SP subsets, we analyzed the frequency of early (CD69$^+$Qa-2$^-$) and late (CD69$^-$Qa-2$^+$) stage CD4 and CD8 SP thymocytes in control and K5.D11 thymi (Figure 9A). The frequency of late stage SP

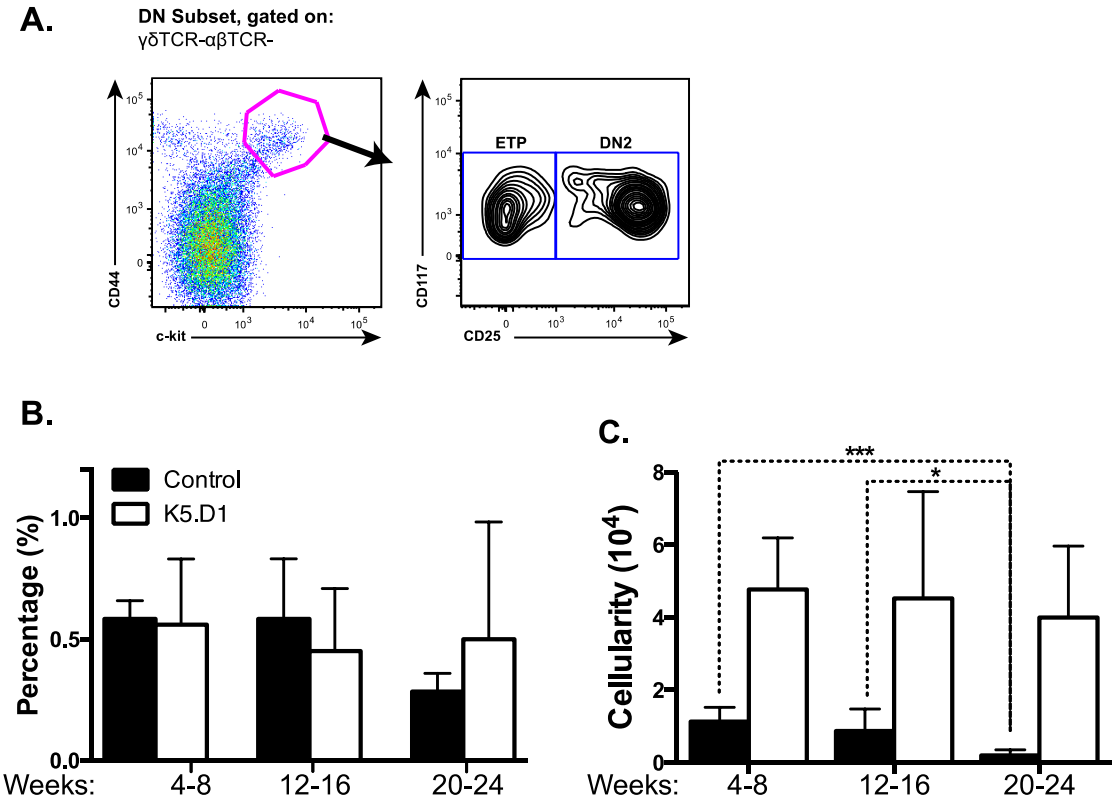
A.
DN Subset, gated on:
γδTCR-αβTCR-
CD44
c-kit
CD117
CD25
ETP
DN2
B.
Control
K5.D1
Percentage (%)
1.0
0.5
0.0
Weeks:
4-8
12-16
20-24
C.
***
*
Cellularity (10^4)
8
6
4
2
0
Weeks:
4-8
12-16
20-24

**Figure 8. The number of ETPs declines with age in control but not in K5.D1 thymi.**

**(A)** Gating scheme to identify ETPs within the thymocyte population. Total thymocytes were gated as $\gamma\delta TCR^{-}\alpha\beta TCR^{-}CD44^{+}CD117^{+}$ subsets, and ETPs were discriminated by $CD25^{-}$ expression. **(B)** Frequency of ETPs in control and K5.D1 with age. **(C)** Number of ETPs in control and K5.D1 with age. Data are presented as mean ±SEM and n≥4 for all data. *P<0.05 and ***P< 0.0001 using an unpaired two-tailed Student T test.

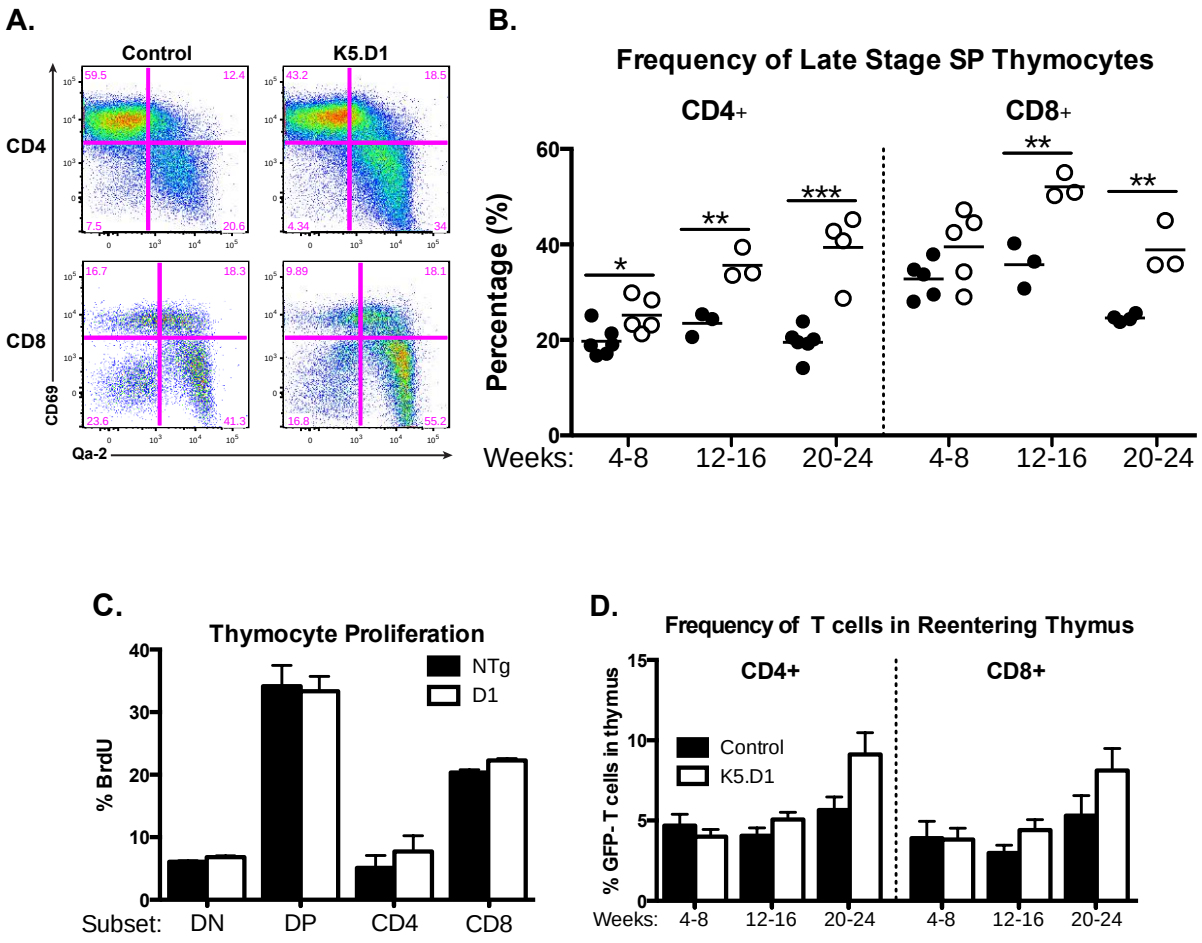
A.
Control
K5.D1
CD4
CD8
CD69
Qa-2
59.5
12.4
7.5
20.6
43.2
18.5
4.34
34
16.7
18.3
23.6
41.3
9.89
18.1
16.8
55.2
B.
Frequency of Late Stage SP Thymocytes
CD4+
CD8+
Percentage (%)
Weeks:
4-8
12-16
20-24
C.
Thymocyte Proliferation
NTg
D1
% BrdU
Subset:
DN
DP
CD4
CD8
D.
Frequency of T cells in Reentering Thymus
CD4+
CD8+
Control
K5.D1
% GFP- T cells in thymus
Weeks:

**Figure 9. SP thymocytes accumulate in the K5.D1 thymus by 12-16 weeks of age.** **(A)** Representative dot plots of early SP thymocytes ($CD69^{+}Qa\text{-}2^{-}$) versus late stage ($CD69^{-}Qa\text{-}2^{+}$) SP thymocyte frequency in control and K5.D1 thymi. **(B)** Scatter graph of the frequency of late stage SP thymocytes with age (n≥3, data from 2+ independent experiments per age group). **(C)** Frequency of BrdU+ thymocytes after 16hr labeling 8-12 week control and K5.D1 thymi (n≥3). **(D)** Frequency of GFP- T cells reentering the CD4 and CD8 SP populations (n≥3). All Bar graphs are represented as mean ±SEM. *P<0.05, **P<0.01, ***P< 0.0001 using an unpaired two-tailed Student T test.

thymocytes does not change appreciably in control mice with age (Figure 9B). However, we observed significant increases of late stage SP thymocytes in K5.D1 thymi with age (Figure 9B).

*Potential mechanisms accounting for the increase in late stage SP thymocytes*

We considered several mechanisms that could explain the increase in late stage SP thymocytes in aged K5.D1 mice. For instance, the increased percentage of late stage SP thymocytes may be due to an increased thymocyte proliferation (Figure 9C). However, we did not observe an increase in the percentage of K5.D1 thymocytes that incorporated BrdU after an overnight pulse. We also considered the possibility that the increased frequency of mature SPs may be due to accumulation of mature peripheral T cells that circulated back into the thymus. To test this possibility, we analyzed the frequency of $GFP^-$ T cells present in the SP thymocytes within RAG2p-GFP control or RAG2p-GFP;K5.D1 transgenic thymi (Figure 9D). While the frequency of recirculating GFP negative cells in the SP thymocyte subsets increased in both control and K5.D1 thymi with age, there was no appreciable difference between these frequencies in aged control and K5.D1. Additionally, the increased frequency of recirculating cells does not account for the increasing size of the SP thymocyte subsets in K5.D1 mice with age.

It is also possible that aberrant selection in the K5.D1 thymic microenvironment could play a role in the altered distribution of thymocyte subsets. We previously examined potential alterations of positive and negative selection in K5.D1 mice using the H-Y TCR transgenic model (135). In this experimental system, all developing thymocytes express a TCR specific for the Y chromosome-encoded male antigen presented by the $H2\text{-}D^b$ MHC molecule. Negative selection deletes these specific thymocytes in male mice, whereas the same TCR transgenic thymocytes undergo

positive selection to become CD8 T cells in female thymi expressing the H2-$D^b$ haplotype. Despite the fact that positive and negative selection appeared normal in H-Y TCR; K5.D1 double transgenic mice, it remained possible that the K5.D1 microenvironment would affect negative or positive selection in non-transgenic thymocytes. However, it is difficult to directly interrogate selection induced by self-peptide/MHC complexes in polyclonal populations. To approach the issue of positive selection, we examined Nur77 expression on DP thymocytes. Nur77 is an immediate early gene upregulated by TCR stimulation. The Nur77-GFP transgene faithfully reports TCR signal strength during thymopoiesis and peripheral T cell stimulation (151). To analyze Nur77 expression on DP thymocytes, we crossed Nur77-GFP transgenic mice with K5.D1 mice, and the double transgenic mice were analyzed for Nur77 expression by flow cytometry to assess TCR activation of DP thymocytes during positive selection (Figure 10A). There was no observed difference in frequency or the mean fluorescence intensity (MFI) of Nur77 expression on DP cells from control or K5.D1 thymi (Figure 10B and 10C). These results suggest that there is no overt defect in positive selection in K5.D1 mice. Additionally, we analyzed CD5 expression as an independent indicator of the strength of TCR engagement (personal communication from KA Hogquist) and confirmed no difference of CD5 expression between control and K5.D1 DP thymocytes (Figure 10D).

Deficient negative selection is another potential explanation for the relative increase in mature SP thymocytes in K5.D1 thymi. To address this possibility, we analyzed CD5 expression on early stage CD4 SP thymocytes identified by the $CD69^+Qa\text{-}2^-$ phenotype. This subset of cells undergoes negative selection by TCR engagement with TRAs presented by mTECs or DCs, and this results in CD5 expression. Low CD5 expression on K5.D1 early CD4 SP thymocytes would suggest

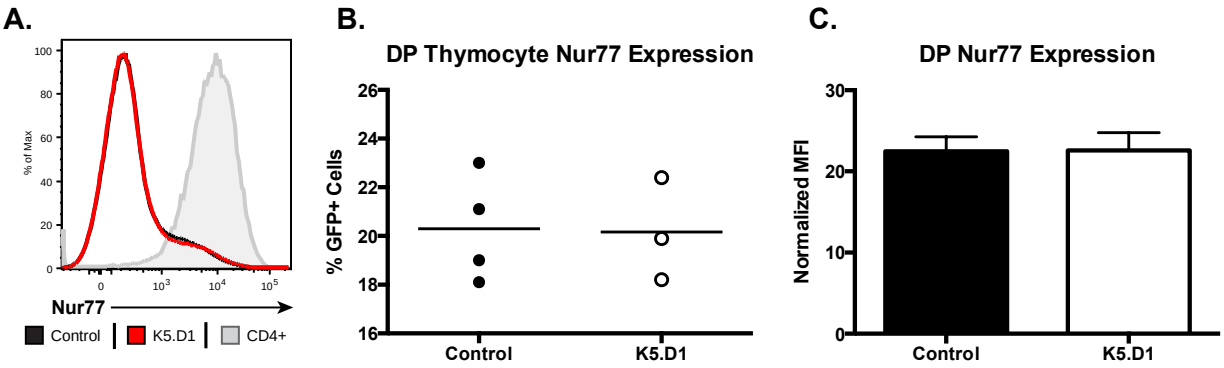
A.
% of Max
Nur77
Control
K5.D1
CD4+
B.
DP Thymocyte Nur77 Expression
% GFP+ Cells
Control
K5.D1
C.
DP Nur77 Expression
Normalized MFI
Control
K5.D1

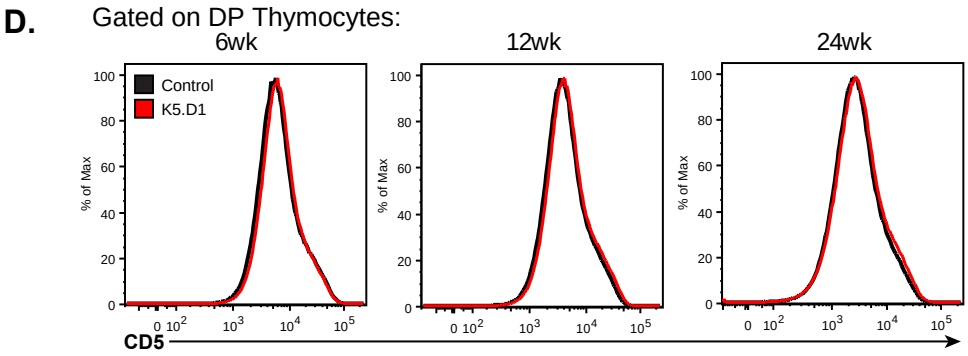
D.
Gated on DP Thymocytes:
6wk
12wk
24wk
Control
K5.D1
% of Max
CD5

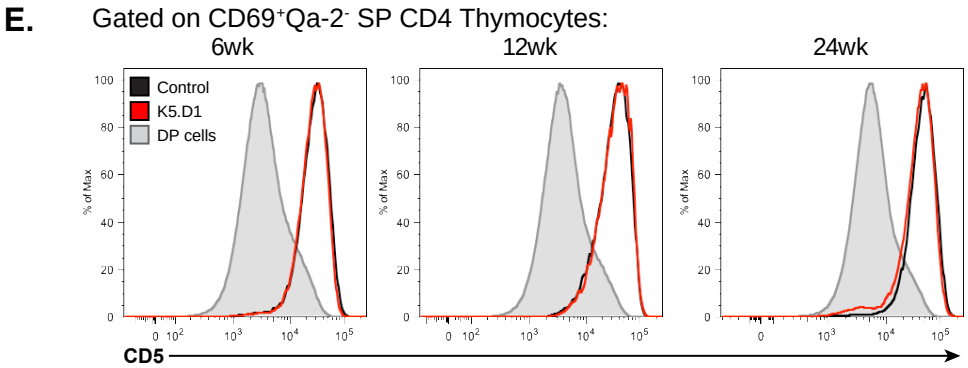
E.
Gated on CD69+Qa-2- SP CD4 Thymocytes:
6wk
12wk
24wk
Control
K5.D1
DP cells
% of Max
CD5

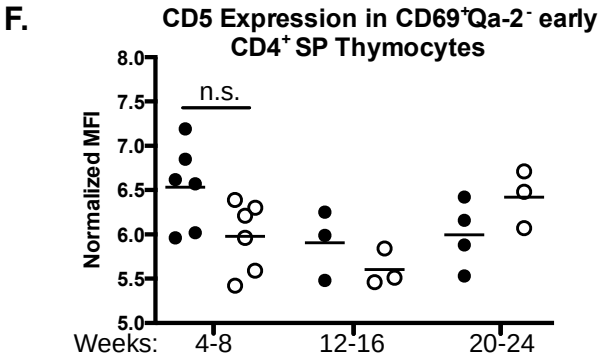
F.
CD5 Expression in CD69+Qa-2- early CD4+ SP Thymocytes
Normalized MFI
n.s.
Weeks:
4-8
12-16
20-24

**Figure 10. Positive and negative selection K5.D1 thymi are comparable to controls.**

**(A)** Representative histogram of Nur77 expression in control and K5.D1 DP thymocytes. **(B)** Frequency of Nur77-GFP$^{+}$ expressing cells in control and K5.D1 DP thymocytes. Data are presented as mean ±SEM and n≥3 for all data. **(C)** Mean fluorescence intensity (MFI) of Nur77-GFP expression in GFP$^{+}$ DP thymocytes from control and K5.D1 thymi. **(D)** Representative histograms of CD5 expression on control and K5.D1 DP thymocytes at 6, 12, and 24 weeks of age. **(E)** CD5 expression on CD4 late stage (CD69$^{-}$Qa-2$^{+}$) thymocytes from control and K5.D1 thymi at 6, 12, and 24 weeks of age.

lower TCR signaling strength and potentially less negative selection in the K5.D1 thymus, whereas increased CD5 expression would suggest higher levels of TCR activation and increased negative selection. However, CD5 expression on K5.D1 early stage SP thymocytes was indistinguishable from expression on thymocytes from control mice (Figure 10D-E). These data suggest that the increased frequency of mature SPs is not a consequence of defective TCR signaling leading to inefficient negative selection. However, other factors such as deficient TRA expression could result in inefficient negative selection. If negative selection were impaired, we would expect an increase in autoimmune symptoms. Therefore, we used several approaches to determine if K5.D1 mice are prone to autoimmunity. First, we treated tissue sections from RAG2$^{-/-}$ skin and kidney with serum from 6-8 month control and K5.D1 mice to assay for the presence of autoantibodies. As a positive control we used CCR7$^{-/-}$ mice, in which negative selection is impaired resulting in the escape of autoreactive T cells and autoantibody production. CCR7$^{-/-}$ serum produced strong immunofluorescence staining on RAG2$^{-/-}$ tissues (Figure 11A, top row). In contrast, serum from K5.D1 mice showed no evidence of increased autoantibodies when compared to serum from control mice (Figure 11A). Histopathological analyses of tissues from 6-8 month old control and K5.D1 mice showed no lymphocyte infiltration in liver, lung, pancreas or extraorbital gland, further suggesting that the K5.D1 microenvironment does not promote autoimmunity (See Appendix 1). However, it remained possible that defective negative selection would generate autoreactive K5.D1 T cells but this potential could be suppressed by repressive influences of Tregs in the K5.D1 environment. To test this premise, we FACS sorted splenic CD4 T cells from control or K5.D1 mice and adoptively transferred them into RAG2$^{-/-}$ recipients that cannot produce T and B cells (Figure 11B). Recipients were weighed every other day for three weeks, and then

**A.**

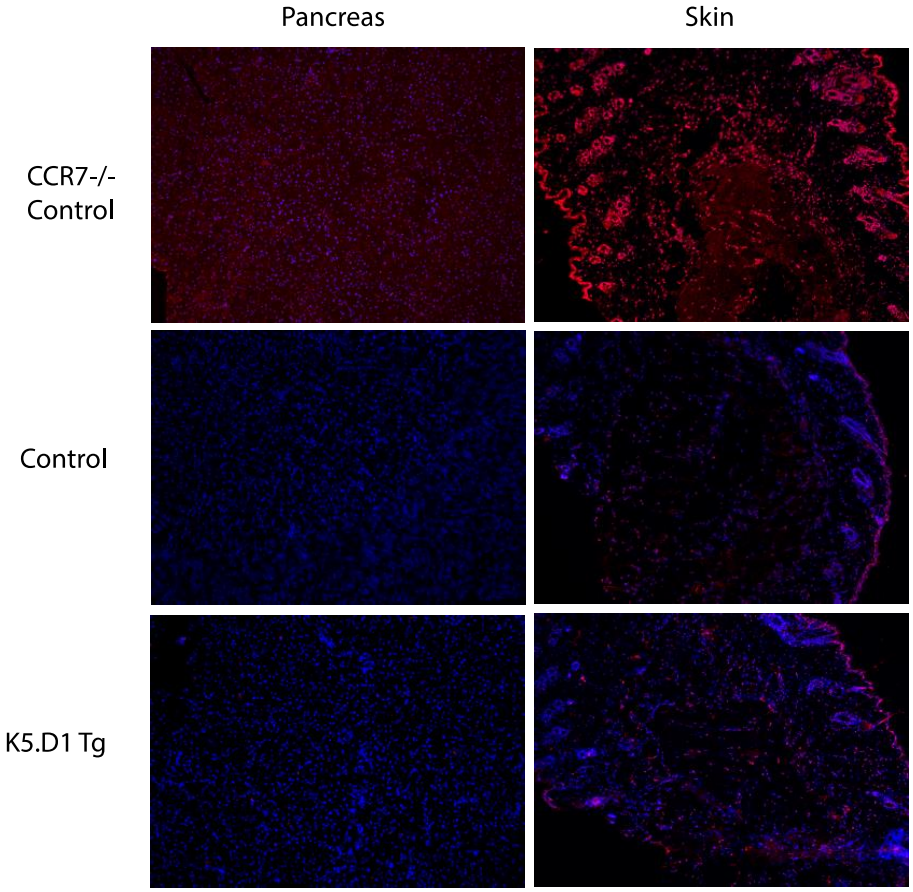
Pancreas
Skin
CCR7-/-
Control
Control
K5.D1 Tg

**B.**

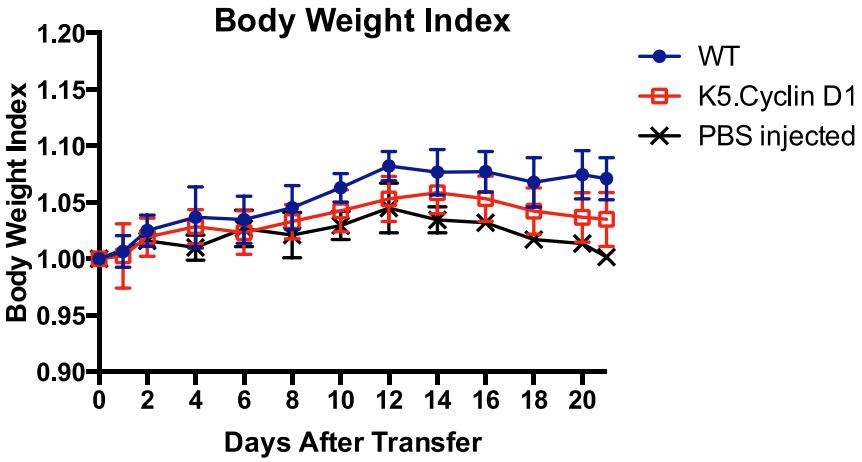
Body Weight Index
Body Weight Index
1.20
1.15
1.10
1.05
1.00
0.95
0.90
0
2
4
6
8
10
12
14
16
18
20
Days After Transfer
WT
K5.Cyclin D1
PBS injected

**Figure 11. K5.D1 T cells do not exhibit autoreactivity when adoptively transferred into RAG2 deficient hosts.** (**A**) IHC images from RAG2-/- tissues stained with sera from K5.D1 or control mice. (**B**) RAG2-/- recipients were injected with sterile PBS or FACS-sorted CD4 T cells (>99% purity) from control or K5.D1 mice and weighed every two days to determine changes in body mass index.

necropsied to determine if the transferred cells generated an autoimmune response in the absence of host regulatory T cells. During this timeframe, recipients given K5.D1 T cells remained healthy and retained body weight indices that were comparable to recipients injected with control CD4 T cells or sterile PBS. Additionally, a blind pathological reading of slides from multiple organs including lung, pancreas, intestines, extraorbital lacrimal and salivary glands did not reveal any lymphocyte infiltrates or other signs of autoreactivity in recipients (Appendix 2). Thus, we conclude that there is no evidence for aberrant central tolerance induction in the K5.D1 thymus and therefore, the accumulation of mature SP thymocytes is unlikely to be due to a defect in negative selection.

Finally, we asked whether the increased frequency of mature SP thymocytes could be due to an accumulation of cells from defective thymic export. Thymic emigration from vessels at the CMJ relies on the expression of S1P1R on thymocytes to follow the S1P cytokine gradient produced by the pericytes lining the vasculature to exit the thymus (42). FACS analysis of S1P1R was not feasible due to poor antibody staining index, which was corroborated by the manufacturer. Instead, we determined whether SP thymocytes were being held up in the perivascular spaces around the vasculature by IHC, which is indicative of defective thymus emigration (42). Paraffin sections of K5.D1 or control littermate thymi at 1, 3 and 6 months of age were stained for CD8, CD31 and ERTR7, which identify CD8 thymocytes, endothelium and epithelial basement membranes, respectively. Surprisingly, there was no accumulation of thymocytes within the perivascular spaces of K5.D1 thymi, regardless of age (Figure 12A). This result suggests that increasing SP thymocyte frequency is not due to emigrating thymocytes held up in perivascular spaces. It is possible that defects prior to entry into the vascular space could affect export. In order to test for this scenario, we

**A.**

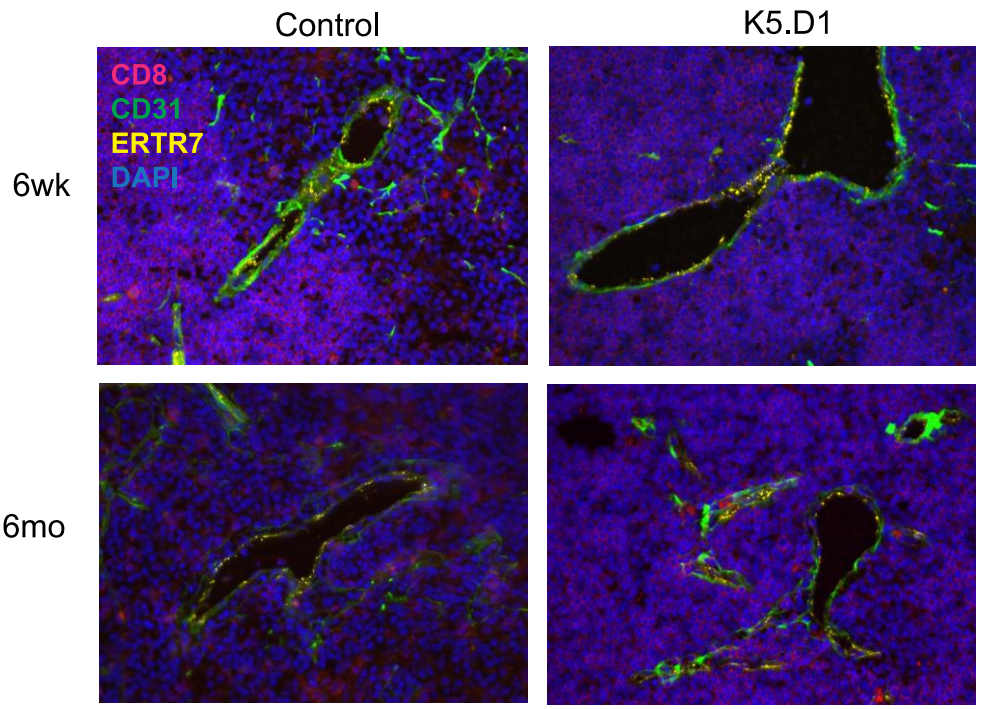
Control
K5.D1
CD8
CD31
ERTR7
DAPI
6wk
6mo

**B.**

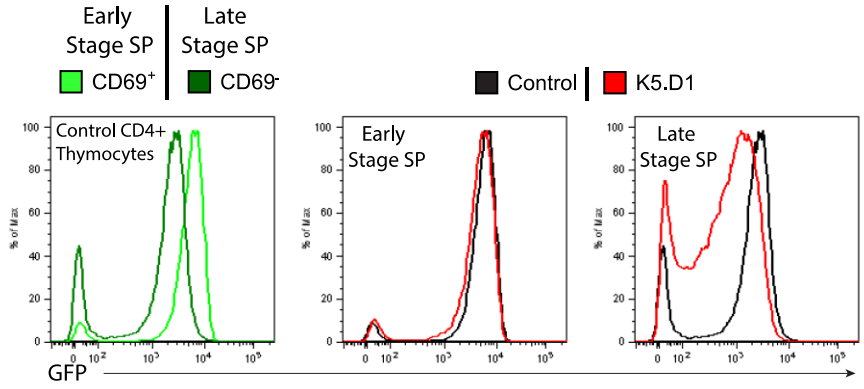
Early Stage SP
CD69+
Late Stage SP
CD69-
Control
K5.D1
Control CD4+ Thymocytes
Early Stage SP
Late Stage SP
% of Max
GFP

**Figure 12. Late stage SP thymocytes do not exhibit defective thymus emigration but experience longer thymus residency than controls**. **(A)** Representative IHC images depicting thymocytes localization around thymus vasculature. **(B)** Representative histograms show GFP expression in early and late stage CD4 SP thymocytes from RAG2p-GFP and K5.D1;RAG2p-GFP mice (data representative of three independent experiments).

analyzed the level of GFP expression in SP thymocytes from K5.D1;RAG2p-GFP thymi and RAG2p-GFP controls. Since the RAG2p-GFP transgene is only expressed during TCR rearrangement, loss of GFP protein in later thymocyte stages can be utilized as a molecular clock to determine the relative rate of thymocyte maturation. To show proof of principle, late stage SP thymocytes exhibit lower levels of GFP than early stage SP thymocytes in control mice (Figure 12B, left histogram). Therefore, we used this scheme to determine if cells were retained in the late stage SP subset. Our data show that K5.D1 early stage SP thymocytes contain similar levels of GFP as control counterparts (Figure 12B, middle histogram). However, late stage SP thymocytes from K5.D1 thymi did contain lower GFP signal (Figure 12B, right histogram). Furthermore, GFP expression was not expressed as a signal peak by histogram, but as a range of GFP intensity implying that many K5.D1 late stage SP thymocytes are retained for a long period of time. Therefore, these results suggest that a delay does exist in the maturation or export of the most mature thymocytes in K5.D1 thymi.

*An increase in thymic K5.D1 Tregs does not equate to increased peripheral Tregs*

The generation of regulatory T cells (Treg) both in the thymus and peripheral tissues is necessary to down modulate the immune response, a process that plays an essential role in preventing autoimmunity. Thymocytes with strong reactivity to self are either deleted or diverted to the Treg developmental program. Because of the expanded thymus size and increased thymopoiesis, we asked if thymic Treg generation was altered in K5.D1 mice. The expression of both CD25 and intracellular Foxp3 identifies CD4 SP mature Treg cells in the thymus (Figure 13A). Using this identification strategy, we have found that there is an increase in both frequency and number of mature Treg cells in the K5.D1 thymus with age (Figure 13B). To determine if there was

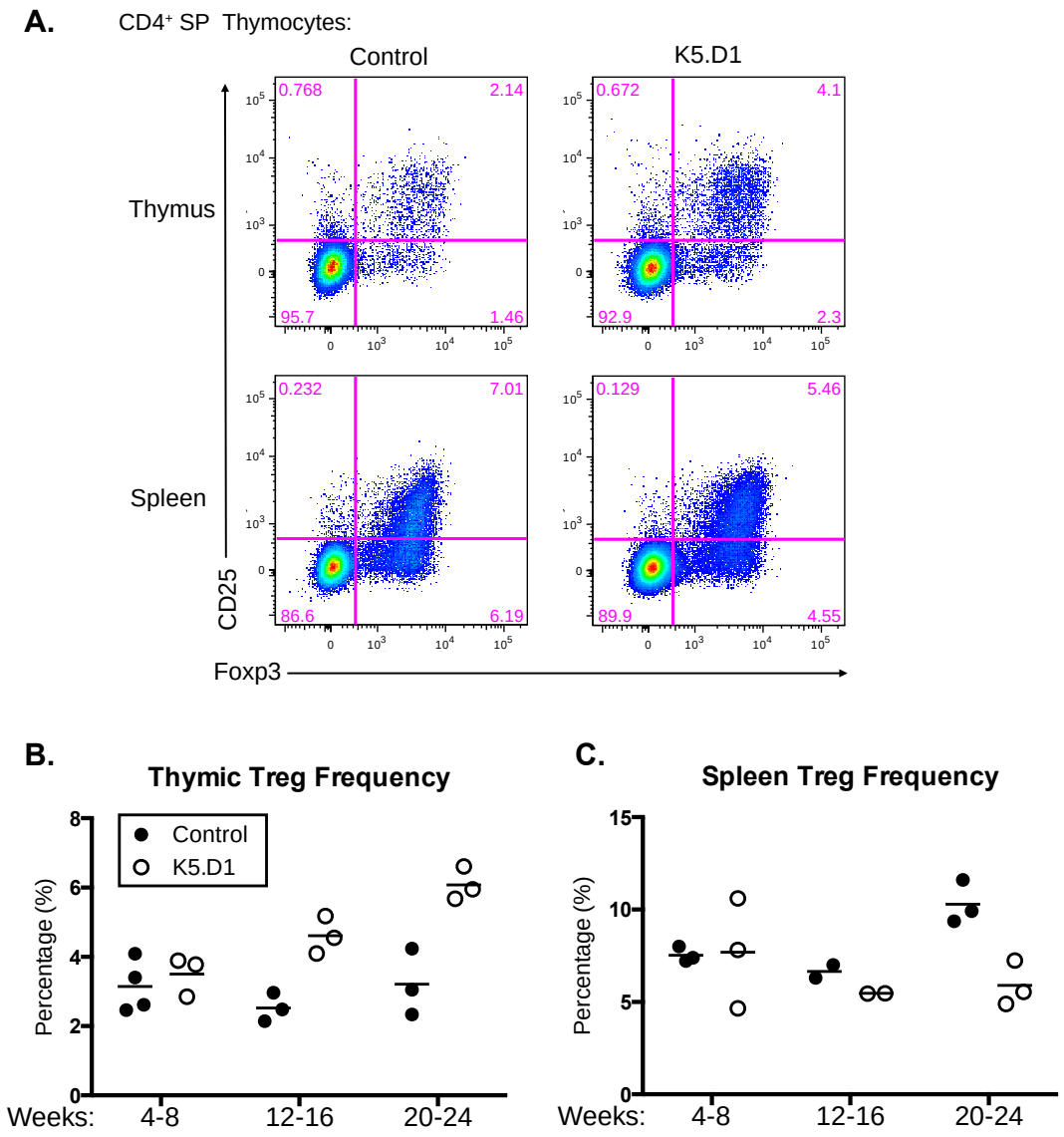
A.
CD4+ SP Thymocytes:
Control
K5.D1
Thymus
Spleen
CD25
Foxp3
0.768
2.14
95.7
1.46
0.672
4.1
92.9
2.3
0.232
7.01
86.6
6.19
0.129
5.46
89.9
4.55
B.
Thymic Treg Frequency
Control
K5.D1
Percentage (%)
Weeks:
4-8
12-16
20-24
C.
Spleen Treg Frequency
Percentage (%)
Weeks:
4-8
12-16
20-24

**Figure 13. The frequency of Tregs is increased in K5.D1 thymi but not in the peripheral T cell pool.** (**A**) Representative dot plots of $CD25^{+}Foxp3^{+}$ Treg thymocytes and splenocytes from control and K5.D1 mice. (**B**) Scatter graph of the % of Tregs in thymocytes (**C**) Scatter graph of the % of Tregs in splenic T cells. Note that thymic Treg frequency is significantly increased in K5.D1 mice, yet splenic Treg frequency is not significantly altered (**C**). **P<0.001 for bracketed values using an unpaired Student's T test.

a corresponding increase in peripheral Treg cells, we analyzed the frequency of mature Treg cells within the splenic CD4 T cell population. The data show that the frequency of peripheral Tregs in K5.D1 spleens remained comparable to controls, and was not influenced by increased Treg frequency in K5.D1 thymi (Figure 13C).

### 3.3 Discussion

Taken together, our data indicate that robust thymopoiesis is supported and increased by expansion of the TEC compartment in aging K5.D1 thymi. Recently, TEC-specific deletion of Retinoblastoma (Rb) family genes was shown to prevent thymic involution and cause thymus expansion similar to the phenotype in K5.D1 mice. Rb family members regulate cell cycle progression and gene expression by binding and inhibiting E2F transcription factors (152). Rb conditional knockout TECs had increased E2F3 activity, which in turn increased Foxn1 expression. The similarities in the K5.D1 transgenic and Rb inactivation models strongly suggest that the CyclinD1-Rb axis is critical for maintaining the TEC compartment and can be manipulated to prevent thymus involution.

The increased TEC niches within the K5.D1 thymus support survival and differentiation of a larger population of ETPs. In fact, we observed a 5-fold increase in ETP number that was maintained with age in K5.D1 thymi. Our results suggest that the decline of ETP numbers with age is secondary to the degeneration of the TEC compartment. Since thymopoiesis relies on ETPs to establish and maintain the developing thymocyte population, the ramifications of involution on the entire thymocyte pool are evident even in early thymus involution. Furthermore, avoiding involution by the K5.D1 transgene increases the size of the developing thymocyte population, thus exemplifying the importance of the TEC microenvironment for thymocyte development.

Stringent positive and negative selection occurs in the K5.D1 thymus, owing to the maintenance of the TEC microenvironment. As evidenced by TCR engagement studies and T cell transfers into immunocompromised mice, developing thymocytes in the K5.D1 thymus are self-restricted and self-tolerant. Moreover, T cells derived from the K5.D1 thymus do not impose autoreactivity on peripheral tissues. These results show that maintaining the thymic architecture is central to the continued output of protective T cells with age.

We observed the increasing frequency of SP thymocytes with age in K5.D1 thymi. Several explanations including increased thymocyte proliferation, delayed thymocyte maturation or perivascular retention failed to explain our observations. Furthermore, SP thymocytes specifically accumulated during the last stage of thymocyte maturation, but were not crowded around the vasculature. Aberrant expression of CD62L necessary for export was not found in the accumulating cells. Thus, the mechanism for this retention remains unclear, but appears to relate in some manner to organ size.

Finally, we observed that the frequency of thymic Tregs significantly increases with age. A recent report showed that peripheral Tregs increasingly recirculate through the thymus with age to inhibit continued Treg generation (153). Unfortunately we cannot definitively state whether the increased frequency of thymic Tregs is due to increased generation or recirculation. However, the frequency of thymic Tregs did not influence the frequency of peripheral Tregs, which suggests that the thymic Treg phenotype is organ-specific.

Taken together, the data in this chapter suggest that thymocyte development in K5.D1 thymi results in increased production of self-tolerant T cells.

# CHAPTER FOUR

# ALTERATIONS TO THE PERIPHERAL T CELL POOL ARE PRECIPITATED BY EARLY THYMUS INVOLUTION

## 4.1 Introduction

The distribution of naïve and memory T cells is severely altered by the decline in naïve T cell output from involuted thymi as well as by life-long antigenic stimulation (Reviewed in (154)). Age-associated changes in the T cell pool are blatant by old age, including the decline of naïve T cell numbers, naïve T cell exhaustion, and increasing memory T cell frequency. The reduction in naïve T cells restricts TCR repertoire diversity, which results in deficient responses to new antigens (5, 112, 134, 155, 156). Therefore, the aging process decreases the capability of the T cell pool to protect against infectious diseases and cancer and is associated with an increased incidence of autoimmunity.

Thymus involution is the major factor responsible for the age-associated decline in naïve T cells. There are a few reports that investigate T cell output during the entire lifespan or chronicle peripheral T cell changes as a result of natural aging (4, 5, 155, 157). However, studies investigating the population dynamics of naïve and memory T cells with age have failed to consider the ramifications of early thymus involution on this process. Furthermore, it has been suggested that preventing thymus involution will preclude the age-associated changes in the T cell pool, including the shift in naïve and memory representation, defects in T cell function and reduced TCR repertoire diversity. To address these points, we analyzed the distribution of naïve and memory T cells during early stages of thymus involution in wildtype mice up to 24 weeks of age. We also performed comparative analyses of these parameters in K5.D1 transgenic mice

that do not undergo thymus involution. To distinguish RTEs from MN T cells in the naïve T cell pool, we used RAG2-pGFP transgenic mice that did or did not express the K5.D1 transgene. In addition to analyzing phenotypic parameters, we also determined the functional potential of naïve T cells in nontransgenic and K5.D1 transgenic mice as a function of age.

## 4.2 Results

*Sustained thymopoiesis in K5.D1 mice prevents loss of naïve T cells during aging*

The majority of studies determining the influence of thymus size and output on the T cell pool utilize mice more than three months of age for a young time point and aged mice over a year old as comparators (4, 5, 155, 157). However, early thymus involution is apparent from the significant decrease in organ size and cellularity by 12-16 weeks of age in control mice (Figure 14A). Therefore, we posed two separate questions: First, we asked whether declining thymopoiesis during early thymus involution (12-24 weeks of age) affected the size of the peripheral T cell pool. Additionally, we questioned whether preventing early involution would affect the composition of the T cell pool. Splenic cellularity remained consistently at ~50 x $10^6$ in control mice up to 24 weeks of age (Figure 14B). However, K5.D1 splenic cell number significantly increased ($p=0.0008$) by 12-16 weeks of age, and was sustained at 20-24 weeks of age. Intriguingly, increased K5.D1 splenic cellularity did not mirror the extreme increase of thymic cell numbers observed with age. This result is consistent with previous studies showing that a peripheral homeostatic mechanism maintains a relatively constant number of total peripheral T cells (158). The modest increase in splenic cellularity in K5.D1 mice was due solely to a three-fold increase in T cell

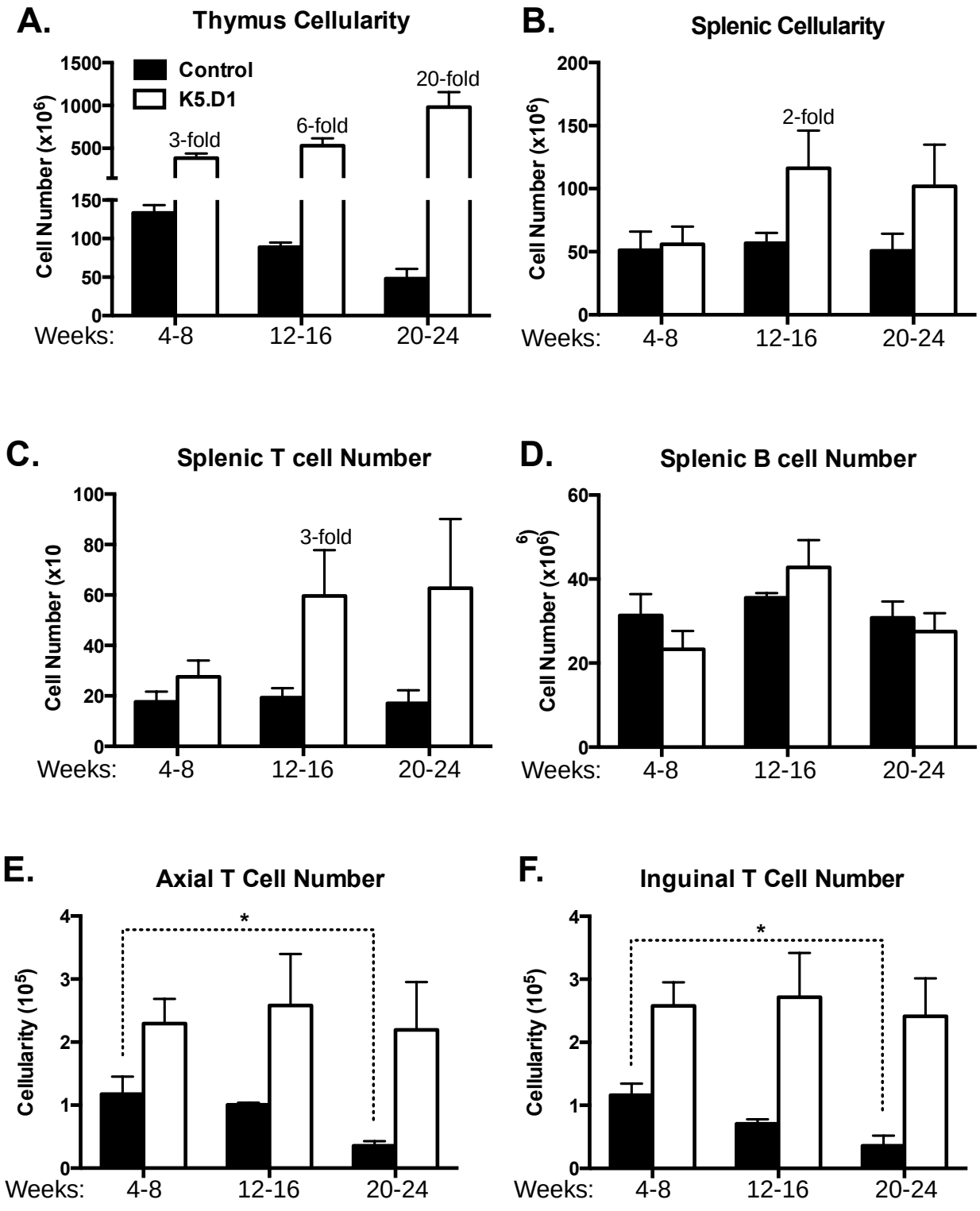
A.
Thymus Cellularity
Control
K5.D1
3-fold
6-fold
20-fold
Cell Number (x10^6)
Weeks:
4-8
12-16
20-24
B.
Splenic Cellularity
2-fold
C.
Splenic T cell Number
3-fold
D.
Splenic B cell Number
E.
Axial T Cell Number
Cellularity (10^5)
*
F.
Inguinal T Cell Number

**Figure 14. Preventing thymus involution in K5.D1 mice increases the size of the peripheral T cell pool.**

(**A**) Thymus cellularity in control and K5.D1 mice with age. (**B**) Splenic cellularity is increased in K5.D1 mice. (**C**) Increased splenic cellularity is due solely to increased T cell numbers in K5.D1 mice. (**D**) Increased splenic numbers are not due to increased B cell numbers. (**E**) T cell numbers decline in control mice in the axial and (**F**) inguinal lymph nodes with age, whereas cell numbers remain inflated in K5.D1 mice with age. n≥3 for all data, *P<0.05 using a two-tailed Student T test.

numbers (Figure 14C). The number of splenic B cells was comparable in control and K5.D1 mice (Figure 14D).

The secondary lymphoid organs (SLO) include lymph nodes throughout the body as well as the spleen. We analyzed the number and frequency of T cells in the control and K5.D1 axial and inguinal lymph nodes to determine if the splenic phenotypes observed in control and K5.D1 spleens were mirrored in other SLO. T cell numbers decreased with age in both lymph node sites in control animals (Figure 14E-F) whereas the increased numbers of T cells in K5.D1 mice were maintained during aging. These results demonstrate that even in young mice, the initial stages of thymus involution drive the reduction of T cell numbers in the spleen and lymph nodes. In contrast, peripheral T cell numbers are elevated in K5.D1 mice. However, the increased cellularity is not altered by aging, and is instead maintained at a relatively constant cellularity up to 24 weeks of age. This result suggests that the T cell numbers are at maximal capacity in K5.D1 SLO.

*Early thymus involution is associated with decreased frequency and number of naïve CD4 T cells and a corresponding increase in memory T cells.*

The helper CD4 T cell population is comprised of both naïve and memory subsets that decrease and increase, respectively, with age. Severe thymus involution in mice one year or older is associated with a skewed frequency of naïve and memory T cells. We asked whether early stages of involution also compromise the composition of the T cell pool in young individuals. To determine the impact of early thymus involution on the distribution of naïve and memory CD4 T cells, we used flow cytometry to identify memory T cells by $CD44^{+}CD62L^{-}$ expression and naïve T cells by $CD44^{-}CD62L^{+}$ expression (Figure 15A). There was a striking decline in the frequency of naïve T cells

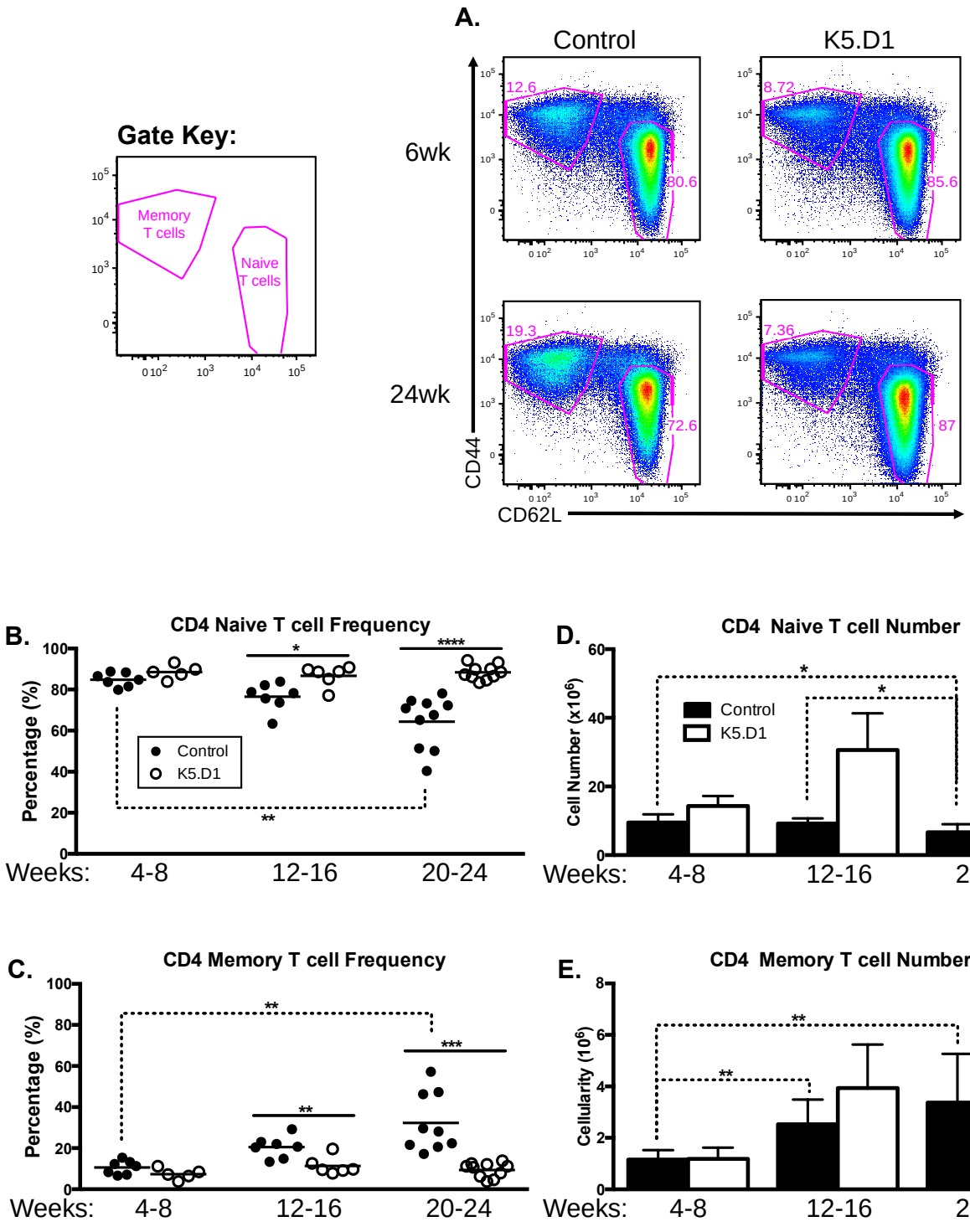
A.
Gate Key:
Memory T cells
Naive T cells
Control
K5.D1
6wk
24wk
12.6
80.6
8.72
85.6
19.3
72.6
7.36
87
CD44
CD62L
B.
CD4 Naive T cell Frequency
Percentage (%)
Control
K5.D1
Weeks: 4-8 12-16 20-24
D.
CD4 Naive T cell Number
Cell Number (x10^6)
Control
K5.D1
Weeks: 4-8 12-16 20-24
C.
CD4 Memory T cell Frequency
Percentage (%)
Weeks: 4-8 12-16 20-24
E.
CD4 Memory T cell Number
Cellularity (10^6)
Weeks: 4-8 12-16 20-24

**Figure 15. Thymus involution alters the distribution of naïve and memory T cells in splenic CD4 T cells.**

(**A**) Representative FACS plots of naïve ($CD44^{-}CD62L^{+}$) and memory ($CD44^{+}CD62L^{-}$) CD4 T cells from 6wk and 24wk control and K5.D1 mice. (**B**) Frequency of naïve $CD4^{+}$ splenic T cells in control and K5.D1 mice with age (**C**) memory T cell frequency increases. (**D**) $CD4^{+}$ naïve T cell number decline significantly in control mice as a result of thymus involution, whereas K5.D1 naïve T cell number increases. (**E**) Memory T cell numbers increase with age in both control and K5.D1 mice. n≥5 for all data, *P<0.05, **P<0.01, ***P< 0.0001 ****P,0.00001 using a two-tailed Student T test.

in control mice with age (Figure 15B), which was accompanied by a corresponding increase in the frequency of memory T cells (Figures 15C). In contrast, there was no change in the frequency of naïve and memory T cells in the K5.D1 T cell pool. Cellularity data revealed a significant decline in the number of naïve T cells (Figure 15D) in control mice, coupled with a significant increase in the number of memory T cells. On the other hand, K5.D1 naïve T cell numbers increase three-fold by 12-16 weeks of age, plateauing by 20-24 weeks of age (Figure 15D). However, the increase in naïve T cell numbers does not affect the generation of memory T cells in K5.D1 mice (Figure 15E). The independent changes in naïve and memory T cell numbers strongly supports the notion that naïve and memory T cells occupy distinct niches. This concept is consistent with the fact that homeostasis of naïve and memory populations are regulated by different cytokines (109, 159). Taken together these results demonstrate that early thymus involution in control mice significantly reduces the cellularity of the naïve T cell compartment and expands the memory T cell compartment. In contrast, the absence of thymus involution in K5.D1 mice prevents the loss of naïve T cells and maintains a relatively constant naïve to memory T cell ratio.

*Early thymus involution is associated with decreased frequency of naïve CD8 T cells and a corresponding increase in memory T cells.*

The frequency of naïve and memory T cells in the CD8 population is driven toward memory T cell dominancy by the reduction of naïve T cells due to reduced thymic output and to expansion of memory T cells. We questioned whether early stages of involution compromise the composition of the T cell pool in young mice. To test this, we turned again to flow cytometry to identify naïve and memory CD8 T cell subsets (Figure 16A). Similar to the CD4 population, naïve T cells in the CD8 population are identified

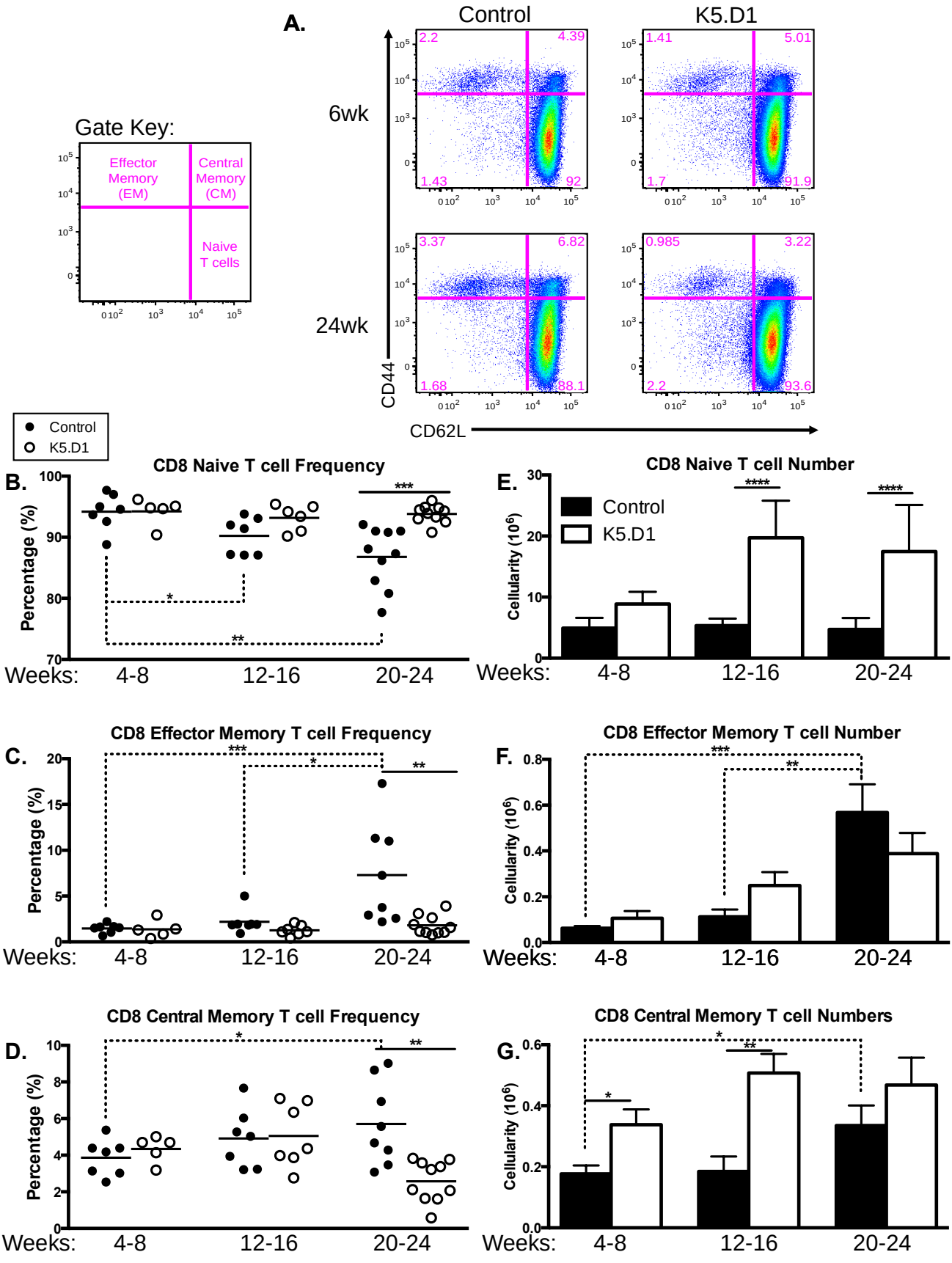
A.
Control
K5.D1
6wk
24wk
CD44
CD62L
Gate Key:
Effector Memory (EM)
Central Memory (CM)
Naive T cells
2.2
4.39
1.43
92
1.41
5.01
1.7
91.9
3.37
6.82
1.68
88.1
0.985
3.22
2.2
93.6
Control
K5.D1
B.
CD8 Naive T cell Frequency
Percentage (%)
Weeks: 4-8 12-16 20-24
E.
CD8 Naive T cell Number
Cellularity (10^6)
Control
K5.D1
Weeks: 4-8 12-16 20-24
C.
CD8 Effector Memory T cell Frequency
Percentage (%)
Weeks: 4-8 12-16 20-24
F.
CD8 Effector Memory T cell Number
Cellularity (10^6)
Weeks: 4-8 12-16 20-24
D.
CD8 Central Memory T cell Frequency
Percentage (%)
Weeks: 4-8 12-16 20-24
G.
CD8 Central Memory T cell Numbers
Cellularity (10^6)
Weeks: 4-8 12-16 20-24

**Figure 16. Thymus involution alters the distribution of naïve and memory T cells in splenic CD8 T cells.**

(**A**) Representative FACS plots of naïve ($CD44^{-}CD62L^{+}$), effector memory ($CD44^{+}CD62L^{-}$) and central memory ($CD44^{+}CD62L^{+}$) CD8 T cells from 6wk and 24wk control and K5.D1 mice. (**B**) The frequency of naïve CD8 splenic T cells decline with age in control mice while (**C**) effector memory and (**D**) central memory T cell frequency increases. (**E**) CD8 naïve T cell numbers remain constant in control mice up to 24 weeks of age, whereas K5.D1 naïve T cell number increase. (**F**) Effector memory T cell numbers in both control and K5.D1 mice. (**G**) Central memory T cell numbers in control mice and K5.D1 mice with age. n≥5 for all data, *P<0.05, **P<0.01, ***P< 0.0001 ****P,0.00001 using a two-tailed Student T test.

by $CD44^{-}CD62L^{+}$ expression. However, the CD8 memory subset is comprised of two easily distinguishable types of T cells that exert separate responses upon reinfection (160). Effector memory (EM) T cells are typically found in the spleen and peripheral tissues after an immune response and are identified by $CD44^{+}CD62L^{-}$ expression. Central memory (CM) T cells, on the other hand, usually home to the lymph nodes and identified by $CD44^{+}CD62L^{+}$ expression (111).

We analyzed the frequency and number of naïve, EM and CM T cells in the CD8 T cell population. The frequency of CD8 naïve T cells in control mice declined significantly with age (Figure 16B), which was accompanied by a corresponding increase in the frequency of both EM and CM T cells (Figures 16C and 16D). In contrast, there was no loss of naïve or increase in memory T cell frequency in the K5.D1 CD8 T cell population (Figure 16B and 16C). Cellularity data revealed sustained numbers of CD8 naïve T cells (Figure 16E) in control mice. This result was not unexpected, as multiple groups have demonstrated that CD8 naïve T cell numbers do not decline until at least 8 months of age in mice (156, 161, 162). Furthermore, we observed a significant increase in the number of both EM and CM T cells with age in control mice (Figure 16F and 16G). In contrast, K5.D1 naïve T cell numbers increased at least three-fold by 12-16 weeks of age and plateaued thereafter (Figure 16E). However, the increase in naïve T cell numbers does not impede the expansion of EM or CM T cells in K5.D1 mice (Figure 16F and 16G). We did note increased numbers of K5.D1 CM T cells at 4-8 and 12-16 weeks of age in the CD8 population compared to controls. However, this change was corrected at 20-24 weeks, such that K5.D1 and control CM numbers were not significantly different at this age. Thus, the independent changes in naïve and memory CD8 T cell numbers further support speculation that naïve and memory T cells reside in distinct niches. Together with our CD4 T cell data,

these results demonstrate that early thymus involution in control mice significantly reduces the frequency of the naïve T cell compartment and expands the memory T cell compartment. In contrast, the absence of thymus involution in K5.D1 mice maintains increased naïve T cell numbers that do not impact the expansion of CD8 memory T cell subsets.

Requirements for T cell entry to the spleen are not as stringent as entry requirements to the lymph nodes, which rely on CD62L and CCR7 expression for migration into lymph node bodies (163, 164). To confirm that the CD4 and CD8 changes were not isolated to the splenic T cell population, we assayed the frequency of naïve and memory T cells in the lymph nodes. Control mice displayed a loss of naïve T cell frequency in the axial lymph nodes along with memory generation that was similar to changes observed in the spleen (Figure 17). In contrast, K5.D1 lymph nodes exhibited no change in the frequency of naïve or memory T cells with age. Analysis of naïve and memory populations in inguinal lymph nodes yielded similar results (data not shown). Therefore, we conclude that early thymus involution drives significant decline of naïve T cell frequency and number coupled with increasing memory T cell frequency and number in SLOs. These novel findings demonstrate that early thymus involution is the precipitating factor behind age-associated changes in the peripheral T cell pool.

*K5.D1 thymi sustain RTE output preventing a decline in MN T cells with age*

The naïve T cell pool consists of phenotypically and functionally heterogeneous cells due to the presence of both RTEs and mature naïve (MN) T cells. RTEs must migrate into SLOs to undergo phenotypic and functional maturation to antigen responsive MN T cells. Continual RTE output from the young thymus not only maintains the size of the naive T cell pool, but also maintains TCR repertoire diversity

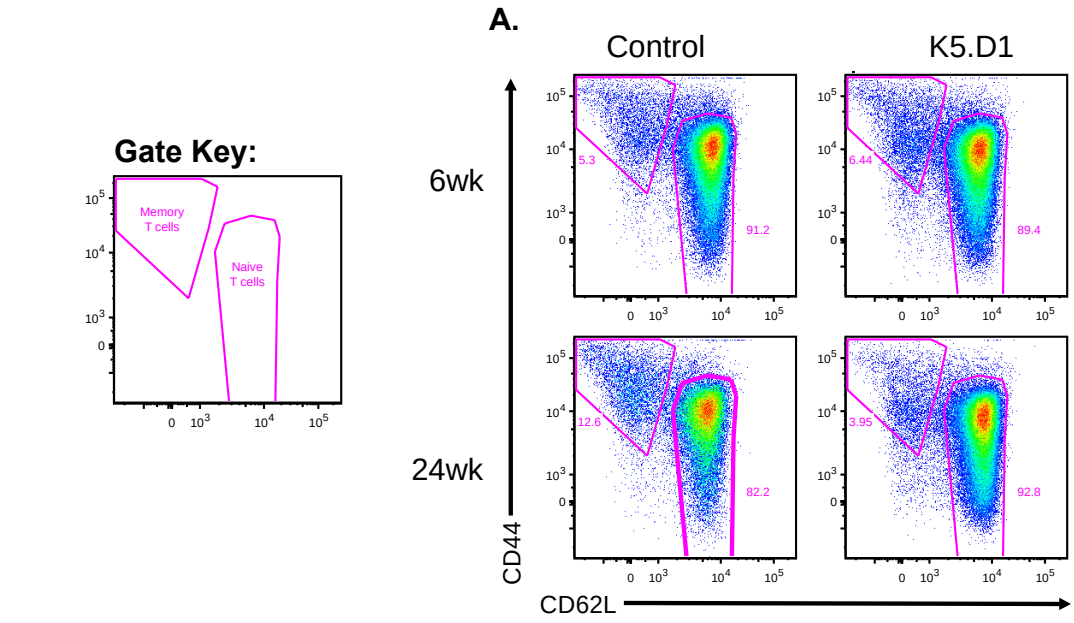
A.
Gate Key:
Memory T cells
Naive T cells
Control
K5.D1
6wk
24wk
CD44
CD62L
5.3
91.2
6.44
89.4
12.6
82.2
3.95
92.8

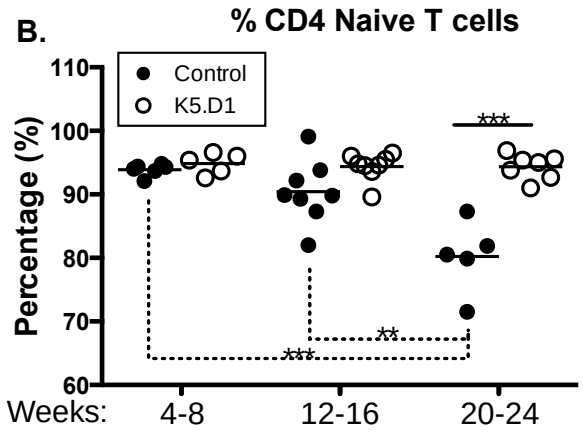
B.
% CD4 Naive T cells
Control
K5.D1
Percentage (%)
Weeks:
4-8
12-16
20-24

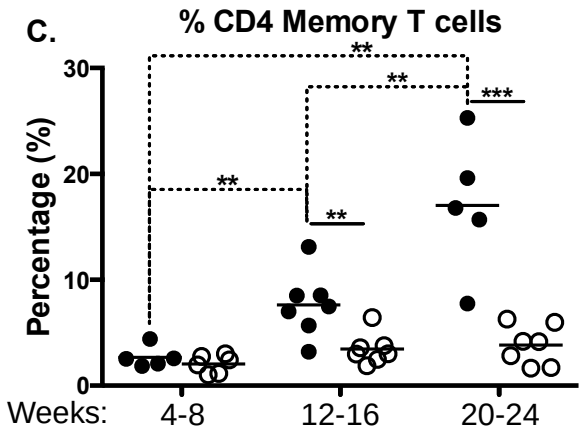
C.
% CD4 Memory T cells
Percentage (%)
Weeks:
4-8
12-16
20-24

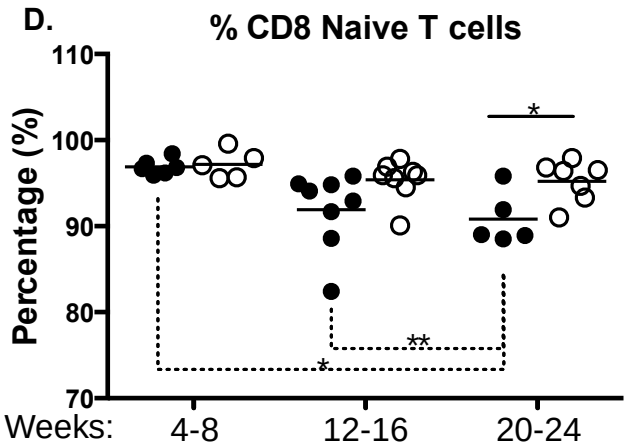
D.
% CD8 Naive T cells
Percentage (%)
Weeks:
4-8
12-16
20-24

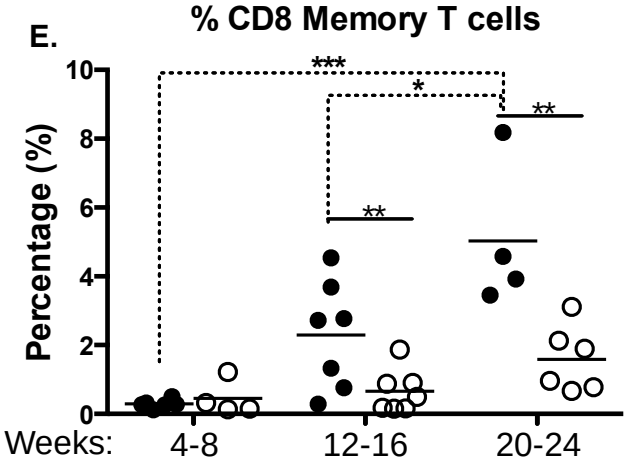
E.
% CD8 Memory T cells
Percentage (%)
Weeks:
4-8
12-16
20-24

**Figure 17. Thymus involution alters the distribution of naïve and memory T cells in lymph nodes.**

(**A**) Representative FACS plots of naïve ($CD44^{-}CD62L^{+}$) and memory ($CD44^{+}CD62L^{-}$) CD4 T cells from 6wk and 24wk control and K5.D1 mice. (**B**) Naïve and (**C**) memory T cell frequency from the CD4 T cell population. (**D**) Naïve and (**E**) memory T cell frequency from the CD8 T cell population. n≥3, *P<0.05 using a two-tailed Student T test.

needed for robust primary T cell responses. However, the number of RTEs produced by the thymus declines during thymus involution (72) To determine if preventing thymus involution sustains the number of RTE and MN T cells during aging, we compared the composition of the naïve T cell pool in control and K5.D1 mice. To identify the RTE and MN T cell subsets, we bred the RAG2p-GFP transgene onto the K5.D1 background to identify RTEs in K5.D1 transgenic and non-transgenic littermates by GFP labeling (Figure 18A). The RAG2p-GFP transgene identifies RTEs released from the thymus within one week of analysis ($GFP^{hi}$), RTEs that have resided for one to three weeks in the periphery ($GFP^{lo}$) and mature naïve (MN) T cells ($GFP^{neg}$) that have resided in the periphery for three or more weeks (Figure 18B). Electronic gates for these subsets were established in CD4 and CD8 splenic naïve T cell subsets. The $GFP^{hi}$ gate was set using SP thymocytes, since all cells in this subset were recently labeled with GFP during the DP stage and indicate the brightest $GFP^{+}$ cells (Figure 18B).

Analysis of GFP expression in naïve CD4 T cells from control mice revealed that the frequency of $GFP^{hi}$ and $GFP^{lo}$ RTEs declines during early involution (Figure 19A-C), whereas MN T cell frequency increases with age (Figure 19D). Furthermore, the absolute number of RTEs also declines, which in turn results in a significant decrease of MN T cells by 20-24 weeks of age (Figure 19E-G). Since MN T cells are required to mount T cell responses to new antigens, these data suggest that even early stages of thymus involution may negatively affect the quality of primary immune responses. However, in the absence of thymus involution in K5.D1 thymi, RTE output does not decline (Figure 19A-C). Instead, the number of RTEs and MN T cells increases between 4-8 and 12-16 weeks of age and is sustained thereafter (Figure 19E-G). Nevertheless, we noted that the frequency of MN T cells is lower than that of RTEs, whereas the reverse is true in controls. This suggests that T cells are lost during

**A.**

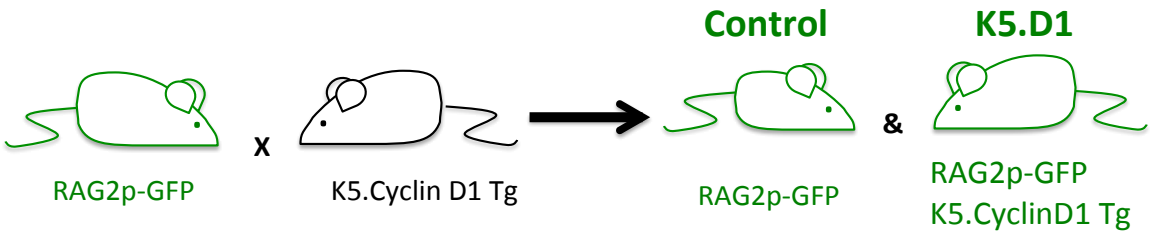
Control
K5.D1
RAG2p-GFP
x
K5.Cyclin D1 Tg
RAG2p-GFP
&
RAG2p-GFP
K5.CyclinD1 Tg

**B.**

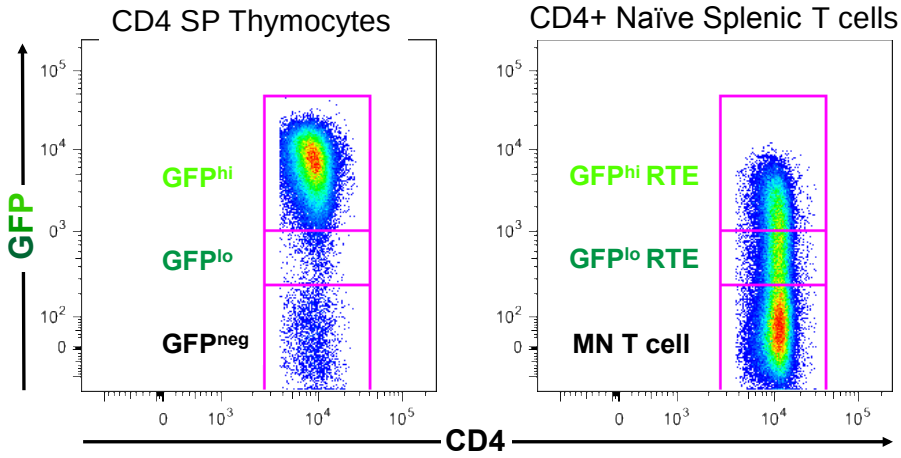
CD4 SP Thymocytes
CD4+ Naïve Splenic T cells
GFP
GFPhi
GFPlo
GFPneg
GFPhi RTE
GFPlo RTE
MN T cell
CD4

**Figure 18. Identification of RTEs and MN T cells in RAG2p-GFP transgenic mice.** (**A**) Breeding scheme to generate Control and K5.D1 mice. (**B**) Gating scheme to define $GFP^{hi}$ $GFP^{lo}$ and $GFP^{neg}$ T cell subsets in the spleen is determined by GFP signal intensity in SP thymocytes.

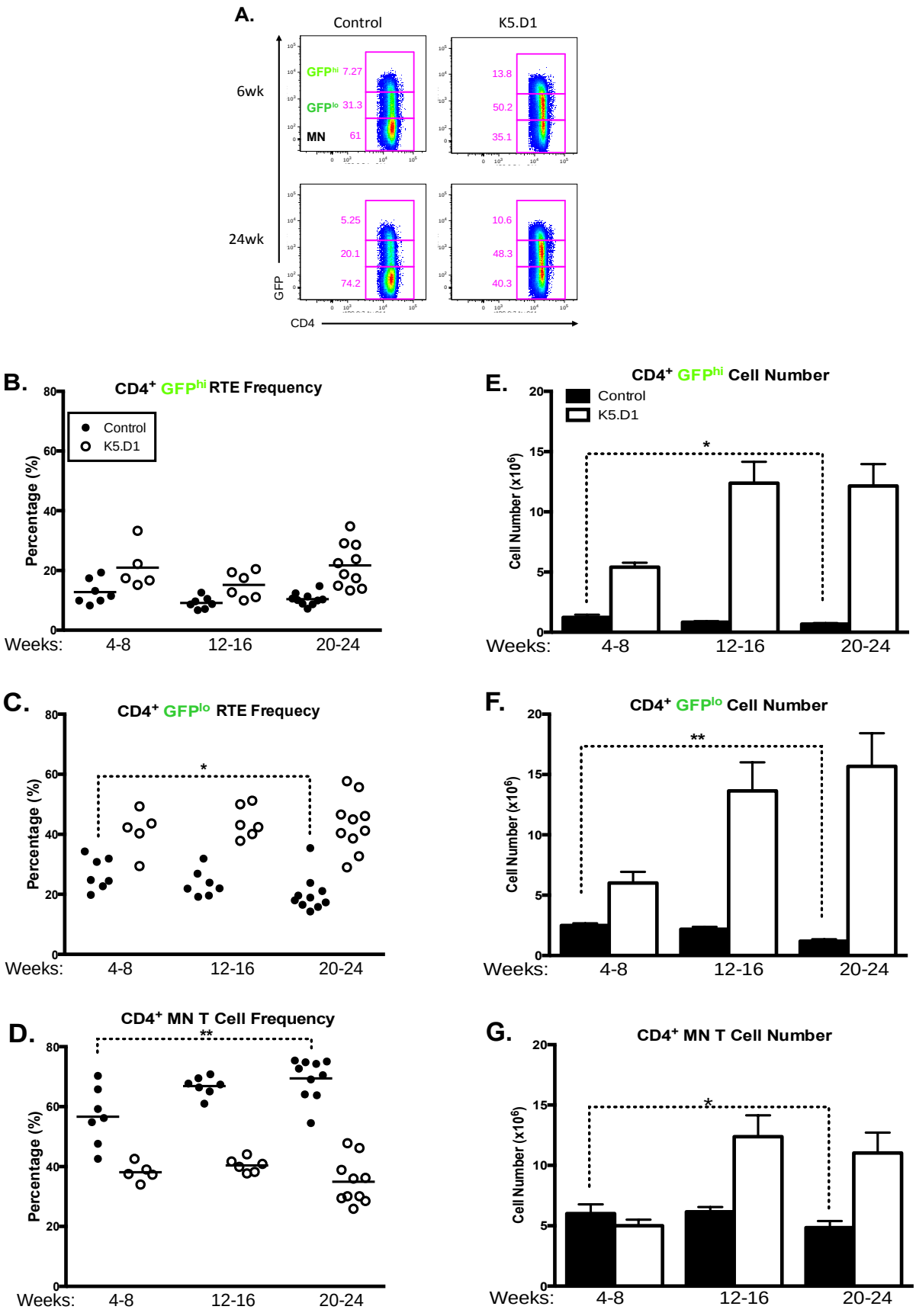
A.
Control
K5.D1
6wk
24wk
GFP
CD4
GFPhi 7.27
GFPlo 31.3
MN 61
13.8
50.2
35.1
5.25
20.1
74.2
10.6
48.3
40.3
B.
CD4+ GFPhi RTE Frequency
Control
K5.D1
Percentage (%)
Weeks: 4-8 12-16 20-24
C.
CD4+ GFPlo RTE Frequecy
*
Percentage (%)
Weeks: 4-8 12-16 20-24
D.
CD4+ MN T Cell Frequency
**
Percentage (%)
Weeks: 4-8 12-16 20-24
E.
CD4+ GFPhi Cell Number
Control
K5.D1
*
Cell Number (x10^6)
Weeks: 4-8 12-16 20-24
F.
CD4+ GFPlo Cell Number
**
Cell Number (x10^6)
Weeks: 4-8 12-16 20-24
G.
CD4+ MN T Cell Number
*
Cell Number (x10^6)
Weeks: 4-8 12-16 20-24

**Figure 19. Changes in the frequency and number of CD4 RTEs and MN T cells with age in control and K5.D1 thymi.**

(**A**) Representative FACS plots of $GFP^{high}$, $GFP^{low}$, and $GFP^{neg}$ mature naïve (MN) CD4 T cells depict the loss of T cell output with age in control mice. (**B**) Frequency of $GFP^{hi}$ RTEs, (**C**) $GFP^{lo}$ RTEs and (**D**) MN CD4 T cells in control and K5.D1 mice with age. (**E**) Number of $GFP^{hi}$ RTEs, (**F**) $GFP^{lo}$ RTEs and (**G**) MN CD4 T cells in control and K5.D1 mice with age. $n \geq 5$ for all data, *$P<0.05$, **$P<0.01$ using a two-tailed Student T test.

maturation of RTEs to the MN T cells stage. This is most likely due to homeostatic constraints, such as the limited availability of IL-7 and MHCII, which cannot sustain large numbers of naïve T cells.

We also analyzed the frequency and number of RTEs and MN T cells in the CD8 naïve T cell compartment (Figure 20). In general, the results were similar to those found in the naïve CD4 subset. Both the frequency and number of $GFP^{hi}$ and $GFP^{lo}$ naïve CD8 T cells declined in controls, but not in K5.D1 thymi. However, the number of MN CD8 T cells did not decline with age in control mice. Others have shown that CD8 naïve T cell numbers do not significantly decline until at least 8 months of age (156, 161, 162). Taken together, these results further support our finding that early thymus involution reduces RTE contribution to the peripheral T cell pool, and promotes the age-associated shift toward memory T cell dominancy.

A previous report demonstrated that RTE output is a function of thymus size and is relatively age-independent (72). In order to determine if RTE output was affected by increased thymopoiesis in K5.D1 mice, we performed a similar analysis by determining the ratio of CD4 RTEs to 100 DP thymocytes (Figure 21A). We observed similar results when comparing CD8 RTEs to 100 DP thymocytes (Figure 21B). The data show that similar to the controls, RTE output/100 DP thymocytes is age independent, emphasizing the importance of thymopoiesis for sustaining the RTE content of the peripheral T cell pool.

Overall, our results demonstrate that in control mice, the contribution of RTEs to the naïve T cell compartment is diminished by 6 months of age. At this age, thymus involution and disorganization of thymic architecture are apparent. However, these changes are not as severe as the thymic degeneration that occurs in mice more than one year of age. Nonetheless, we find that even the apparently minor alterations that

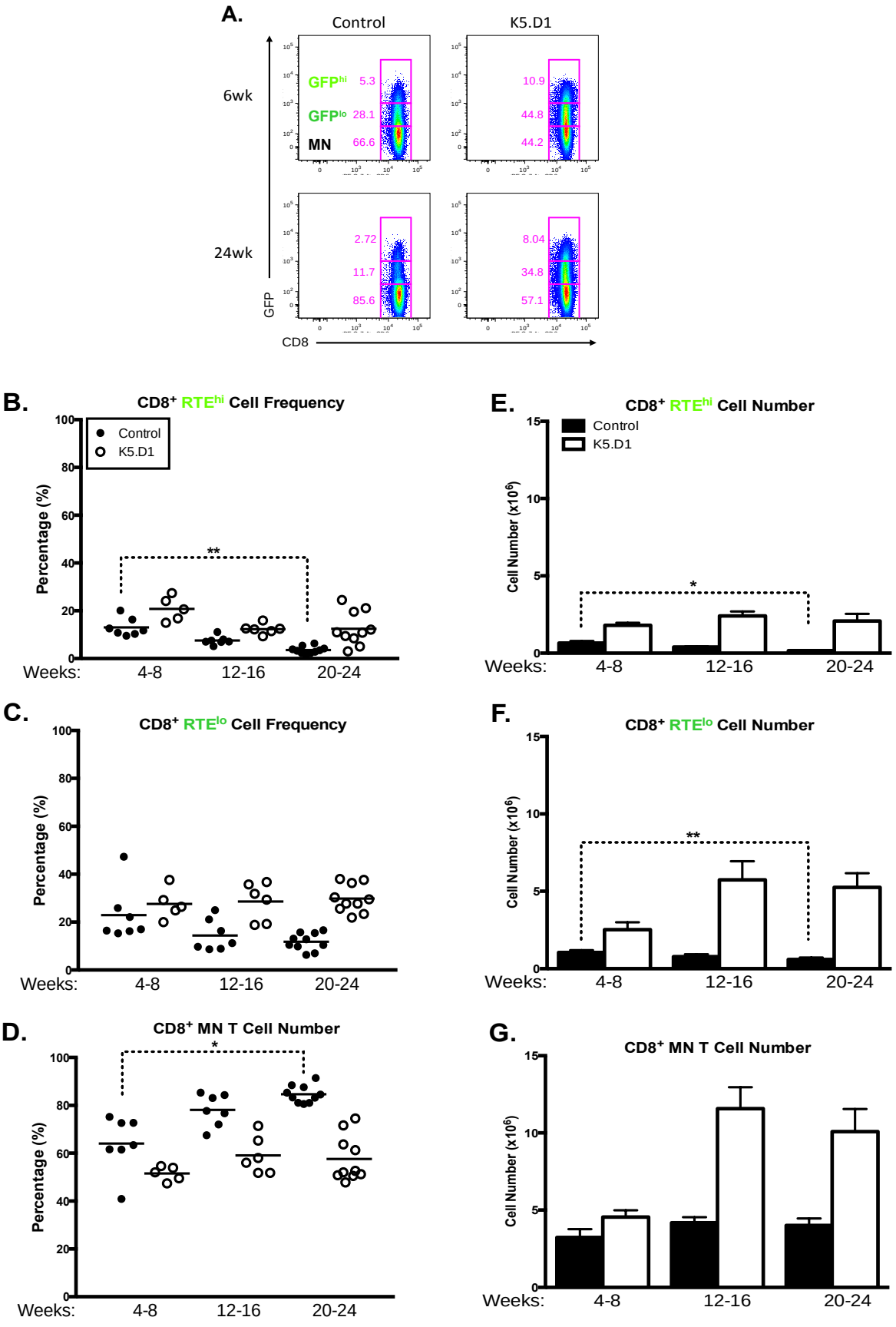
A.
Control
K5.D1
6wk
24wk
GFP
CD8
GFPhi 5.3
GFPlo 28.1
MN 66.6
10.9
44.8
44.2
2.72
11.7
85.6
8.04
34.8
57.1
B.
CD8+ RTEhi Cell Frequency
Control
K5.D1
Percentage (%)
Weeks:
4-8
12-16
20-24
**
E.
CD8+ RTEhi Cell Number
Cell Number (x10^6)
*
C.
CD8+ RTElo Cell Frequency
F.
CD8+ RTElo Cell Number
**
D.
CD8+ MN T Cell Number
*
G.
CD8+ MN T Cell Number

**Figure 20. Changes in the frequency and number of CD8 RTEs and MN T cells with age in control and K5.D1 thymi.**

(**A**) Representative FACS plots of $GFP^{high}$, $GFP^{low}$, and $GFP^{neg}$ mature naïve (MN) CD8 T cells depict the loss of T cell output with age in control mice. (**B**) Frequency of $GFP^{hi}$ RTEs, (**C**) $GFP^{lo}$ RTEs and (**D**) MN CD8 T cells in control and K5.D1 mice with age. (**E**) Number of $GFP^{hi}$ RTEs, (**F**) $GFP^{lo}$ RTEs and (**G**) MN CD8 T cells in control and K5.D1 mice with age. $n \geq 5$ for all data, $^{*}P<0.05$, $^{**}P<0.01$ using a two-tailed Student T test.

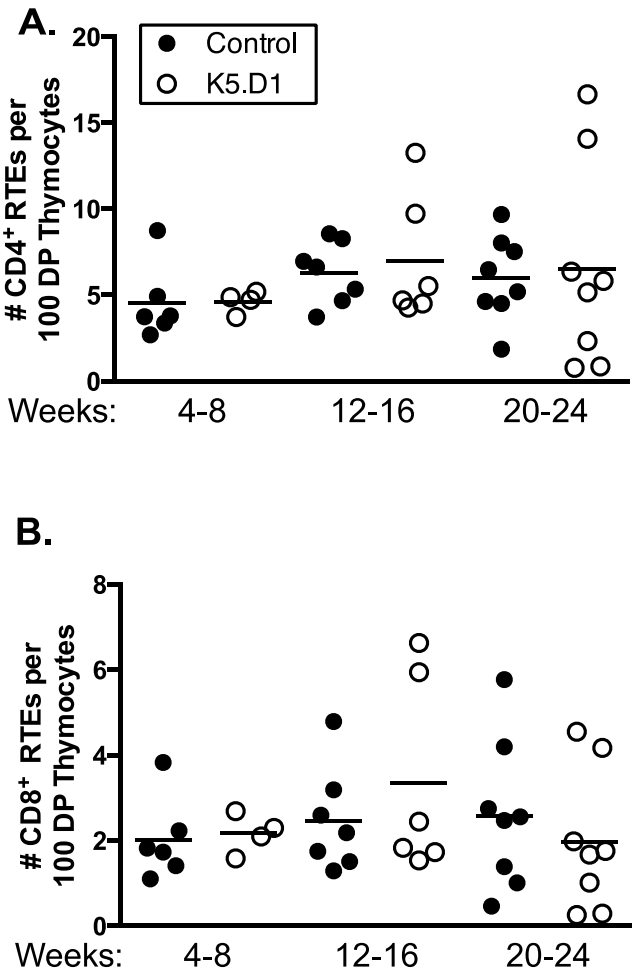
A.
Control
K5.D1
# CD4+ RTEs per 100 DP Thymocytes
20
15
10
5
0
Weeks:
4-8
12-16
20-24
B.
# CD8+ RTEs per 100 DP Thymocytes
8
6
4
2
0
Weeks:
4-8
12-16
20-24

**Figure 21. RTE output in K5.D1 and control mice is independent of age.**

(**A**) Ratio of CD4 $GFP^+$ RTEs compared to 100 DP thymocytes from control and K5.D1 mice. (**B**) Ratio of CD8 $GFP^+$ RTEs compared to 100 DP thymocytes from control and K5.D1 mice. n≥4 for all data.

occur during early stages of thymus involution influence the composition of the peripheral T cell pool. Moreover, the age-related decline in RTE output and naïve T cell numbers can be overcome by maintaining the TEC compartment, which prevents thymus involution.

*Phenotypic Maturation of RTEs in Control and K5.D1 mice*

As RTEs transition to the MN stage, there are consistent changes in the expression of various cell surface proteins that regulate interactions with the surrounding environment to provide optimal survival and activation signals (115, 117). Entry into secondary lymphoid organs is crucial for the execution of RTE maturation (120). Due to the increased number of RTEs present in K5.D1 peripheral T cell pool, we questioned whether RTE maturation might be altered in K5.D1 mice. If RTE maturation were delayed in K5.D1 mice, we would expect to see significant expression differences of RTE maturation markers during the transition from $GFP^{hi}$ RTE to MN T cells. Therefore, we analyzed CD4 and CD8 naïve T cells to determine if phenotypic maturation was comparable in $GFP^{hi}$, $GFP^{lo}$ or $GFP^{neg}$ cells from control and K5.D1 mice at 12 weeks of age (Figure 22). The expression of L-7Rα, Qa-2 and CD45RB increases as control RTEs mature from $GFP^{hi}$ to $GFP^{neg}$ MN T cells (72). We found that a similar pattern when analyzing expression of the same surface markers on K5.D1 RTEs and MN T cells. These data suggest that K5.D1 RTEs undergo typical phenotypic maturation. It has been reported that RTE maturation is delayed in old mice (>year of age, (72)). To determine if RTE maturation was affected even earlier, we performed similar analyses at 5-6 months of age. The data showed no delay in the kinetics of maturation in control or K5.D1 RTEs (data not shown).

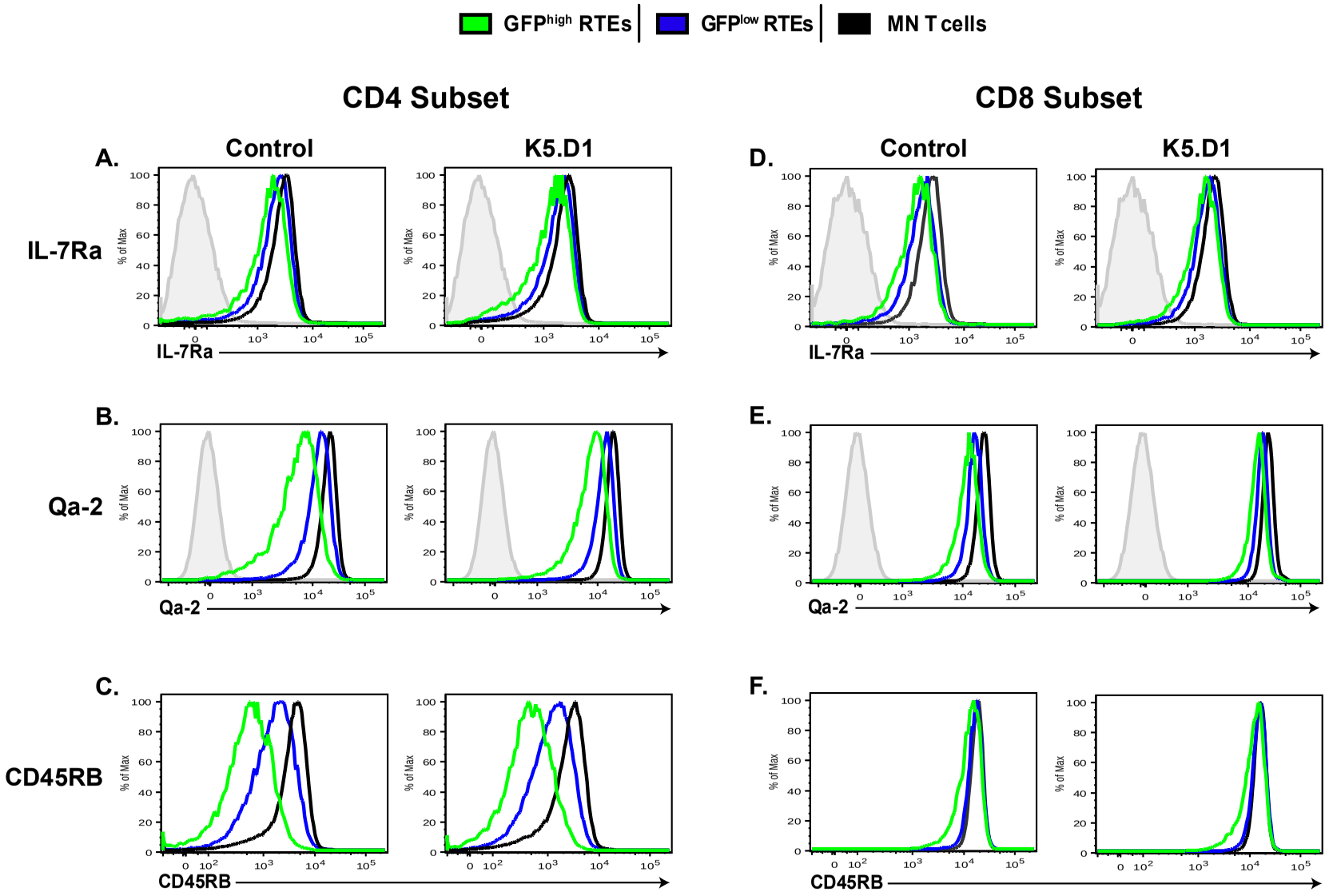
GFP^high RTEs
GFP^low RTEs
MN T cells
CD4 Subset
CD8 Subset
A.
Control
K5.D1
D.
Control
K5.D1
IL-7Ra
% of Max
IL-7Ra
B.
Qa-2
% of Max
Qa-2
E.
Qa-2
% of Max
Qa-2
C.
CD45RB
% of Max
CD45RB
F.
% of Max
CD45RB

**Figure 22. Phenotypic RTE maturation in control and K5.D1 mice at 12 weeks of age.**

CD4 RTE maturation was identified in naïve T cells by the expression of (**A**) IL-7Rα, (**B**) Qa-2 and (**C**) CD45RB in the $GFP^{hi}$ RTE, $GFP^{lo}$ RTE and $GFP^{neg}$ MN T cell subsets of control and K5.D1 mice. CD8 RTE maturation was identified in naïve T cells by the expression of (**D**) IL-7Rα, (**E**) Qa-2 and (**F**) CD45RB in the $GFP^{hi}$ RTE, $GFP^{lo}$ RTE and $GFP^{neg}$ MN T cell subsets of control and K5.D1 mice. Data are representative of at least 5 control or K5.D1 mice from four independent experiments.

We assessed mean fluorescence intensity (MFI) to directly compare the level of expression of IL-7Rα, Qa-2 and CD45RB on control and K5.D1 $GFP^{hi}$, $GFP^{lo}$ and $GFP^{neg}$ naïve T cells (Figure 23). The expression level of Qa-2 and CD45RB was comparable between control and K5.D1 RTEs and MN T cells at each age analyzed. We also found comparable levels of IL-7Rα expression on RTEs from control and K5.D1 mice. Interestingly, however, we observed a significant increase in the MFI of IL-7Rα expression on MN T cells from K5.D1 compared to control littermates at 12-16 and 20-24 weeks of age (Figure 23G-I). This finding suggests that increased IL-7Rα expression on K5.D1 T cells may confer a survival advantage that promotes persistence of MN T cells in the crowded K5.D1 periphery.

*Functional Maturation of RTEs in Control and K5.D1 mice*

In addition to changes in surface phenotype, RTEs undergo functional maturation in the periphery as they progress to the MN T cell stage (117). Previous studies have shown that CD4 RTEs from young mice do not proliferate or up-regulate CD25 expression as extensively as MN T cells in response to anti-CD3 plus anti-CD28 stimulation in vitro in the presence of APCs (115, 132). Adding IL-2 to the cultures in these studies did not correct this deficiency. Furthermore, RTEs produce less IL-2, IFN-g and IL-4 than MN T cells. CD8 RTEs also are less competent than MN T cells in proliferating and generating cytotoxic T cells in response to anti-CD3 stimulation in vitro (115, 132).

Regardless of naïve T cell maturation status, previous studies have shown that in general the responsiveness of naïve T cells to TCR stimulation is reduced with age both in vitro and in vivo. (5, 112, 155-157). These studies have generally been performed in young three month old mice and compared to >1 year old mice. However,

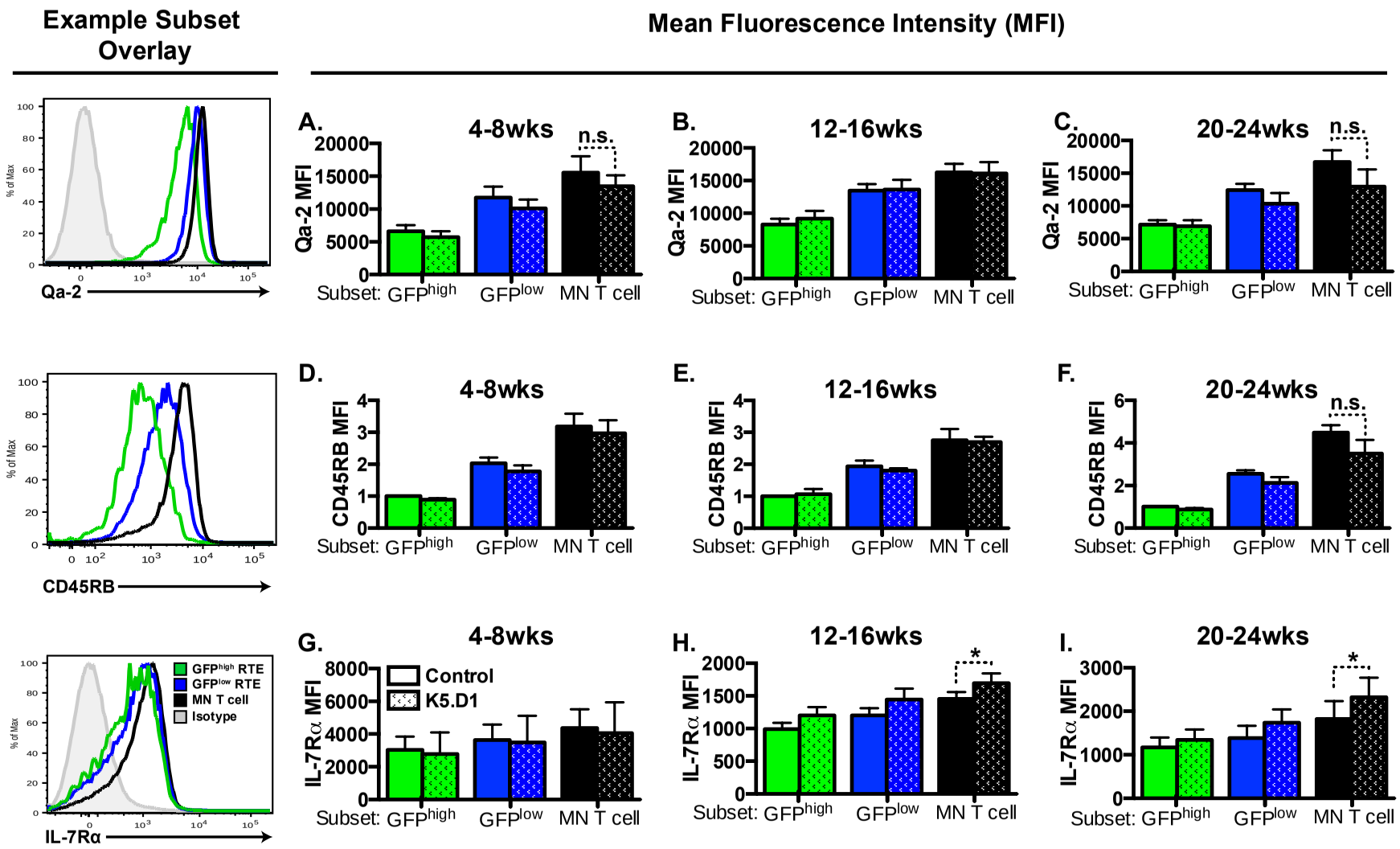
Example Subset Overlay
Mean Fluorescence Intensity (MFI)
% of Max
Qa-2
CD45RB
IL-7Rα
GFPhigh RTE
GFPlow RTE
MN T cell
Isotype
A.
4-8wks
B.
12-16wks
C.
20-24wks
n.s.
Qa-2 MFI
D.
CD45RB MFI
E.
F.
G.
Control
K5.D1
IL-7Rα MFI
H.
I.
*
Subset: GFPhigh
GFPlow
MN T cell

**Figure 23. IL-7Rα expression is increased on K5.D1 compared to control MN T cells.**

The mean fluorescent intensity (MFI) for Qa-2, CD45RB and IL-7Rα expression was determined on $GFP^{hi}$ RTE, $GFP^{lo}$ RTE and $GFP^{neg}$ MN T cell subsets of control and K5.D1 mice at the indicated ages. n≥5 for all data, combined from at least three independent experiments. *P<0.05 using a paired two-tailed Student T test.

little attention has been paid to potential defects in peripheral T cell immune function during early stages of thymic involution. Thus, we asked two separate questions regarding the functional maturation of RTEs from control and K5.D1 mice. First, we wanted to know if RTE and/or MN T cell proliferation and cytokine production declines during the first six months of life. Second, we wanted to compare these functional parameters in RTEs and MN T cells from control and K5.D1 mice. We cultured FACS sorted RTEs and MN T cells in the presence of APCs with anti-CD28 antibody and varying amounts of anti-CD3 antibody. In agreement with previous reports, control RTEs failed to produce as much IFNγ and IL-4 as control MN T cells when given suboptimal doses of anti-CD3 regardless of whether the donors were 6 or 30 weeks of age (Figure 24A and 11B, (132)). RTEs also failed to produce as much of these cytokines at optimal doses of anti-CD3, showing that RTE are not as responsive as MN T cells after TCR stimulation (data not shown). Proliferation of activated T cells was assessed by CFSE label dilution. In agreement with a previous report, we found that the frequency of proliferating control RTEs is less than MN T cells after stimulation (Figure 24C and 24D, (132). Cytokine production and proliferation of K5.D1 RTEs and MN T cells were comparable to controls RTE and MN T cells, respectively. These results indicate that the cytokine and proliferative responses of RTEs and MN T cells are comparable prior to and at early stages of thymus involution in both control and K5.D1 mice.

*K5.D1 MN T cells out-persist control MN T cells in a lymphoreplete environment*

RTEs have been shown to compete poorly with MN T cells after competitive adoptive transfer into a lymphoreplete environment, but out-persist MN T cells in a lymphopenic host (113, 118). We have also observed similar disparities in RTE

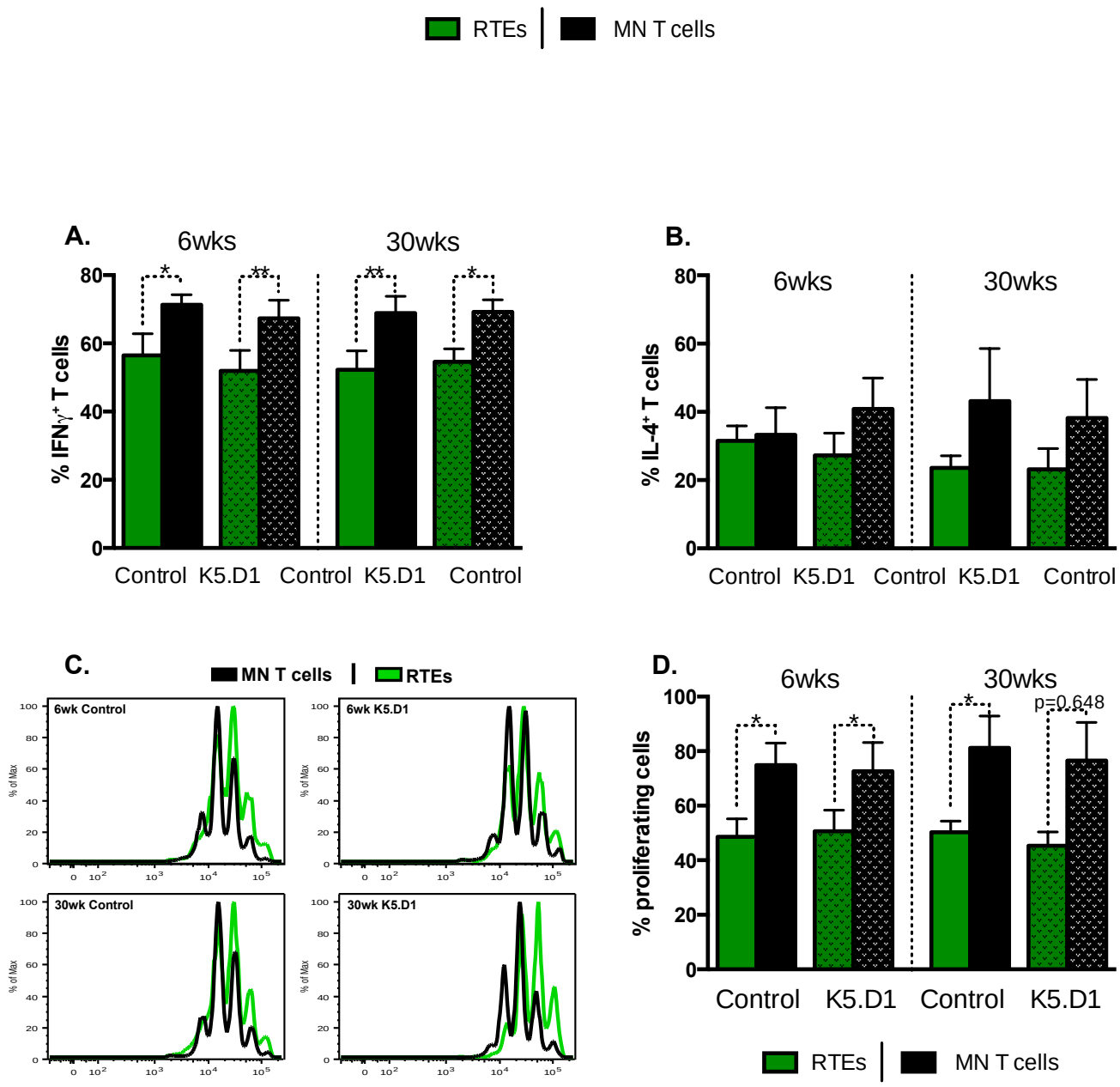
RTEs
MN T cells
A.
6wks
30wks
% IFNγ+ T cells
Control
K5.D1
Control
K5.D1
Control
B.
6wks
30wks
% IL-4+ T cells
Control
K5.D1
Control
K5.D1
Control
C.
MN T cells
RTEs
6wk Control
6wk K5.D1
30wk Control
30wk K5.D1
% of Max
D.
6wks
30wks
p=0.648
% proliferating cells
Control
K5.D1
Control
K5.D1
RTEs
MN T cells

**Figure 24**. **T cell activation occurs in K5.D1 T cells.**

(**A**) IFNγ and (**B**) IL-4 expression after 72hr *in vitro* stimulation with 100ng anti-CD3 and 1ug anti-CD28. (**C**) Representative histograms of RTE and MN T cell CFSE dilution 72hr after *in vitro* stimulation using 100ng anti-CD3 and 1ug anti-CD28 antibody. (**D**) The frequency of CFSE-diluting proliferative cells after stimulation. n≥3, *P<0.05, **P<0.01 using a two-tailed paired Student T test.

incorporation versus the MN T cells from control mice (data not shown). We questioned whether K5.D1 RTEs and MN T cells could compete as well as their wildtype counterparts for incorporation into a lymphoreplete periphery. To answer this question, we mixed congenically marked control and K5.D1 CD4 RTEs or MN T cells at a 1:1 ratio and transferred them into unmanipulated, lymphoreplete recipients (Figure 25A). We analyzed the injected cell mixture to obtain a precise ratio of control to K5.D1 cells in order to compare the input ratio to the ratio of control and K5.D1 T cells recovered from recipient spleen or lymph nodes (For example FACS data, see Figure 25B). This approach facilitates comparisons among multiple experiments. A detailed description of the calculations used in this adoptive transfer approach is presented in Chapter 2.

We found no competitive advantage in recovery of control and K5.D1 RTEs from spleen, axial and inguinal lymph nodes at one or six weeks after transfer (Figure 26A). These results imply that K5.D1 RTEs possess no overt survival characteristics relative to control RTEs. However, K5.D1 MN T cells outcompeted control MN T cells as early as one week as well as at six weeks post-transfer (Figure 26B).

The increased persistence of K5.D1 MN T cells suggested that they might possess a survival advantage over their counterparts from control mice. Since we observed increased expression of IL-7Rα on MN T cells from K5.D1 mice (Figure 23), we hypothesized that IL-7 signaling might enhance their survival after adoptive transfer. To test this, we FACS sorted MN T cells from control and K5.D1 mice and cultured them in the presence or absence of IL-7 for up to 48 hours (Figure 26C). Both control and K5.D1 T cells die rapidly without IL-7, with more than 70% of cells dying within 24 hours after being placed in culture (Figure 26C, solid points). When cultured in the presence of IL-7, both control and K5.D1 T cell survival improved (Figure 26C, open points). However, K5.D1 T cells survival was significantly higher at 24 and 48 hours

A.

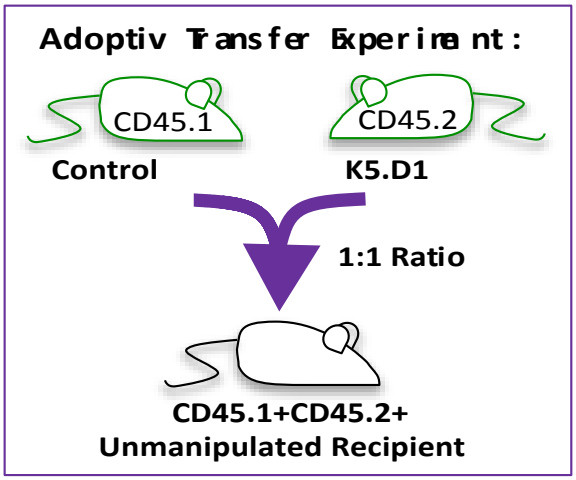
Adoptiv Transfer Experiment:
CD45.1
CD45.2
Control
K5.D1
1:1 Ratio
CD45.1+CD45.2+
Unmanipulated Recipient

B.

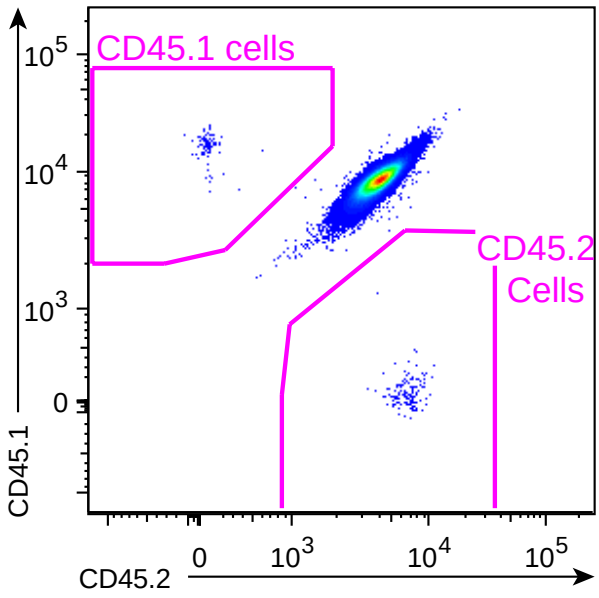
CD45.1 cells
CD45.2
Cells
$10^5$
$10^4$
$10^3$
0
CD45.1
0
$10^3$
$10^4$
$10^5$
CD45.2

**Figure 25. Competitive adoptive transfer into lymphoreplete recipients.**

(**A**) Experimental scheme to identify and adoptively transfer donor cells into unmanipulated recipients. (**B**) Representative FACS plot identifying CD45.1 and CD45.2 donor cells within a CD45.1/CD45.2 unmanipulated recipient CD4 splenic naïve T cell pool.

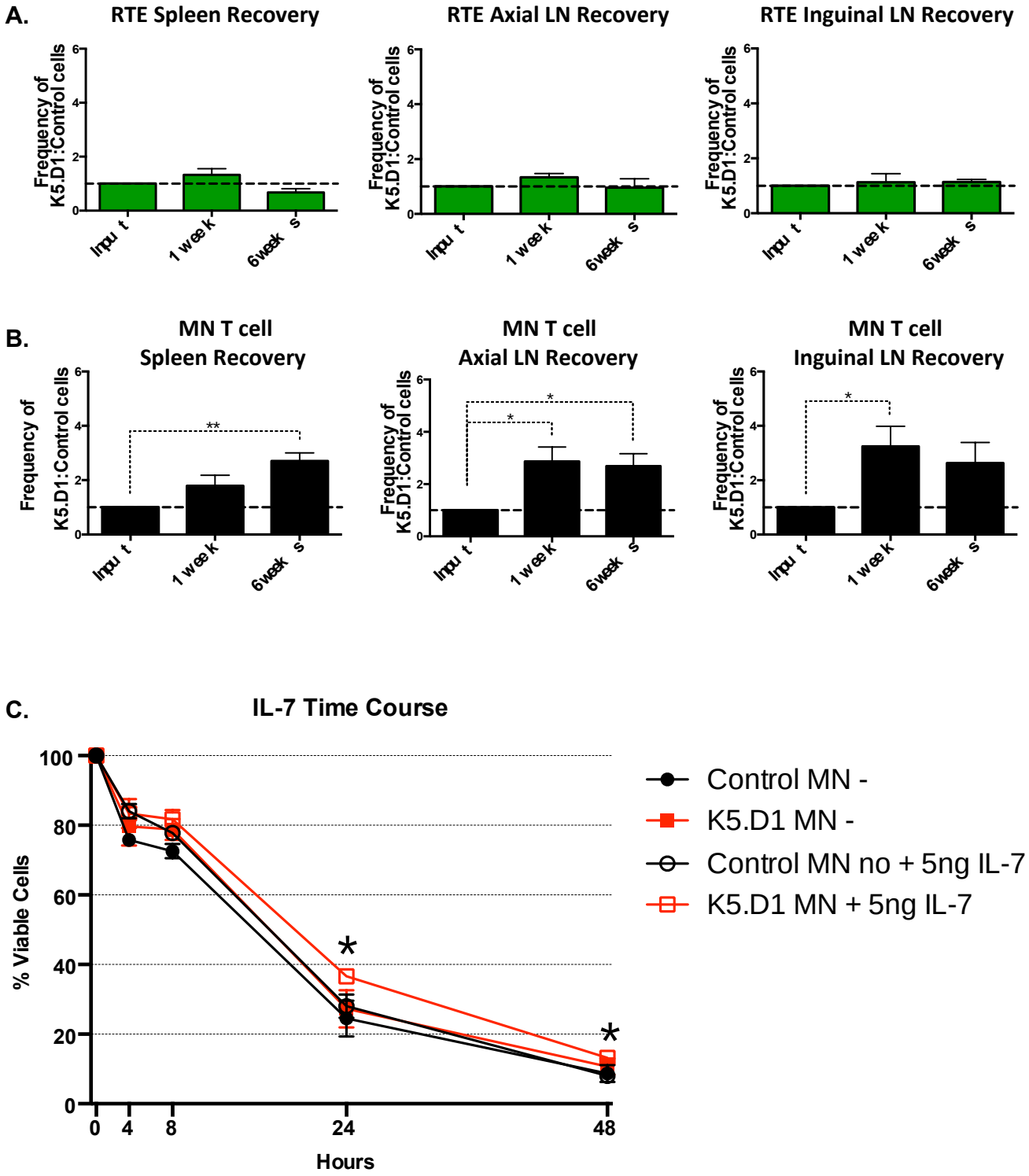
A.
RTE Spleen Recovery
RTE Axial LN Recovery
RTE Inguinal LN Recovery
Frequency of K5.D1:Control cells
Input
1 week
6 weeks
B.
MN T cell Spleen Recovery
MN T cell Axial LN Recovery
MN T cell Inguinal LN Recovery
**
*
C.
IL-7 Time Course
% Viable Cells
Hours
Control MN -
K5.D1 MN -
Control MN no + 5ng IL-7
K5.D1 MN + 5ng IL-7

**Figure 26. K5.D1 MN T cells out-persist control MN T cells in a lymphoreplete environment.**

(**A**) Recovery of K5.D1 vs. Control RTEs in the spleen, axial and inguinal LNs of recipient mice after 1 or 6wk after transfer. (**B**) Recovery of K5.D1 vs. Control mature naïve (MN) T cells in the spleen, axial and inguinal LNs of recipient mice after 1 or 6wk after transfer. (**C**) Survival Assay of control or K5.D1 T cells cultured in the presence or absence of 5ng IL-7. n≥3, *P<0.05 and **P<0.01 using a two-tailed unpaired Student T test or paired Student T test (Figure C).

than control T cells when IL-7 was supplemented. Interestingly, these differences were neutralized when cells were cultured in the presence of higher concentrations of IL-7. Therefore, our results suggest that the increased IL-7Rα expression does play a role in K5.D1 T cell survival.

*T cell receptor diversity is maintained in K5.D1 mice*

Naïve T cell TCR repertoire diversity is severely altered in aged mice, and stems from the decline in RTE output and homeostatic proliferation of peripheral T cells (1, 3). Because we observed significant changes in the frequency of naïve T cells in control mice as early at 12-16 weeks of age, we wanted to determine if TCR repertoire diversity was impacted by this decline. We addressed this question by assaying the usage frequency of fifteen different TCR $V_\beta$ segments that can make up the CDR3 region of the TCR beta chain (Figure 27). Using an antibody panel, and FACS analysis, we did find slight alterations in the frequencies of some $V_\beta$s with age, including $V_{\beta 4,}$ $V_{\beta 8.1/8.2,}$ and $V_{\beta 10b}$ in the CD4 naïve subset and $V_{\beta 5.1/5.2}$ in the CD8 naïve T cell subset of control mice. However, K5.D1 mice exhibited similar changes in the usage of these same $V_\beta$ regions, indicating that declining T cell output in control mice did not drive these changes.

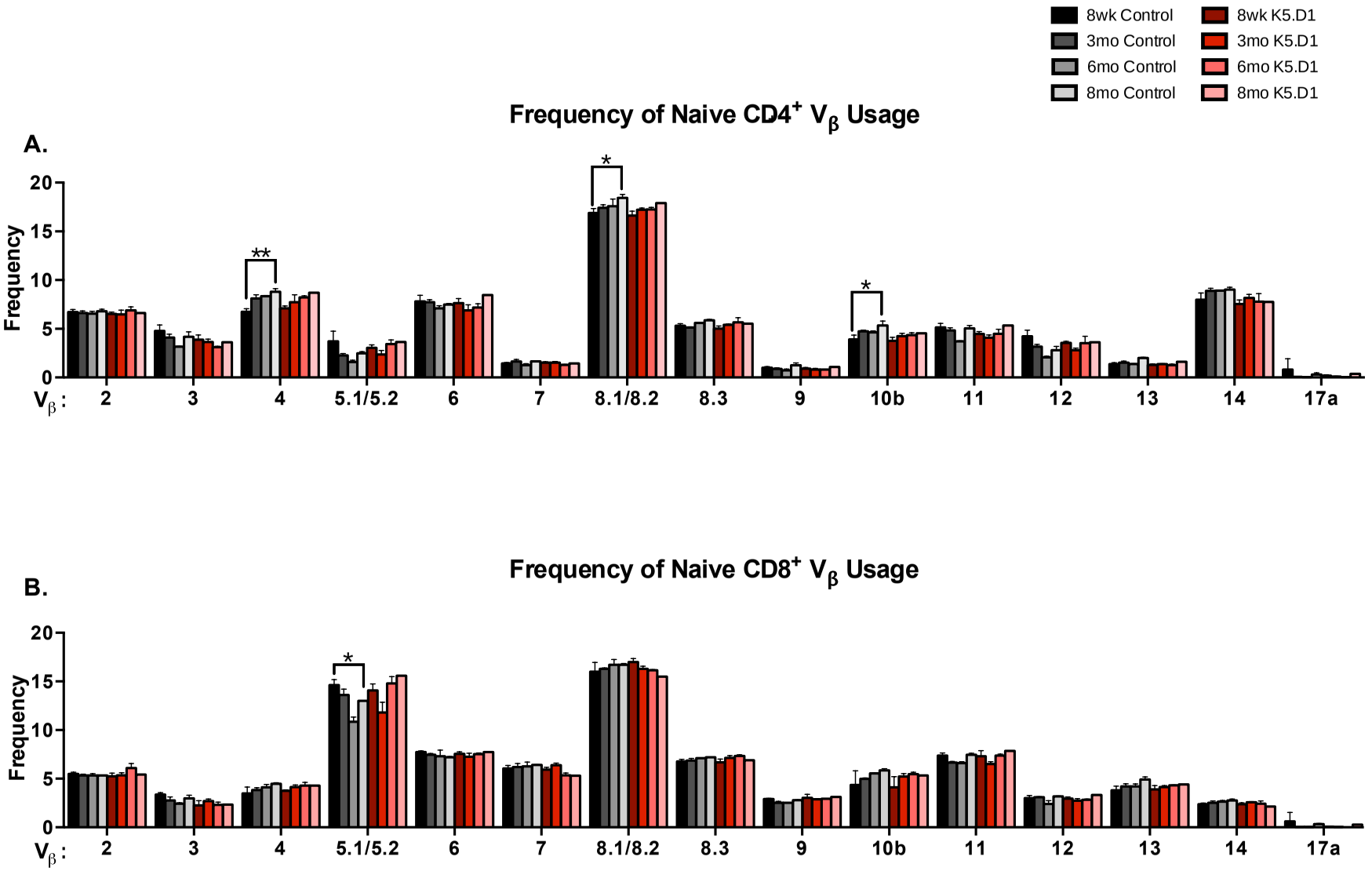
8wk Control
3mo Control
6mo Control
8mo Control
8wk K5.D1
3mo K5.D1
6mo K5.D1
8mo K5.D1
A.
Frequency of Naive CD4+ Vβ Usage
Frequency
20
15
10
5
0
**
*
*
Vβ: 2 3 4 5.1/5.2 6 7 8.1/8.2 8.3 9 10b 11 12 13 14 17a
B.
Frequency of Naive CD8+ Vβ Usage
Frequency
20
15
10
5
0
*
Vβ: 2 3 4 5.1/5.2 6 7 8.1/8.2 8.3 9 10b 11 12 13 14 17a

**Figure 27. The usage of TCR $V_\beta$ segments is altered with age.**

(**A**) The frequency of $V_\beta$ usage in the CD4 naïve T cell populations from control and K5.D1 mice with age. (**B**) The frequency of $V_\beta$ usage in the CD8 naïve T cell populations from control and K5.D1 mice. n≥3 for all data, from three independent experiments.

## 4.3 Discussion

Age-associated changes in the T cell pool that result from severe thymus involution have been investigated in mice over one year of age. These studies concluded that thymus involution is associated with severe impairment in T cell immune responses (76, 134, 165, 166). Here we show that the earliest phases of thymus involution initiate the age-associated shift from naïve to memory cell dominancy within the T cell pool. Declining RTE output is evident by 12-16 weeks of age in the control mice from our studies, resulting in decreased naïve T cell numbers. The naïve T cell loss from these events is filled by the generation of memory T cells to maintain the cellularity of the T cell pool.

There has been much speculation that preventing thymus involution is an important goal to sustain naïve T cell output and robust immune response capabilities. Expression of the K5.D1 transgene in TECs prevents thymus involution and increases RTE output with age. Moreover, the K5.D1 RTEs do not impede the establishment of the mature naïve T cell subset. Not all of these RTEs survive to the MN T cells stage. However, enough survive to result in a significantly increased number of MN T cells at 20-24 weeks of age compared to controls in which MN T cell numbers have declined at that point. Thus, maintaining a functional thymus translates into preventing the loss of MN T cells, which are required to generate T cell immune responses to newly encountered antigens.

The crowded K5.D1 naïve T cell pool does not impact the generation of memory T cell subsets, supporting previous speculation that the naïve and memory T cell populations reside in separate niches in the periphery. We conclude that sustaining T cell output maintains large numbers of naïve T cells that prevent the age-associated shift from naïve to memory dominancy in the T cell pool.

The kinetics of RTE maturation have been shown to slow with age (72). We found no significant difference in RTE maturation in control mice 4 to 24 weeks of age. This result suggests that early involution does not alter RTE maturation. We also observed comparable RTE maturation in K5.D1 mice up to 24 weeks of age. Interestingly, IL-7Ra expression was increased on MN T cells from K5.D1 mice. This result suggested that K5.D1 MN T cells might be more apt to survive via IL-7 signaling in lymphoreplete conditions. Indeed K5.D1 MN T cells out-persisted control MN T cells at a three to one ratio in adoptive transfer experiments.

Naïve T cell homeostasis requires critical factors including the availability of IL-7 and MHC. Although we do not yet know if IL-7 signaling mediates the enhanced survival observed *in vivo,* the *in vitro* survival studies demonstrated that K5.D1 T cells do survive better than control cells in low concentrations of IL-7. We speculate that the increased number of T cells in K5.D1 mice drives down the availability of IL-7 on a per cell basis. The expression of IL-7R has been shown to increase during times of low IL-7 availability, and is rapidly downregulated upon ligand-receptor interaction (Reviewed in (110). Therefore, we suspect that low levels of IL-7 availability in the K5.D1 periphery may lead to the increased IL-7R expression observed on K5.D1 MN T cells. Then, when these cells are transferred into a wildtype lymphoreplete recipient, they are better poised to interact with available IL-7 and persist than wildtype cells.

TCR diversity is essential for maintaining robust primary immune responses. Our data show that TCR activation in K5.D1 T cells is comparable to control T cells up to 30 weeks of age. Furthermore, TCR diversity, as assayed by Vβ usage frequency shows no clonal expansion of any particular TCR in K5.D1 mice. These results support our notion that the K5.D1 thymus sustains the generation of diverse and responsive T cells.

Taken together, the work presented throughout this chapter support our hypothesis that preventing involution sustains a large, responsive naïve T cell pool.

# CHAPTER FIVE

# DISCUSSION

The negative influence of thymus involution on the peripheral T cell pool has been established in both mouse and man. As the thymus atrophies, thymopoiesis is reduced and the output of naïve T cells declines. This deficit in the production and exit of naïve T cells leads to peripheral T cell proliferation to maintain peripheral homeostasis. The naïve to memory T cell ratio declines as a consequence, and this age and involution-associated trend is associated with restricted TCR diversity and defects in the ability to mount protective immune responses to newly encountered antigens (1, 134).

Thymus involution is driven primarily by disintegration of the TEC compartment (57, 81, 147). Therefore we chose to determine whether preventing the loss of TECs ablated involution and peripheral T cell pool dynamics. Previously our lab showed that the TEC microenvironment is maintained in K5.CyclinD1 (K5.D1) mice, which in turn sustained thymopoiesis (135, 143). We became particularly interested in determining how early stages of thymus involution affect the composition of the peripheral T cell pool. Most studies of involution concentrated on thymi from old (1 to 2 years of age) mice that are completely atrophied. Thus, changes in the composition and function of peripheral T cells in very old mice measure end stage effects. However, we and others have shown that thymus involution actually is initiated early in life (57, 141). Therefore, we undertook this study to determine: 1) the consequences of early stage involution on peripheral T cells and 2) whether involution-associated defects in peripheral T cells would be averted in K5.D1 mice that do not undergo thymus involution.

Our investigations have resulted in four significant findings: First, we showed that increased Foxn1 expression is associated with sustained TEC numbers and differentiation, which helps to sustain the functional microenvironment necessary for continued thymopoiesis with age. Second, we found that early thymus involution in control mice precipitates a decline in RTEs that initiates an early age-associated shift toward memory T cell dominancy evident in aged mice and elderly patients. Third, we showed that the absence of thymus involution prevents age-associated changes to the composition of the T cell pool without inhibiting the generation of memory T cells. Fourth, we demonstrated that K5.D1 MN T cells have a competitive advantage over nontransgenic MN T cells in adoptive transfer studies. These results demonstrate that maintenance of the TEC microenvironment is essential not only for continued thymopoiesis, but also for the sustaining a large and diverse naïve T cell population.

*Foxn1 expression is maintained indefinitely in K5.D1 TECS*

The FOXN1 transcription factor has been heralded as the 'master regulator' of TEC maintenance and differentiation in both fetal and postnatal thymi. To this end, multiple groups have reported that early termination of *Foxn1* expression results in premature involution (81, 167), whereas the maintenance of *Foxn1* expression slows but does not prevent involution (82). These previous findings demonstrated that maintenance of the TEC microenvironment requires *Foxn1* expression, likely in concert with other factors. The fact that thymopoiesis relies on interactions with a well-differentiated TEC microenvironment to produce competent T cells reinforces the close relationship between TEC degeneration and diminished thymopoiesis during thymus involution. Our data in Chapter Three revealed that TECs from young K5.D1 mice express elevated levels of *Foxn1* expression compared to control littermate TECs. With

age, the high level of Foxn1 expression in K5.D1 TECs is maintained in stark contrast to TECs from age-matched wildtype mice, which lose Foxn1 expression with the onset of thymus involution.

While Foxn1 expression does not account solely for the increased number of TECs and avoided involution in K5.D1 thymi, it does suggest that Cyclin D1 expression has an important influence on preserving steady-state signaling conditions in aging TECs. It remains to be determined if the K5.D1 transgene exerts a direct or indirect role in maintaining the Foxn1 expression, although another experimental mouse model employing the same cell cycle pathway was shown to directly influence transcription of *Foxn1* in TECs. Work from Garfin and colleagues showed that knocking out Rb, the downstream target of the CyclinD1/Cdk heterodimer, de-repressed the E2F transcription factor family to allow binding of E2F3 to the Foxn1 promoter. While investigation of this mechanism was not pursued in our studies and may not fully explain the K5.D1 phenotype, we speculate that this same pathway likely plays a role in the increased Foxn1 expression observed. Furthermore, the K5.D1 TEC compartment is well organized into differentiated cTEC and mTEC subsets. This finding is consistent with other studies in which thymus size was maintained or rebounded when Foxn1 expression was driven in TECs (82, 83, 152). In these models increased *Foxn1* expression promoted crucial TEC differentiation that supports thymopoiesis and continued T cell output. Thus, these data and our own support the central dogma that maintaining *Foxn1* expression is a key factor in the sustaining both a differentiated TEC microenvironment and continued thymopoiesis past the time frame of normal age-associated involution.

*The K5.D1 TEC microenvironment supports thymopoiesis and sustains the output of self-tolerant RTEs with age*

We previously reported a normal frequency of major thymocyte subsets in K5.D1 mice. In that same report, positive and negative selection were shown to be intact in mice that expressed the K5.D1 transgene as well as the H-Y TCR transgene (135). Since the H-Y TCR is expressed on DN thymocytes, a developmental stage in which TCRs are not yet expressed in wildtype mice, we performed additional studies to assess selection in the K5.D1 TEC environment for this thesis. Our data showed that that the percentage of post-positive selection ($CD69^{+}$) DP thymocytes was comparable to that in nontransgenic controls. We also determined that the strength of TCR engagement on K5.D1 DP thymocytes is comparable to controls by means of Nur77 and CD5 expression. These findings support our previous work indicating that positive selection in K5.D1 thymi is indistinguishable from that in control littermates. We performed a more thorough analysis of negative selection and demonstrated that serum from K5.D1 mice did not contain detectable autoantibodies. Moreover, transferring K5D1 T cells into RAG2-/- recipients that cannot generate Tregs failed to produce autoimmune symptoms. Considering that the TEC microenvironment is instrumental for negative and positive selection, and is maintained in K5.D1 mice, these results confirm that the K5.D1 model is an excellent tool for studying how the absence of thymus involution affects peripheral T cells with age without skewing TCR diversity toward autoimmunity.

The precursors for all subsequent stages of thymocyte development are the ETP subset, which have been shown to decline with age and involution (149, 168). Our results from control mice agree with these published findings. Interestingly, preventing thymus involution in K5.D1 mice maintains ETP cellularity, and suggests that the K5.D1

TEC microenvironment continues to provide available intrathymic niches necessary to support ETP survival and differentiation with age. Furthermore, the fact that TEC cellularity increases with age in the K5.D1 thymus, whereas the number of TECs in control nontransgenic thymi decreases with age supports the premise that the TEC microenvironment is necessary for ETP survival and persistence.

Our data agrees with a previous report showing that thymic output is dependent on organ size. (72). The ratio of RTEs to DP thymocytes is relatively stable in control and K5.D1 mice with age. This demonstrates that the amount of RTEs in the periphery is a function of the size of the developing thymocyte pool.

*Thymus egress is delayed in K5.D1 mice*

Thymus emigration is the final step of thymopoiesis, and is a highly controlled process to prevent the escape of immature or autoreactive T cells. Unexpectedly, we observed an accumulation of late stage SP thymocytes in K5.D1 mice that increased with age. We determined that proliferation and maturation could not account for the observed phenotype. Importantly, the late SP stage is the last maturation step before thymus emigration. To prevent immature thymocytes from emigrating, the early activation marker CD69 is expressed after TCR engagement on SP cells. CD69 expression stalls cells that require additional maturation by preventing the expression of KLF2 target genes necessary for exit, including CD62L and S1P1R (169). We observed appropriate downregulation of CD69, as well as expression of CD62L on K5.D1 thymocytes, which confirmed that SP thymocytes were undergoing maturation and preparing for thymus emigration. Furthermore, we found that late stage SP thymocytes were actually retained longer in K5.D1 mice than littermate controls by using the intensity of RAG2p-GFP signal as an indicator of the length of thymus

residency. While altered S1P1R expression cannot be fully dismissed as the cause of the retained K5.D1 SP cells, we did not observe any accumulation of cells in the perivascular spaces that would suggest low S1P1R expression. Interestingly, there are multiple mouse models that display late stage SP retention much like the K5.D1 model, including S1P1R$^{-/-}$ Aire$^{-/-}$, PI3K$^{-/-}$ and SOCS1$^{-/-}$ mice (46, 170-172). The similarities between these models and our own suggest additional avenues that should be considered for determining the mechanism behind this K5.D1 phenotype. These include altered chemokine/receptor expression, as well as minor defects in negative selection that our studies have not exposed. Thus, further investigation is necessary to determine the mechanistic underpinnings of accumulating late stage thymocytes in the aging K5.D1 thymus.

*Thymic Treg generation versus recirculation*

The generation of Tregs is essential for the suppression of inflammatory and autoreactive T cells in the periphery. We observed an increased frequency of Tregs in the K5.D1 thymus with age. However, we did not find an increased frequency of Tregs in the periphery. We initially speculated that increased thymopoiesis in the K5.D1 thymus might lead to increased numbers of thymocytes undergoing apoptosis due to negative selection, which has been reported to promote the apoptosis-TGFβ-Foxp3 axis to induce Treg generation (173). However, a recent publication has highlighted the tendency of peripheral Tregs to recirculate into the thymus, thus artificially inflating thymic Treg frequency (153). Therefore we cannot definitively say whether the increased frequency of thymic Tregs in K5.D1 mice is due to generation or recirculation. In an attempt to determine whether the phenotype was due to *de novo* Treg generation or peripheral Treg circulation we utilized the RAG2p-GFP reporter to

identify newly generated Tregs. Unfortunately, our current method of Foxp3 identification relies on cell fixation and analysis of Foxp3 transcription factor expression by flow cytometry, which completely destroyed GFP signal in our preliminary experiments. In order to visualize Tregs in K5.D1 mice, either a third transgene for Foxp3 identification would need to be utilized in our RAG2p-GFP system, or Tregs from congenically distinct mice could be injected into K5.D1 mice and analyzed after a chase period to determine the rate of Treg homing to the thymus. Nonetheless, the implications from either increased Treg generation or peripheral recirculation will impact the characterization of this mouse model, and which might prove the K5.D1 model useful for Treg studies in the future.

*Early thymus involution in young mice precipitates age-associated changes in the composition of peripheral T cells*

Age-associated changes to the composition of the T cell pool have been defined in both aged mice and elderly patients. Our studies focused on the ramifications of early thymus involution on the peripheral T cell pool, and revealed that early stages of involution promote changes to the frequency and number of naïve and memory T cells. Furthermore, we were able to show that these changes are due to reduced RTE output by involuting thymi that fails to sustain naïve T cell numbers. To our knowledge, this is the first description of the influence early thymus involution has upon the established T cell pool in young mice. Furthermore, our data contradicts popular opinion regarding when naïve T cell numbers decline (134), and shows that this occurs much earlier than previously appreciated.

In stark contrast to the decreased ratio of naïve to memory peripheral T cells in nontransgenic controls during early involution, the pre-involution ratio of naïve to

memory cells was maintained in K5.D1 mice due to sustained RTE production. This finding agrees with reports of other mouse models in which the TEC microenvironment and thymopoiesis are sustained or regenerated at older ages, thus maintaining or reversing the shift between naïve and memory T cell dominancy (82, 83, 152). Importantly, the number of K5.D1 MN T cells is nearly double that of control MN T cells by just 12-16 weeks of age. This result suggests that the periphery can accommodate a limited increase in T cell number despite the homeostatic control that normally preserves a relatively constant number of cells in the periphery. The fact that the increase in naïve peripheral T cells does not mirror the increase in thymocytes suggests that homeostatic signals are limiting. Previous studies have shown that the major signals regulating homeostasis of naïve T cells include IL-7 and MHCII (Reviewed in (106, 109, 110, 159)). However, homeostatic cytokine signaling cannot support an indefinite amount of cells, as evidenced by our findings. In support of this concept, transplantation of up to nine thymic lobes under the kidney capsule of wildtype mice only leads to a doubling of the size of the T cell pool (158).

We also found that the increase of naïve T cells in K5.D1 mice did not impact the number of memory T cells. This agrees with previous speculation that naïve and memory T cell populations occupy distinct niches within the peripheral T cell pool (174). Indeed, naïve T cell numbers are largely controlled by IL-7 and MHC interactions, whereas memory T cell numbers are sustained by a combination of IL-7 and IL-15 (Reviewed in (106, 109, 110, 159)). Therefore, the loss of naïve T cell numbers with age is not a necessary prerequisite to create room for antigen-experienced memory T cells, but occurs solely as a consequence of thymus microenvironmental degeneration for naive T cell output. Whether the continual output of naïve T cells impacts the long-term response of memory T cells in our K5.D1 mice remains to be seen. The memory T

cell population should be investigated to determine whether the continual output of naïve T cells affects the clonal diversity, longevity and response of the memory T cell population.

*The relationship between RTEs and MN T cells*

Since the naïve T cell population consists of both phenotypically and functionally distinct RTEs and MN T cells, we analyzed these subsets through the use of the RAG2p-GFP transgenic mouse model. Interestingly, the frequency of $GFP^{hi}$ and $GFP^{lo}$ RTEs in K5.D1 mice was much higher than in controls. While in controls a low frequency of $GFP^{hi}$ RTEs gave way to a higher frequency of $GFP^{lo}$ RTEs that maintained the MN T cell population, this was not the case in K5.D1 mice. Although the frequency of $GFP^{hi}$ RTEs was lower than $GFP^{lo}$ RTEs, the MN T cell subset in K5.D1 mice was much smaller than the $GFP^{lo}$ RTE subset. This demonstrates that the excess RTEs that are produced by the K5.D1 thymus do not survive for more than ~3 weeks in the periphery. We do not have direct evidence that most $GFP^{lo}$ RTEs undergo apoptosis. However, others have shown that RTEs do not incorporate into a lymphoreplete environment as well as MN T cells, perhaps due to a reduced ability to respond to homeostatic signals, (118). Therefore, K5.D1 RTEs may undergo apoptosis due to limited availability of homeostatic signals in the periphery.

Notably, IL-7Rα expression was increased on K5.D1 MN T cells compared to control T cells. We speculate that the increased number of naïve T cells in the K5.D1 periphery is indirectly responsible for the increased IL-7Rα expression on MN T cells. Expression of IL-7Rα is modulated by IL-7 availability (Reviewed in (110)). Thus IL-7Rα expression is increased in the presence of low levels of IL-7, whereas IL-7Rα expression declines on T cells in higher concentrations of IL-7. The cyclical regulation

of the IL7-Rα is thought to improve the likelihood of ligand interaction when IL7 availability is low. IL7-IL7R interaction promotes receptor internalization and transcriptional downregulation, which is thought to conserve IL-7 ligand for interactions with a larger fraction of T cells so as to support homeostasis of the entire population (110, 175). Because the K5.D1 mouse contains nearly three times the number of T cells present in littermate controls, we speculate that the availability of IL-7 for any one cell is greatly reduced. Therefore, we suspect that low IL-7 availability promotes increased IL-7Rα expression on K5.D1 T cells, which in turn promotes cellular survival in the crowded K5.D1 periphery.

We tested the survival capabilities of K5.D1 MN T cells by directly competing these cells with control MN T cells in an adoptive transfer experiment using lymphoreplete recipients. These experiments demonstrated that K5.D1 MN T cells out-persist control T cells in a lymphoreplete environment, and suggests that the K5.D1 T cells have an inherent survival or proliferative advantage compared to control T cells in this system. This, coupled with the increased IL-7Rα expression present on K5.D1 MN T cells, led us to speculate that the IL-7 signaling pathway plays a role in sustaining the K5.D1 MN T cells *in vivo*. Our short-term *in vitro* culture results suggests that increased IL-7Rα expression on K5.D1 T cells does, in fact, promote the viability of these cells. We also performed additional IL-7 culture experiments that demonstrated enhanced proliferation does not account for K5.D1 MN T cell persistence *in vitro* (data not shown). While additional factors that promote T cell persistence cannot be ruled out, including increased cell lifespan and the support of other homeostatic cytokines, the enhanced survival of MN T cells in the presence of IL-7 is consistent with the notion that IL-7Rα expression plays an important role in supporting MN T cell homeostasis in the K5.D1 periphery.

*Preventing involution: beneficial or detrimental?*

There is little question that thymopoiesis is a biologically expensive process, with only 1-2% of all thymocytes completing maturation and exiting the thymus. This leads some immunologists to speculate that the involution process is an evolutionarily conserved attempt to curb the energy-expensive production of T cells after T cell pool has been established (176). However, there has been no established feedback loop between the periphery and thymus to account for this hypothesis. Nonetheless, there is a strong correlation between increasing thymus atrophy and the onset of puberty, which supports the idea that metabolic resources are diverted toward reproduction at the expense of T cell development to ultimately support the persistence of the species (176). Still others believe that the involution process represents biological adaptation at work. Since the life expectancy in developed countries has nearly doubled since the industrial revolution, perhaps the sustainment of thymus size has not yet adapted to the increased human lifespan. Whether thymus involution is evolutionarily driven or represents ongoing adaptation remains to be seen, but does not negate the fact that T cell-mediated immune responses decline significantly with age.

Adverting or reverting thymus involution has been suggested as a remedy for many of the age-related defects in T cell production and response. The research presented herein supports this view and show that a large and diverse T cell pool can be maintained by preventing TEC-driven thymus involution. However, our studies were not conducted beyond the age of six months due to the physical constraints of the mouse model, and therefore leaves unanswered the question of whether maintaining thymus size into old age is beneficial or detrimental to immune function. There has been speculation that thymus involution is necessary to prevent the development of a

large autoimmune T cell population with age (77). This perspective stems from the correlation between the skewed TRA expression observed in TECs from aged, involuted thymi and the increased numbers of autoimmune T cells escaping selection in these thymi. Furthering this idea, thymic regeneration in mice fails to restore the TEC microenvironment and expression of TRAs after involution (177). Thus, the thought is that T cells produced in a regenerated thymus are likely to respond suboptimally and may even promote autoimmunity. Both of these observations have been made in involuted thymi but have not addressed the TRA situation in thymi that have avoided involution. Studies utilizing would put to bed this disagreement among the immunology field and clarify the help or harm a productive thymus can deliver to the aging immune system.

We've shown that even early thymus involution has a significant consequence on the size and composition of the naïve T cell population, which is essential for recognizing newly encountered antigens. Our results suggest that preventing thymus involution is truly central to preventing age-associated changes to the peripheral T cell pool. Furthermore, the T cells derived from the non-involuting K5.D1 thymus appear to be normal – there are no apparent defects in negative or positive selection of K5.D1 thymocytes, TCR diversity is maintained and the RTEs generated from the K5.D1 thymus undergo appropriate phenotypic and functional maturation in the periphery. Though K5.D1 mouse model is highly artificial, it proves that sustaining the thymic microenvironment is central to maintaining competent T cell output. Whether preventing the loss and diversity of TEC subsets adverts the skewing of TRAs expressed in the thymus remains to be seen.

*Final Thoughts*

The K5.D1 model serves as a useful tool for investigating the mechanisms responsible for loss of the TEC compartment during the stages of thymus involution. The next major question that should be answered by this model is whether preventing thymus involution enhances the T cell response to pathogen and tumor antigens throughout the lifespan. The implications from this work, whether positive or negative, would help shape the field's viewpoint on the benefits involution prevention and thymic regeneration can bring to the table as a potential therapeutic approach.

# APPENDIX 1
# AGED K5.D1 HISTOPATHOLOGY

Control and K5.D1 animals were aged to 6-8 months and necropsied to determine what, if any, autoimmunity occurred as a consequence of the K5.D1 transgene. The following representative images and histopathology report demonstrate that K5.D1 T cells do not promote autoimmunity in the peripheral organs. Furthermore, these studies have been replicated at least three separate times, with three or more control and K5.D1 replicates within each study. Therefore, we are confident that thymus hyperplasia in the K5.D1 transgenic mouse does not promote systemic autoimmunity.

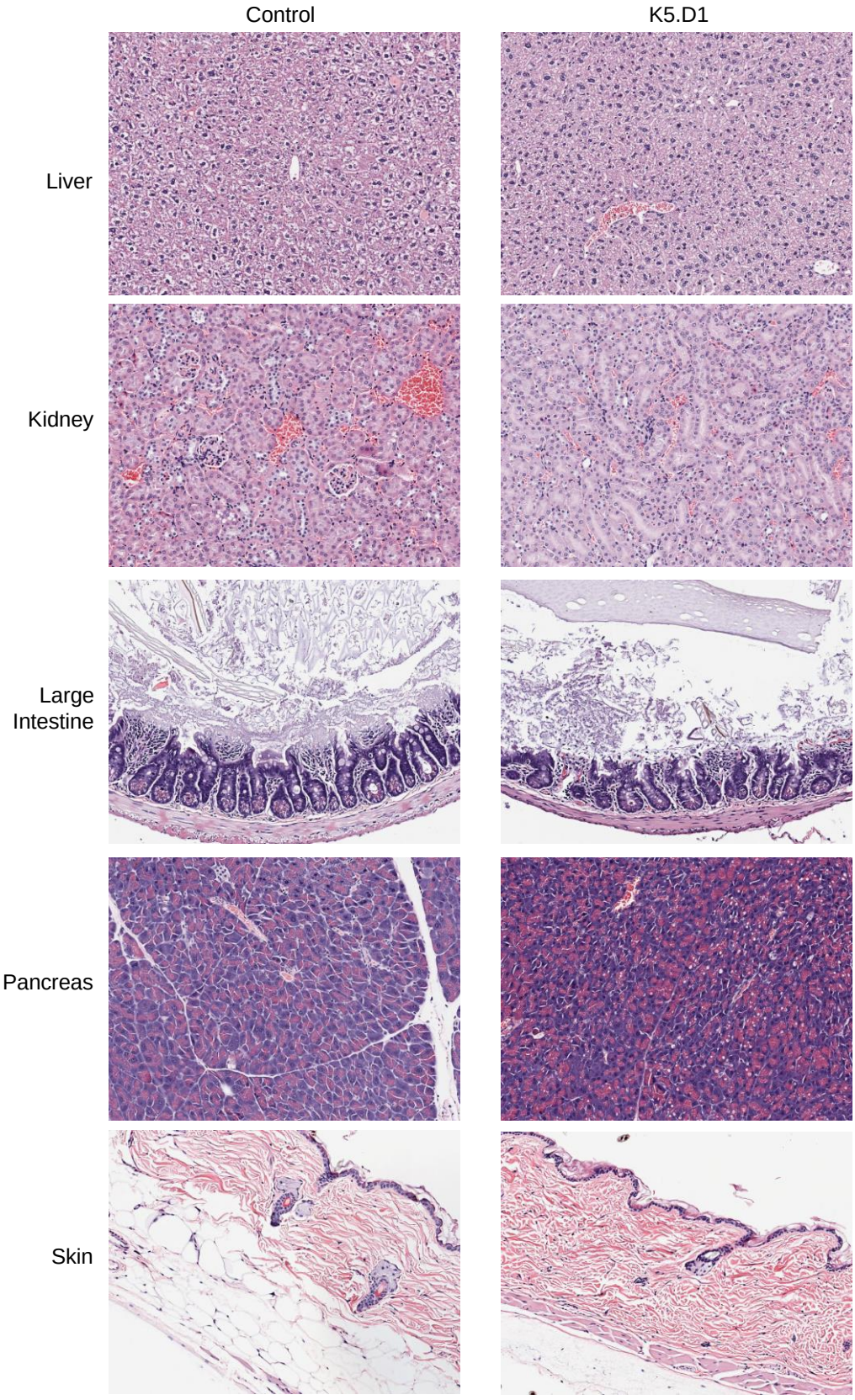
Control
K5.D1
Liver
Kidney
Large Intestine
Pancreas
Skin

| Animal # | Slide # | Tissue | Diagnosis |
|---|---|---|---|
| 2592 WT | 1 | Liver | Triaditis, lymphocytic, multifocal, minimal<br>EMH, focal, minimal |
| 2592 WT | 1 | Kidney | NSL |
| 2592 WT | 2 | Small intestine | Lamina propria - NSL<br>Peyer's patch - NP |
| 2592 WT | 2 | Large intestine | Lamina propria - NSL |
| 2592 WT | 3 | Salivary gland | Sialoadenitis, lymphoplasmacytic, multifocal, moderate |
| 2592 WT | 3 | Cervical l.n. | NSL |
| 2592 WT | 3 | Extraorbital lacrimal gland | Adenitis, lymphocytic, multifocal, mild |
| 2592 WT | 4 | Pancreas | NSL |
| 2592 WT | 4 | Skin | NSL |
| 2593 WT | 1 | Liver | Triaditis, lymphocytic, multifocal, minimal<br>EMH, multifocal, minimal |
| 2593 WT | 1 | Kidney | ISN, lymphoplasmacytic, multifocal, moderate |
| 2593 WT | 2 | Small intestine | Lamina propria - lymphoid hyperplasia, minimal<br>Peyer's patch - NSL |
| 2593 WT | 2 | Large intestine | Lamina propria - NSL |
| 2593 WT | 3 | Salivary gland | Sialoadenitis, lymphocytic, focal, mild |
| 2593 WT | 3 | Cervical l.n. | Lymphoid hyperplasia, mild |
| 2593 WT | 3 | Extraorbital lacrimal gland | Adenitis, lymphocytic, multifocal, moderate |
| 2593 WT | 4 | Pancreas | Pancreatitis, lymphocytic, focal, mild |
| 2593 WT | 4 | Skin | NSL |
| 2594 WT | 1 | Liver | Triaditis, lymphocytic, multifocal, minimal<br>Vacuolar change, centrilobular, focally extensive, moderate |
| 2594 WT | 1 | Kidney | ISN, lymphoplasmacytic, multifocal, mild |
| 2594 WT | 2 | Small intestine | Lamina propria – lymphoid hyperplasia, minimal<br>Peyer's patch - NSL |
| 2594 WT | 2 | Large intestine | Lamina propria - NSL |
| 2594 WT | 3 | Salivary gland | Sialodenitis, lymphocytic, multifocal, mild |
| 2594 WT | 3 | Cervical l.n. | Section too small to evaluate |
| 2594 WT | 3 | Extraorbital lacrimal gland | Adenitis, lymphocytic, multifocal, mild |
| 2594 WT | 4 | Pancreas | NSL |
| 2594 WT | 4 | Skin | NSL |
| 2595 D1 | 1 | Liver | Triaditis, lymphocytic, multifocal, minimal |
| 2595 D1 | 1 | Kidney | ISN, lymphoplasmacytic, multifocal, minimal |
| 2595 D1 | 2 | Small intestine | Lamina propria – lymphoid hyperplasia, |

| | | | |
|---|---|---|---|
| | | | mild<br>Peyer's patch – lymphoid hyperplasia, minimal |
| 2595 D1 | 2 | Large intestine | Lamina propria - NSL |
| 2595 D1 | 3 | Salivary gland | NSL |
| 2595 D1 | 3 | Cervical l.n. | Not present on slide |
| 2595 D1 | 3 | Extraorbital lacrimal gland | Adenitis, lymphocytic, multifocal, moderate |
| 2595 D1 | 4 | Pancreas | NSL |
| 2595 D1 | 4 | Skin | NSL |
| 2596 WT | 1 | Liver | Pyogranulomas, multiple, minimal |
| 2596 WT | 1 | Kidney | ISN, lymphoplasmacytic, multifocal, mild<br>Hydronephrosis, mild, unilateral |
| 2596 WT | 2 | Small intestine | Lamina propria - NSL<br>Peyer's patch - not present on slide |
| 2596 WT | 2 | Large intestine | Lamina propria - NSL |
| 2596 WT | 3 | Salivary gland | Sialoadenitis, lymphoplasmacytic, multifocal, moderate |
| 2596 WT | 3 | Cervical l.n. | Lymphoid hyperplasia, mild |
| 2596 WT | 3 | Extraorbital lacrimal gland | Adenitis, lymphocytic, multifocal, mild |
| 2596 WT | 4 | Pancreas | NSL |
| 2596 WT | 4 | Skin | NSL |
| 2597 D1 | 1 | Liver | Triaditis, lymphocytic, multifocal, minimal |
| 2597 D1 | 1 | Kidney | ISN, lymphocytic, multifocal, minimal |
| 2597 D1 | 2 | Small intestine | Lamina propria - NSL<br>Peyer's patch – lymphoid hyperplasia, mild |
| 2597 D1 | 2 | Large intestine | Lamina propria - NSL |
| 2597 D1 | 3 | Salivary gland | NSL |
| 2597 D1 | 3 | Cervical l.n. | NSL |
| 2597 D1 | 3 | Extraorbital lacrimal gland | Adenitis, lymphocytic, multifocal, mild |
| 2597 D1 | 4 | Pancreas | NSL |
| 2597 D1 | 4 | Skin | NSL |
| 2598 D1 | 1 | Liver | Triaditis, lymphocytic, multifocal, mild<br>Bile duct hyperplasia, multifocal, mild |
| 2598 D1 | 1 | Kidney | ISN, lymphocytic, multifocal, mild<br>Malformation of pelvis with focal epithelial hyperplasia, bilateral, moderate |
| 2598 D1 | 2 | Small intestine | Lamina propria - NSL<br>Peyer's patch – lymphoid hyperplasia, mild |
| 2598 D1 | 2 | Large intestine | Lamina propria - NSL |
| 2598 D1 | 3 | Salivary gland | Sialoadenitis, lymphocytic, multifocal, mild |
| 2598 D1 | 3 | Cervical l.n. | Lymphoid hyperplasia, moderate |
| 2598 D1 | 3 | Extraorbital lacrimal gland | Adenitis, lymphocytic, multifocal, moderate |
| 2598 D1 | 4 | Pancreas | NSL |

| | | | |
|---|---|---|---|
| 2598 D1 | 4 | Skin | NSL |

Comment:
Triaditis and lymphoid hyperplasia of lamina propria are within normal limits.

# APPENDIX 2

## RAG2$^{-/-}$ T CELL RECIPIENT HISTOPATHOLOGY

To determine peripheral environment dampens the extent of autoreactivity of T cells from K5.D1 mice, we injected FACS sorted CD4 T cells from control or K5.D1 mice into immunocompromised recipients. These mice were weighed every other day for three weeks and necropsied. A blind pathological reading of slides from multiple organs did not reveal any lymphocyte infiltrates or other signs of autoreactivity in recipients. Presented below are representative images from RAG2$^{-/-}$ recipients that received control or K5.D1 T cells, as well as the final histopathology report created by Dr. Donna Kusewitt. Taken together, we conclude that K5.D1 T cells do not possess the potential for autoreactivity.

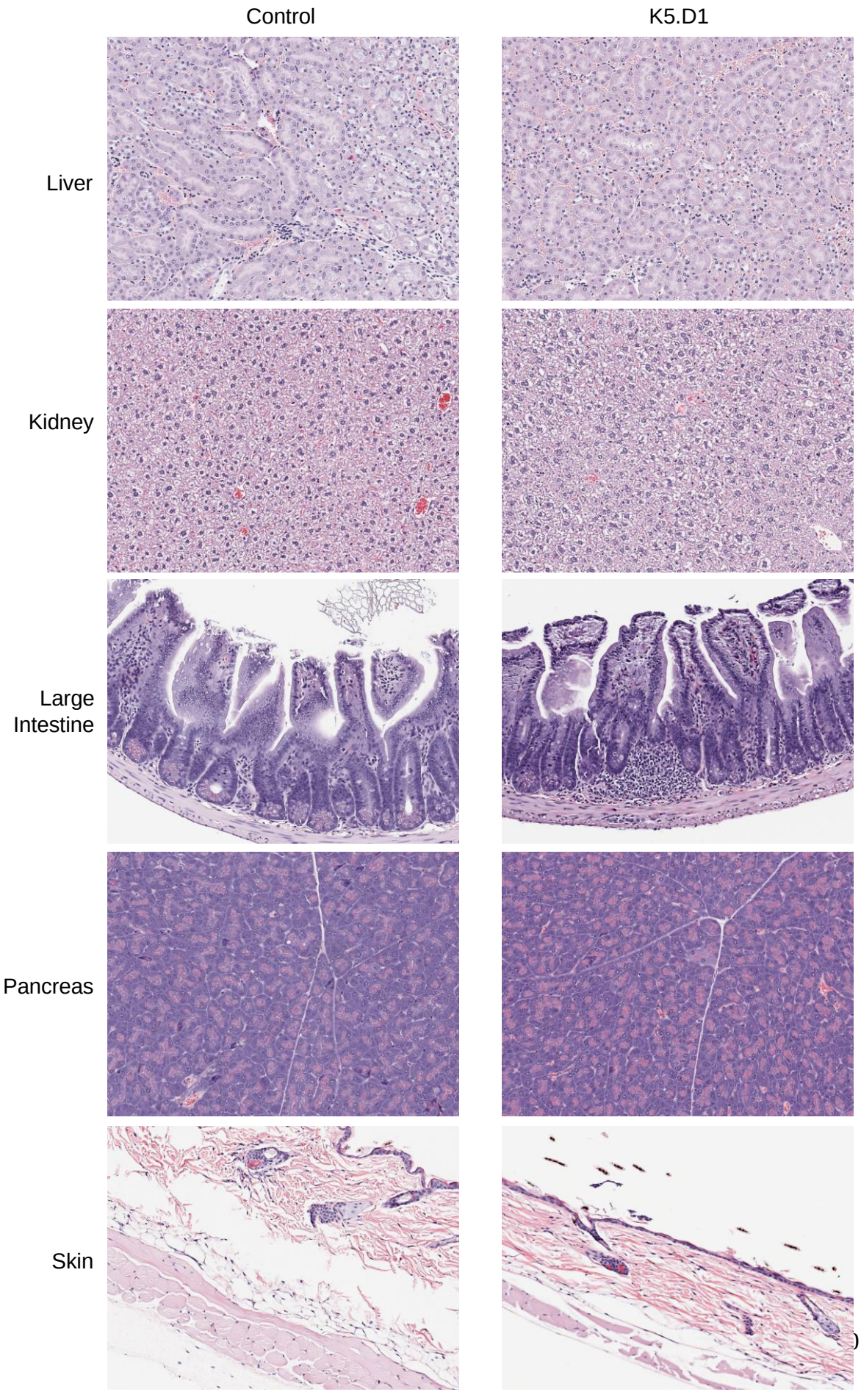
Control
K5.D1
Liver
Kidney
Large Intestine
Pancreas
Skin

FINAL REPORT
Necropsy/Histopathology Report

MM
PS #
679
INVESTIGATOR:
Ellen Richie
SUBMITTOR:
Michelle Bolner DATE
SUBMITTED: 5/7/15
DATE COMPLETED:
5/12/15

Microscopic Findings:

| Animal # | Slide # | Tissue | Diagnosis |
|---|---|---|---|
| WT 1L | 2613 - 1 | Liver | NSL |
| WT 1L | 1 | Kidney | ISN, lymphocytic, focal, mild |
| WT 1L | 2 | Small intestine | Lamina propria - NSL<br>Peyer's patch - NP |
| WT 1L | 2 | Large intestine | Lamina propria - NSL |
| WT 1L | 3 | Salivary gland | NSL |
| WT 1L | 3 | Cervical l.n. | Lymphoid hypoplasia, marked |
| WT 1L | 3 | Extraorbital lacrimal gland | NSL |
| WT 1L | 4 | Pancreas | NSL |
| WT 1L | 4 | Skin | NSL |
| WT 1L | 5 | Spleen | Lymphoid hypoplasia, moderate<br>EMH, moderate |
| WT 1L | 5 | Thymus | Hypoplasia, moderate, with no cortico-medullary demarcation |
| WT 1L | 6 | Lung | NSL |
| WT 2R | 2614 - 1 | Liver | NSL |
| WT 2R | 1 | Kidney | ISN, lymphocytic, focal, mild |
| WT 2R | 2 | Small intestine | Lamina propria - NSL<br>Peyer's patch - NP |
| WT 2R | 2 | Large intestine | Lamina propria - NSL |
| WT 2R | 3 | Salivary gland | Sialoadenitis, lymphoplasmacytic, multifocal, moderate |
| WT 2R | 3 | Cervical l.n. | NSL |
| WT 2R | 3 | Extraorbital lacrimal gland | Adenitis, lymphocytic, multifocal, mild |
| WT 2R | 4 | Pancreas | NSL |
| WT 2R | 4 | Skin | NSL |
| WT 2R | 5 | Spleen | Lymphoid hypoplasia, marked<br>EMH, moderate |

| | | | |
|---|---|---|---|
| WT 2R | 5 | Thymus | Hypoplasia, moderate, with no cortico-medullary demarcation<br>Cyst, epithelial |
| WT 2R | 6 | Lung | PB/PV, lymphocytic, focal, minimal |
| WT 3B | 2615 - 1 | Liver | Triaditis, lymphocytic, multifocal, minimal |
| WT 3B | 1 | Kidney | NSL |
| WT 3B | 2 | Small intestine | Lamina propria - NSL<br>Peyer's patch – Lymphoid hypoplasia, marked |
| WT 3B | 2 | Large intestine | Lamina propria - NSL |
| WT 3B | 3 | Salivary gland | NSL |
| WT 3B | 3 | Cervical l.n. | NP |
| WT 3B | 3 | Extraorbital lacrimal gland | NSL |
| WT 3B | 4 | Pancreas | NSL |
| WT 3B | 4 | Skin | NSL |
| WT 3B | 5 | Spleen | Lymphoid hypoplasia, moderate<br>EMH, mild |
| WT 3B | 5 | Thymus | Hypoplasia, moderate, with no cortico-medullary demarcation<br>Cysts |
| WT 3B | 6 | Lung | PB/PV, lymphocytic, multifocal, moderate<br>(lung not fully expanded) |
| WT 9L | 2621 - 1 | Liver | Triaditis, lymphocytic, multifocal, mild |
| WT 9L | 1 | Kidney | ISN, lymphocytic, multifocal, minimal |
| WT 9L | 2 | Small intestine | Lamina propria – enteritis, lymphocytic, multifocal, minimal<br>Peyer's patch – lymphoid hypoplasia, marked |
| WT 9L | 2 | Large intestine | Lamina propria - NSL |
| WT 9L | 3 | Salivary gland | NSL |
| WT 9L | 3 | Cervical l.n. | Lymphoid hypoplasia, moderate |
| WT 9L | 3 | Extraorbital lacrimal gland | NSL |
| WT 9L | 4 | Pancreas | Pancreatitis (periductal), lymphocytic, multifocal, minimal |
| WT 9L | 4 | Skin | Folliculitis, lymphocytic, multifocal, minimal |
| WT 9L | 5 | Spleen | Lymphoid hypoplasia, moderate<br>EMH, marked |
| WT 9L | 5 | Thymus | Hypoplasia, moderate, with no cortico-medullary demarcation |
| WT 9L | 6 | Lung | PB/PV, lymphocytic, multifocal, mild |
| D1 4 2R | 2616 - 1 | Liver | Triaditis, lymphocytic, multifocal, mild<br>Microgranuloma, single, minimal |
| D1 4 2R | 1 | Kidney | NSL |

| | | | |
|---|---|---|---|
| D1 4 2R | 2 | Small intestine | Lamina propria – enteritis, lymphocytic, multifocal, minimal<br>Peyer's patch – lymphoid hypoplasia, moderate |
| D1 4 2R | 2 | Large intestine | Lamina propria - NSL |
| D1 4 2R | 3 | Salivary gland | NSL |
| D1 4 2R | 3 | Cervical l.n. | Lymphoid hypoplasia, moderate |
| D1 4 2R | 3 | Extraorbital lacrimal gland | Adenitis, lymphocytic, multifocal, mild |
| D1 4 2R | 4 | Pancreas | Pancreatitis (periductal), lymphocytic, multifocal, mild |
| D1 4 2R | 4 | Skin | NSL |
| D1 4 2R | 5 | Spleen | Lymphoid hypoplasia, moderate<br>EMH, moderate |
| D1 4 2R | 5 | Thymus | Hypoplasia, marked, with no cortico-medullary demarcation |
| D1 4 2R | 6 | Lung | PB/PV, lymphocytic, multifocal, moderate |
| D1 5N | 2617 - 1 | Liver | Triaditis, lymphocytic, multifocal, mild |
| D1 5N | 1 | Kidney | ISN, lymphocytic, focal, mild |
| D1 5N | 2 | Small intestine | Lamina propria – NSL<br>Peyer's patch – NP |
| D1 5N | 2 | Large intestine | Lamina propria - NSL |
| D1 5N | 3 | Salivary gland | NSL |
| D1 5N | 3 | Cervical l.n. | Lymphoid hypoplasia, moderate |
| D1 5N | 3 | Extraorbital lacrimal gland | NSL |
| D1 5N | 4 | Pancreas | NSL |
| D1 5N | 4 | Skin | NSL |
| D1 5N | 5 | Spleen | Lymphoid hypoplasia, moderate<br>EMH, moderate |
| D1 5N | 5 | Thymus | Hypoplasia, moderate, with no cortico-medullary demarcation<br>Cysts, multiple |
| D1 5N | 6 | Lung | PB/PV, lymphocytic, multifocal, minimal |
| D1 6R | 2618 - 1 | Liver | Triaditis, lymphocytic, multifocal, minimal |
| D1 6R | 1 | Kidney | ISN, lymphocytic, multifocal, mild |
| D1 6R | 2 | Small intestine | Lamina propria – enteritis, lymphocytic, multifocal, minimal<br>Peyer's patch – NP |
| D1 6R | 2 | Large intestine | Lamina propria - NSL |
| D1 6R | 3 | Salivary gland | NSL |
| D1 6R | 3 | Cervical l.n. | NP |
| D1 6R | 3 | Extraorbital lacrimal gland | Adenitis, lymphocytic, multifocal, marked |

| | | | |
|---|---|---|---|
| D1 6R | 4 | Pancreas | NSL |
| D1 6R | 4 | Skin | Perifolliculitis, lymphocytic, multifocal, mild |
| D1 6R | 5 | Spleen | Lymphoid hypoplasia, marked<br>EMH, marked |
| D1 6R | 5 | Thymus | Hypoplasia, moderate, with no cortico-medullary demarcation |
| D1 6R | 6 | Lung | PB/PV, lymphocytic, multifocal, moderate |
| D1 7B | 2619 - 1 | Liver | Triaditis, lymphocytic, multifocal, minimal |
| D1 7B | 1 | Kidney | NSL |
| D1 7B | 2 | Small intestine | Lamina propria – enteritis, lymphocytic, multifocal, minimal<br>Peyer's patch – lymphoid hypoplasia, marked |
| D1 7B | 2 | Large intestine | Lamina propria - NSL |
| D1 7B | 3 | Salivary gland | NSL |
| D1 7B | 3 | Cervical l.n. | Lymphoid hypoplasia, marked |
| D1 7B | 3 | Extraorbital lacrimal gland | Adenitis, lymphocytic, multifocal, minimal |
| D1 7B | 4 | Pancreas | NSL |
| D1 7B | 4 | Skin | Folliculitis, lymphocytic, focal, minimal |
| D1 7B | 5 | Spleen | Lymphoid hypoplasia, marked<br>EMH, marked |
| D1 7B | 5 | Thymus | Hypoplasia, moderate, with no cortico-medullary demarcation |
| D1 7B | 6 | Lung | PB/PV, lymphocytic, multifocal, minimal |
| D1 10R | 2622 - 1 | Liver | Hepatitis, pyogranulomatous, multifocal, marked |
| D1 10R | 1 | Kidney | ISN, lymphocytic, multifocal, mild |
| D1 10R | 2 | Small intestine | Lamina propria- enteritis, lymphocytic, multifocal, minimal<br>Peyer's patch – lymphoid hypoplasia, moderate |
| D1 10R | 2 | Large intestine | Lamina propria - NSL |
| D1 10R | 3 | Salivary gland | NSL |
| D1 10R | 3 | Cervical l.n. | NP |
| D1 10R | 3 | Extraorbital lacrimal gland | NSL |
| D1 10R | 4 | Pancreas | NSL |
| D1 10R | 4 | Skin | NSL |
| D1 10R | 5 | Spleen | Lymphoid hypoplasia, moderate<br>EMH, marked |
| D1 10R | 5 | Thymus | Hypoplasia, moderate, with no cortico-medullary demarcation |
| D1 10R | 6 | Lung | PB/PV, lymphocytic, multifocal, mild |
| D1 11B | 2623 - 1 | Liver | Triaditis, lymphocytic, multifocal, minimal |

| | | | |
|---|---|---|---|
| D1 11B | 1 | Kidney | NSL |
| D1 11B | 2 | Small intestine | Lamina propria- enteritis, lymphocytic, multifocal, mild<br>Peyer's patch – lymphoid hypoplasia, marked |
| D1 11B | 2 | Large intestine | Lamina propria – colitis, diffuse, mild |
| D1 11B | 3 | Salivary gland | NSL |
| D1 11B | 3 | Cervical l.n. | Lymphoid hypoplasia, moderate |
| D1 11B | 3 | Extraorbital lacrimal gland | Adenitis, granulocytic and lymphocytic, multifocal, marked |
| D1 11B | 4 | Pancreas | Pancreatitis, lymphocytic, focal, minimal<br>Periarteritis, granulomatous, focal, moderate |
| D1 11B | 4 | Skin | Folliculitis, lymphocytic, focal, minimal |
| D1 11B | 5 | Spleen | Lymphoid hypoplasia, marked<br>EMH, marked |
| D1 11B | 5 | Thymus | Hypoplasia, moderate, with no cortico-medullary demarcation |
| D1 11B | 6 | Lung | PB/PV, lymphocytic, multifocal, moderate |
| PBS 8 2R | 2620 - 1 | Liver | Triaditis, lymphocytic, multifocal, minimal |
| PBS 8 2R | 1 | Kidney | NSL |
| PBS 8 2R | 2 | Small intestine | Lamina propria- enteritis, lymphocytic, multifocal, minimal<br>Peyer's patch - NP |
| PBS 8 2R | 2 | Large intestine | Lamina propria - NSL |
| PBS 8 2R | 3 | Salivary gland | NSL |
| PBS 8 2R | 3 | Cervical l.n. | NP |
| PBS 8 2R | 3 | Extraorbital lacrimal gland | NSL |
| PBS 8 2R | 4 | Pancreas | Pancreatitis (periductal), lymphocytic, focal, minimal |
| PBS 8 2R | 4 | Skin | NSL |
| PBS 8 2R | 5 | Spleen | Lymphoid hypoplasia, marked<br>EMH, moderate |
| PBS 8 2R | 5 | Thymus | Hypoplasia, moderate, with no cortico-medullary demarcation<br>Cyst |
| PBS 8 2R | 6 | Lung | Eosinophilic macrophage pneumonia, focal, moderate |
| PBS 12 2L | 2624 - 1 | Liver | Triaditis, lymphocytic, multifocal, minimal |
| PBS 12 2L | 1 | Kidney | ISN, lymphocytic, multifocal, minimal |
| PBS 12 2L | 2 | Small intestine | Lamina propria- enteritis, lymphocytic, multifocal, minimal<br>Peyer's patch – lymphoid hypoplasia, marked |
| PBS 12 2L | 2 | Large intestine | Lamina propria - NSL |

| | | | |
|---|---|---|---|
| PBS 12 2L | 3 | Salivary gland | Adenitis, granulocytic and lymphocytic, focal, minimal |
| PBS 12 2L | 3 | Cervical l.n. | NP |
| PBS 12 2L | 3 | Extraorbital lacrimal gland | NSL |
| PBS 12 2L | 4 | Pancreas | NSL |
| PBS 12 2L | 4 | Skin | Perifolliculitis, lymphocytic, focal, minimal |
| PBS 12 2L | 5 | Spleen | Lymphoid hypoplasia, marked<br>EMH, moderate |
| PBS 12 2L | 5 | Thymus | Hypoplasia, marked, with no cortico-medullary demarcation |
| PBS 12 2L | 6 | Lung | PB/PV, lymphocytic, multifocal, minimal |

Interpretation: Inflammatory infiltrates termed “lymphocytic” are composed primarily of mononuclear cells admixed with small numbers of granulocytes. The identity of the mononuclear cells as lymphocytes should be verified by IHC.

Lymphocytes in these mice do not appear to be fully mature, as they have large, poorly condensed nuclei.

Lesions termed “minimal” likely represent findings within normal limits, and probably should not be counted as true lesions.

The eosinophilic macrophage pneumonia in mouse PBS 8 2R is likely an incidental finding.
.

Donna F. Kusewitt 5/12/15

Donna F. Kusewitt, DVM, PhD, ACVP Date

## Bibliography


1. Yager, E. J., M. Ahmed, K. Lanzer, T. D. Randall, D. L. Woodland, and M. A. Blackman. 2008. Age-associated decline in T cell repertoire diversity leads to holes in the repertoire and impaired immunity to influenza virus. *The Journal of experimental medicine* 205: 711-723.

2. Goronzy, J. J., G. Li, Z. Yang, and C. M. Weyand. 2013. The janus head of T cell aging - autoimmunity and immunodeficiency. *Frontiers in immunology* 4: 131.

3. Ahmed, M., K. G. Lanzer, E. J. Yager, P. S. Adams, L. L. Johnson, and M. A. Blackman. 2009. Clonal expansions and loss of receptor diversity in the naive CD8 T cell repertoire of aged mice. *Journal of immunology* 182: 784-792.

4. Lefebvre, J. S., A. C. Maue, S. M. Eaton, P. A. Lanthier, M. Tighe, and L. Haynes. 2012. The aged microenvironment contributes to the age-related functional defects of CD4 T cells in mice. *Aging cell* 11: 732-740.

5. Haynes, L., S. M. Eaton, E. M. Burns, T. D. Randall, and S. L. Swain. 2003. CD4 T cell memory derived from young naive cells functions well into old age, but memory generated from aged naive cells functions poorly. *Proceedings of the National Academy of Sciences of the United States of America* 100: 15053-15058.

6. Manley, N. R. R., E.R.; Blackburn, C.C.; Condie, B.G.; Sage, J. 2011. Structure and function of the thymic microenvironment. *Frontiers in Bioscience* 16: 2461-2477.

7. Petrie, H. T., and J. C. Zuniga-Pflucker. 2007. Zoned out: functional mapping of stromal signaling microenvironments in the thymus. *Annual review of immunology* 25: 649-679.

8. Lind, E., Prockop SE, Porritt HE, Petrie HT. 2001. Mapping Precursor Movement through the Postnatal Thymus Reveals Specific Microenvironments Supporting Defined Stages of Early Lymphoid Development. *Journal of Experimental Medicine* 194: 127-134.

9. Bhandoola, A., H. von Boehmer, H. T. Petrie, and J. C. Zuniga-Pflucker. 2007. Commitment and developmental potential of extrathymic and intrathymic T cell precursors: plenty to choose from. *Immunity* 26: 678-689.

10. Koch, U., and F. Radtke. 2011. Mechanisms of T cell development and transformation. *Annual review of cell and developmental biology* 27: 539-562.

11. Goldschneider, I. 2006. Cyclical mobilization and gated importation of thymocyte progenitors in the adult mouse: evidence for a thymus-bone marrow feedback loop. *Immunological reviews* 209: 58-75.

12. Shortman K, W., L. 1996. Early T Lymphocyte Progenitors. *Annual review of immunology*: 29-47.

13. Bell, J. J., and A. Bhandoola. 2008. The earliest thymic progenitors for T cells possess myeloid lineage potential. *Nature* 452: 764-767.

14. Schmitt, T. M., M. Ciofani, H. T. Petrie, and J. C. Zuniga-Pflucker. 2004. Maintenance of T cell specification and differentiation requires recurrent notch receptor-ligand interactions. *The Journal of experimental medicine* 200: 469-479.

15. Koch, U., E. Fiorini, R. Benedito, V. Besseyrias, K. Schuster-Gossler, M. Pierres, N. R. Manley, A. Duarte, H. R. Macdonald, and F. Radtke. 2008. Delta-like 4 is the essential, nonredundant ligand for Notch1 during thymic T cell lineage commitment. *The Journal of experimental medicine* 205: 2515-2523.

16. Hozumi, K., C. Mailhos, N. Negishi, K. Hirano, T. Yahata, K. Ando, S. Zuklys, G. A. Hollander, D. T. Shima, and S. Habu. 2008. Delta-like 4 is indispensable in thymic environment specific for T cell development. *The Journal of experimental medicine* 205: 2507-2513.

17. Shah, D. K., and J. C. Zuniga-Pflucker. 2014. An overview of the intrathymic intricacies of T cell development. *Journal of immunology* 192: 4017-4023.

18. Feyerabend, T. B., G. Terszowski, A. Tietz, C. Blum, H. Luche, A. Gossler, N. W. Gale, F. Radtke, H. J. Fehling, and H. R. Rodewald. 2009. Deletion of Notch1 converts pro-T cells to dendritic cells and promotes thymic B cells by cell-extrinsic and cell-intrinsic mechanisms. *Immunity* 30: 67-79.

19. Wada, H., K. Masuda, R. Satoh, K. Kakugawa, T. Ikawa, Y. Katsura, and H. Kawamoto. 2008. Adult T-cell progenitors retain myeloid potential. *Nature* 452: 768-772.

20. Wilson, A., H. R. MacDonald, and F. Radtke. 2001. Notch 1-deficient common lymphoid precursors adopt a B cell fate in the thymus. *The Journal of experimental medicine* 194: 1003-1012.

21. Murphy, K. T., P.; Walport, M.; Janeway, C. 2012. *Janeway's Immunobiology*. Garland Science, New York.

22. Kang, J. V., A.; Raulet, DH. 2001. Evidence That γδ versus αβ T Cell Fate Determination Is Initiated Independently of T Cell Receptor Signaling. *Journal of Experimental Medicine* 193: 689-698.

23. Ciofani, M., and J. C. Zuniga-Pflucker. 2010. Determining gammadelta versus alphass T cell development. *Nature reviews. Immunology* 10: 657-663.

24. Michie, A. M., and J. C. Zúñiga-Pflücker. 2002. Regulation of thymocyte differentiation: pre-TCR signals and β-selection. *Seminars in Immunology* 14: 311-323.

25. von Boehmer, H. 2005. Unique features of the pre-T-cell receptor α-chain: not just a surrogate. *Nature reviews. Immunology* 5: 571-577.

26. Penit, C., B. Lucas, and F. Vasseur. 1995. Cell expansion and growth arrest phases during the transition from precursor (CD4-8-) to immature (CD4+8+) thymocytes in normal and genetically modified mice. *Journal of immunology* 154: 5103-5113.

27. Klein, L., M. Hinterberger, G. Wirnsberger, and B. Kyewski. 2009. Antigen presentation in the thymus for positive selection and central tolerance induction. *Nature reviews. Immunology* 9: 833-844.

28. Takada, K., and Y. Takahama. 2015. Positive-selection-inducing self-peptides displayed by cortical thymic epithelial cells. *Advances in immunology* 125: 87-110.

29. Kurobe, H., C. Liu, T. Ueno, F. Saito, I. Ohigashi, N. Seach, R. Arakaki, Y. Hayashi, T. Kitagawa, M. Lipp, R. L. Boyd, and Y. Takahama. 2006. CCR7-dependent cortex-to-medulla migration of positively selected thymocytes is essential for establishing central tolerance. *Immunity* 24: 165-177.

30. Klein, L., B. Kyewski, P. M. Allen, and K. A. Hogquist. 2014. Positive and negative selection of the T cell repertoire: what thymocytes see (and don't see). *Nature reviews. Immunology* 14: 377-391.

31. Overgaard, N. H., J. Jung, R. J. Steptoe, and J. W. Wells. 2015. CD4+/CD8+ double-positive T cells: more than just a developmental stage? *Journal of leukocyte biology* 97: 31-38.

32. McCaughtry, T. M., R. Etzensperger, A. Alag, X. Tai, S. Kurtulus, J. H. Park, A. Grinberg, P. Love, L. Feigenbaum, B. Erman, and A. Singer. 2012. Conditional deletion of cytokine receptor chains reveals that IL-7 and IL-15 specify CD8 cytotoxic lineage fate in the thymus. *The Journal of experimental medicine* 209: 2263-2276.

33. Singer, A., S. Adoro, and J. H. Park. 2008. Lineage fate and intense debate: myths, models and mechanisms of CD4- versus CD8-lineage choice. *Nature reviews. Immunology* 8: 788-801.

34. Brugnera, E. B., A.; Cibotti, R.; Yu, Q.; Guinter, T.I.; Yamashita, Y.; Sharrow, S.O.; Singer, A. 2000. Coreceptor Reversal in the thymus: signaled CD4+8+ thymocytes initially terminate CD8 transcription even when differentiating into CD8+ T cells. *Immunity* 13: 59-71.

35. Kyewski, B., and L. Klein. 2006. A central role for central tolerance. *Annual review of immunology* 24: 571-606.

36. Koble, C., and B. Kyewski. 2009. The thymic medulla: a unique microenvironment for intercellular self-antigen transfer. *The Journal of experimental medicine* 206: 1505-1513.

37. Stritesky, G. L., Y. Xing, J. R. Erickson, L. A. Kalekar, X. Wang, D. L. Mueller, S. C. Jameson, and K. A. Hogquist. 2013. Murine thymic selection quantified using a unique method to capture deleted T cells. *Proceedings of the National Academy of Sciences of the United States of America* 110: 4679-4684.

38. Anderson, M. S. V., E. S.; Klein, L.; Chen, Z.; Berzins, S. P.; Turley, S. J.; von Boehmer, H.; Bronson, R.; Dierich, A.; Benoist, C.; Mathis, D. 2002. Projection of an immunological self shadow within the thymus by the aire protein. *Science* 298: 1395-1401.

39. Coquet, J. M., J. C. Ribot, N. Babala, S. Middendorp, G. van der Horst, Y. Xiao, J. F. Neves, D. Fonseca-Pereira, H. Jacobs, D. J. Pennington, B. Silva-Santos, and J. Borst. 2013. Epithelial and dendritic cells in the thymic medulla promote CD4+Foxp3+ regulatory T cell development via the CD27-CD70 pathway. *The Journal of experimental medicine* 210: 715-728.

40. Xu, X., S. Zhang, P. Li, J. Lu, Q. Xuan, and Q. Ge. 2013. Maturation and emigration of single-positive thymocytes. *Clinical & developmental immunology* 2013: 282870.

41. Carlson, C. M., B. T. Endrizzi, J. Wu, X. Ding, M. A. Weinreich, E. R. Walsh, M. A. Wani, J. B. Lingrel, K. A. Hogquist, and S. C. Jameson. 2006. Kruppel-like factor 2 regulates thymocyte and T-cell migration. *Nature* 442: 299-302.

42. Zachariah, M. A., and J. G. Cyster. 2010. Neural crest-derived pericytes promote egress of mature thymocytes at the corticomedullary junction. *Science* 328: 1129-1135.

43. Cyster, J. G., and S. R. Schwab. 2012. Sphingosine-1-phosphate and lymphocyte egress from lymphoid organs. *Annual review of immunology* 30: 69-94.

44. Matloubian, M. L., C.G.; Cinamon, G.; Lesneski, M.J.; Xu, Y.; Brinkmann, V.; Allende, M.L.; Proia, R.L.; Cyster, J.G. 2004. Lymphocyte egress from thymus and peripheral lymphoid organs is dependent on S1P receptor 1. *Nature* 427: 355-360.

45. Feng, C. W., K.J.; Vance, B.A.; El-Khoury, D.; Canelles, M.; Lee, J.; Gress, R.; Fowlkes, B.J.; Shores, E.W.; Love, P.E. 2002. A potential role for CD69 in thymocyte emigration. *International Immunology* 14: 535-544.

46. Barbee, S. D., and J. Alberola-Ila. 2005. Phosphatidylinositol 3-Kinase Regulates Thymic Exit. *The Journal of Immunology* 174: 1230-1238.

47. Suniara R.K.; Jenkinson, E. J. O., J.J. 2000. An essential role for thymic mesenchyme in early t cell development. *The Journal of experimental medicine* 191: 1051-1056.

48. Calderon, L., and T. Boehm. 2011. Three chemokine receptors cooperatively regulate homing of hematopoietic progenitors to the embryonic mouse thymus. *Proceedings of the National Academy of Sciences of the United States of America* 108: 7517-7522.

49. Shitara, S. H., T.; Liang, B.; Wagatsuma, K.; Zuklys, S.; Hollander, G. A.; Nakase, H.; Chiba, T.; Tani-ichi, S.; Ikuta, K. 2013. IL-7 produced by thymic epithelial cells plays a major role in the development of thymocytes and TCRγδ+ Intraepithelial Lymphocytes. *Journal of immunology* 190: 6173-6179.

50. Xing, Y., S. C. Jameson, and K. A. Hogquist. 2013. Thymoproteasome subunit-beta5T generates peptide-MHC complexes specialized for positive selection. *Proceedings of the National Academy of Sciences of the United States of America* 110: 6979-6984.

51. Murata, S., K. Sasaki, T. Kishimoto, S. Niwa, H. Hayashi, Y. Takahama, and K. Tanaka. 2007. Regulation of CD8+ T cell development by thymus-specific proteasomes. *Science* 316: 1349-1353.

52. Yano, M., N. Kuroda, H. Han, M. Meguro-Horike, Y. Nishikawa, H. Kiyonari, K. Maemura, Y. Yanagawa, K. Obata, S. Takahashi, T. Ikawa, R. Satoh, H. Kawamoto, Y. Mouri, and M. Matsumoto. 2008. Aire controls the differentiation program of thymic epithelial cells in the medulla for the establishment of self-tolerance. *The Journal of experimental medicine* 205: 2827-2838.

53. Blackburn, C. C. A., C.L.; Li, R.; Harvey, R.P.; Malin, M.A.; Boyd, R.L.; Miller, J.F.A.P.; Morahan, G. 1996. The nu geneacts cell-autonomously and is required for differentiation of thymic epithelia lprogenitors. *Proc Natl Acad Sci U S A* 93: 5742-5746.

54. Corbeaux, T. H., I.; Swann, J.B.; Kanzler, B.; Haas-Assenbaum, A.; Boehm, T. 2010. Thymopoiesis in mice depends on a Foxn1-positive thymic epithelial cell lineage. *Proceedings of the National Academy of Sciences of the United States of America* 107: 16613-16618.

55. Rossi, S. W., W. E. Jenkinson, G. Anderson, and E. J. Jenkinson. 2006. Clonal analysis reveals a common progenitor for thymic cortical and medullary epithelium. *Nature* 441: 988-991.

56. Bennett, A. R., A. Farley, N. F. Blair, J. Gordon, L. Sharp, and C. C. Blackburn. 2002. Identification and characterization of thymic epithelial progenitor cells. *Immunity* 16: 803-814.

57. Gray, D. H., N. Seach, T. Ueno, M. K. Milton, A. Liston, A. M. Lew, C. C. Goodnow, and R. L. Boyd. 2006. Developmental kinetics, turnover, and stimulatory capacity of thymic epithelial cells. *Blood* 108: 3777-3785.

58. Alves, N. L., Y. Takahama, I. Ohigashi, A. R. Ribeiro, S. Baik, G. Anderson, and W. E. Jenkinson. 2014. Serial progression of cortical and medullary thymic epithelial microenvironments. *European journal of immunology* 44: 16-22.

59. Wong, K., N. L. Lister, M. Barsanti, J. M. Lim, M. V. Hammett, D. M. Khong, C. Siatskas, D. H. Gray, R. L. Boyd, and A. P. Chidgey. 2014. Multilineage potential and self-renewal define an epithelial progenitor cell population in the adult thymus. *Cell reports* 8: 1198-1209.

60. Ucar, A., O. Ucar, P. Klug, S. Matt, F. Brunk, T. G. Hofmann, and B. Kyewski. 2014. Adult thymus contains FoxN1(-) epithelial stem cells that are bipotent for medullary and cortical thymic epithelial lineages. *Immunity* 41: 257-269.

61. Anderson, G., and Y. Takahama. 2012. Thymic epithelial cells: working class heroes for T cell development and repertoire selection. *Trends in immunology* 33: 256-263.

62. Ripen, A. M., T. Nitta, S. Murata, K. Tanaka, and Y. Takahama. 2011. Ontogeny of thymic cortical epithelial cells expressing the thymoproteasome subunit beta5t. *European journal of immunology* 41: 1278-1287.

63. Anderson, G., S. Baik, J. E. Cowan, A. M. Holland, N. I. McCarthy, K. Nakamura, S. M. Parnell, A. J. White, P. J. Lane, E. J. Jenkinson, and W. E. Jenkinson. 2014. Mechanisms of thymus medulla development and function. *Current topics in microbiology and immunology* 373: 19-47.

64. Klug, D. B., C. Carter, I. B. Gimenez-Conti, and E. R. Richie. 2002. Cutting Edge: Thymocyte-Independent and Thymocyte-Dependent Phases of Epithelial Patterning in the Fetal Thymus. *The Journal of Immunology* 169: 2842-2845.

65. Fiorini, E., I. Ferrero, E. Merck, S. Favre, M. Pierres, S. A. Luther, and H. R. MacDonald. 2008. Cutting Edge: Thymic Crosstalk Regulates Delta-Like 4 Expression on Cortical Epithelial Cells. *The Journal of Immunology* 181: 8199-8203.

66. Penit, C., B. Lucas, F. Vasseur, T. Rieker, and R. L. Boyd. 1996. Thymic medulla epithelial cells acquire specific markers by post-mitotic maturation. *Developmental immunology* 5: 25-36.

67. Surh, C. D. E., B.; Sprent, J. 1992. Growth of Epithelial Cells in the Thymic Medulla Is Under the Control of Mature T Cells. *Journal of Experimental Medicine* 176: 611-616.

68. Naspetti, M. A.-L., M.; DeKoning, J,; Malissen, M.; Galland, F.; Lo, D.; Naquet, P. 1997. Thymocytes and RelB-dependent medullary epithelial cells provide growth-promoting and organization signals, respectively, to thymic medullary stromal cells. *European journal of immunology* 27: 1392-1397.

69. Hikosaka, Y., T. Nitta, I. Ohigashi, K. Yano, N. Ishimaru, Y. Hayashi, M. Matsumoto, K. Matsuo, J. M. Penninger, H. Takayanagi, Y. Yokota, H. Yamada, Y. Yoshikai, J. Inoue, T. Akiyama, and Y. Takahama. 2008. The cytokine RANKL produced by positively selected thymocytes fosters medullary thymic epithelial cells that express autoimmune regulator. *Immunity* 29: 438-450.

70. Rossi, S. W., M. Y. Kim, A. Leibbrandt, S. M. Parnell, W. E. Jenkinson, S. H. Glanville, F. M. McConnell, H. S. Scott, J. M. Penninger, E. J. Jenkinson, P. J. Lane, and G. Anderson. 2007. RANK signals from CD4(+)3(-) inducer cells regulate development of Aire-expressing epithelial cells in the thymic medulla. *The Journal of experimental medicine* 204: 1267-1272.

71. Steinmann, G. G. K., B.; Muller-Hermelink, H.K. 1985. The Involution of the Ageing Human Thymic Epithelium is Independent of Puberty. *Scandinavian journal of immunology* 22: 563-575.

72. Hale, J. S., T. E. Boursalian, G. L. Turk, and P. J. Fink. 2006. Thymic output in aged mice. *Proceedings of the National Academy of Sciences of the United States of America* 103: 8447-8452.

73. Lynch, H. E., G. L. Goldberg, A. Chidgey, M. R. Van den Brink, R. Boyd, and G. D. Sempowski. 2009. Thymic involution and immune reconstitution. *Trends in immunology* 30: 366-373.

74. Qi, Q., Y. Liu, Y. Cheng, J. Glanville, D. Zhang, J. Y. Lee, R. A. Olshen, C. M. Weyand, S. D. Boyd, and J. J. Goronzy. 2014. Diversity and clonal selection in the human T-cell repertoire. *Proceedings of the National Academy of Sciences of the United States of America* 111: 13139-13144.

75. Maue, A. C., E. J. Yager, S. L. Swain, D. L. Woodland, M. A. Blackman, and L. Haynes. 2009. T-cell immunosenescence: lessons learned from mouse models of aging. *Trends in immunology* 30: 301-305.

76. Haynes, L., and S. L. Swain. 2006. Why aging T cells fail: implications for vaccination. *Immunity* 24: 663-666.

77. Boehm, T., and J. B. Swann. 2013. Thymus involution and regeneration: two sides of the same coin? *Nature reviews. Immunology* 13: 831-838.

78. Mackall, C. L., J. A. Punt, P. Morgan, A. G. Farr, and R. E. Gress. 1998. Thymic function in young/old chimeras: substantial thymic T cell regenerative capacity despite irreversible age-associated thymic involution. *European journal of immunology* 28: 1886-1893.

79. Zhu, X. G., J.; Dohkan, J.; Cheng, L.; Barnes, P. F.; Su, D. 2007. Lymphohematopoietic progenitors do not have a synchronized defect with age-related thymic involution. *Aging cell* 6: 663-672.

80. Ortman, C. L. D., K.A.; Witte, P.L.; Le, P.T. 2002. Molecular characterization of the mouse involuted thymus: aberrations in expression of transcription regulators in thymocyte and epithelial compartments. *International Immunology* 14: 813-822.

81. Chen, L., S. Xiao, and N. R. Manley. 2009. Foxn1 is required to maintain the postnatal thymic microenvironment in a dosage-sensitive manner. *Blood* 113: 567-574.

82. Zook, E. C., P. A. Krishack, S. Zhang, N. J. Zeleznik-Le, A. B. Firulli, P. L. Witte, and P. T. Le. 2011. Overexpression of Foxn1 attenuates age-associated thymic involution and prevents the expansion of peripheral CD4 memory T cells. *Blood* 118: 5723-5731.

83. Bredenkamp, N., C. S. Nowell, and C. C. Blackburn. 2014. Regeneration of the aged thymus by a single transcription factor. *Development* 141: 1627-1637.

84. Jin, X. N., C.S.; Ulyanchenko, S.; Stenhouse, F.H.; Blackburn, C.C. 2014. Long-term persistence of functional thymic epithelial progenitor cells in vivo under conditions of low FOXN1 expression. *PloS one* 9: 1-16.

85. Youm, Y. H., H. Yang, Y. Sun, R. G. Smith, N. R. Manley, B. Vandanmagsar, and V. D. Dixit. 2009. Deficient ghrelin receptor-mediated signaling compromises thymic

stromal cell microenvironment by accelerating thymic adiposity. *The Journal of biological chemistry* 284: 7068-7077.

86. Sempowski, G. D., L. P. Hale, J. S. Sundy, J. M. Massey, R. A. Koup, D. C. Douek, D. D. Patel, and B. F. Haynes. 2000. Leukemia Inhibitory Factor, Oncostatin M, IL-6, and Stem Cell Factor mRNA Expression in Human Thymus Increases with Age and Is Associated with Thymic Atrophy. *The Journal of Immunology* 164: 2180-2187.

87. Yang, H., Y. H. Youm, and V. D. Dixit. 2009. Inhibition of thymic adipogenesis by caloric restriction is coupled with reduction in age-related thymic involution. *Journal of immunology* 183: 3040-3052.

88. Yang, H. Y., Y.; Vandanmagsar, B.; Rood, J.; Kumar, G.; Butler, A.A.; Dixit, V.D. 2009. Obesity accelerates thymic aging. *Blood* 114: 3803-3812.

89. Henderson, J. 1904. On the relationship of the thymus to the sexual organs. *J Physiol* 31: 222-229.

90. Heng, T. S., J. J. Reiseger, A. L. Fletcher, G. R. Leggatt, O. J. White, K. Vlahos, I. H. Frazer, S. J. Turner, and R. L. Boyd. 2012. Impact of sex steroid ablation on viral, tumour and vaccine responses in aged mice. *PloS one* 7: e42677.

91. Alpdogan, O., V. M. Hubbard, O. M. Smith, N. Patel, S. Lu, G. L. Goldberg, D. H. Gray, J. Feinman, A. A. Kochman, J. M. Eng, D. Suh, S. J. Muriglan, R. L. Boyd, and M. R. van den Brink. 2006. Keratinocyte growth factor (KGF) is required for postnatal thymic regeneration. *Blood* 107: 2453-2460.

92. Rossi, S. W. U., T.; Kuse, S.; Keller, M.P.; Zuklys, S.; Gudkov, A.V.; Takahama, Y.; Krenger, W.; Blazar, B.R.; Hollander, G.A. 2007. Keratinocyte growth factor (KGF) enhances postnatal T-cell development via enhancements in proliferation and function of thymic epithelial cells. *Immunobiology* 109: 3803-3811.

93. Erickson, M., S. Morkowski, S. Lehar, G. Gillard, C. Beers, J. Dooley, J. S. Rubin, A. Rudensky, and A. G. Farr. 2002. Regulation of thymic epithelium by keratinocyte growth factor. *Blood* 100: 3269-3278.

94. Griffith, A. V., M. Fallahi, H. Nakase, M. Gosink, B. Young, and H. T. Petrie. 2009. Spatial mapping of thymic stromal microenvironments reveals unique features influencing T lymphoid differentiation. *Immunity* 31: 999-1009.

95. Vrisekoop, N., J. P. Monteiro, J. N. Mandl, and R. N. Germain. 2014. Revisiting thymic positive selection and the mature T cell repertoire for antigen. *Immunity* 41: 181-190.

96. O'Shea, J. J., and W. E. Paul. 2010. Mechanisms underlying lineage commitment and plasticity of helper CD4+ T cells. *Science* 327: 1098-1102.

97. Abbas, A. K., K. M. Murphy, and A. Sher. 1996. Functional diversity of helper T lymphocytes. *Nature* 383: 787-793.

98. Stockinger, B. V., M.; Martin, B. 2007. Th17 T cells: Linking innate and adaptive immunity. *Seminars in Immunology* 19: 353-361.

99. King, C. T., S. G.; Mackay, C. R. 2008. T follicular helper (Tfh) cells in normal and dysregulated immune responses. *Annual review of immunology* 26: 741-766.

100. Sakaguchi, S. Y., T.; Nomura, T.; Ono, M. 2008. Regulatory T cells and Immune Tolerance. *Cell* 133: 775-787.

101. Li, Z., D. Li, A. Tsun, and B. Li. 2015. FOXP3 regulatory T cells and their functional regulation. *Cellular & molecular immunology*.

102. Bradley, L. M. W., S.R.; Swain, S.L. 1994. Entry of Naive CD4 T Cells into Peripheral Lymph Nodes Requires L-Selectin. *Journal of Experimental Medicine* 180: 2401-2406.

103. Forster, R. S., A.; Breitfeld, D.; Kremmer, E.; Renner-Muller, I.; Wolf, E.; Lipp, M. 1999. CCR7 Coordinates the Primary Immune Response by Establishing Functional Microenvironments
in Secondary Lymphoid Organs. *Cell* 99: 23-33.

104. Mueller, S. N., T. Gebhardt, F. R. Carbone, and W. R. Heath. 2013. Memory T cell subsets, migration patterns, and tissue residence. *Annual review of immunology* 31: 137-161.

105. Kennedy, M. K., M. Glaccum, S. N. Brown, E. A. Butz, J. L. Viney, M. Embers, N. Matsuki, K. Charrier, L. Sedger, C. R. Willis, K. Brasel, P. J. Morrissey, K. Stocking, J. C. Schuh, S. Joyce, and J. J. Peschon. 2000. Reversible defects in natural killer

and memory CD8 T cell lineages in interleukin 15-deficient mice. *The Journal of experimental medicine* 191: 771-780.

106. Surh, C. D., and J. Sprent. 2005. Regulation of mature T cell homeostasis. *Semin Immunol* 17: 183-191.

107. Tanchot, C., F. A. Lemonnier, B. Perarnau, A. A. Freitas, and B. Rocha. 1997. Differential requirements for survival and proliferation of CD8 naive or memory T cells. *Science* 276: 2057-2062.

108. Takeda, S., H. R. Rodewald, H. Arakawa, H. Bluethmann, and T. Shimizu. 1996. MHC class II molecules are not required for survival of newly generated CD4+ T cells, but affect their long-term life span. *Immunity* 5: 217-228.

109. Surh, C. D., and J. Sprent. 2008. Homeostasis of naive and memory T cells. *Immunity* 29: 848-862.

110. Carrette, F., and C. D. Surh. 2012. IL-7 signaling and CD127 receptor regulation in the control of T cell homeostasis. *Semin Immunol* 24: 209-217.

111. Chiu, B. C., B. E. Martin, V. R. Stolberg, and S. W. Chensue. 2013. Cutting edge: Central memory CD8 T cells in aged mice are virtual memory cells. *Journal of immunology* 191: 5793-5796.

112. Renkema, K. R., G. Li, A. Wu, M. J. Smithey, and J. Nikolich-Zugich. 2014. Two separate defects affecting true naive or virtual memory T cell precursors combine to reduce naive T cell responses with aging. *Journal of immunology* 192: 151-159.

113. Opiela, S. J., T. Koru-Sengul, and B. Adkins. 2009. Murine neonatal recent thymic emigrants are phenotypically and functionally distinct from adult recent thymic emigrants. *Blood* 113: 5635-5643.

114. Scollay, R. G., E. C. Butcher, and I. L. Weissman. 1980. Thymus cell migration. Quantitative aspects of cellular traffic from the thymus to the periphery in mice. *European journal of immunology* 10: 210-218.

115. Boursalian, T. E., J. Golob, D. M. Soper, C. J. Cooper, and P. J. Fink. 2004. Continued maturation of thymic emigrants in the periphery. *Nature immunology* 5: 418-425.

116. Fink, P. J., and D. W. Hendricks. 2011. Post-thymic maturation: young T cells assert their individuality. *Nature reviews. Immunology* 11: 544-549.

117. Fink, P. J. 2013. The biology of recent thymic emigrants. *Annual review of immunology* 31: 31-50.

118. Houston, E. G., Jr., L. E. Higdon, and P. J. Fink. 2011. Recent thymic emigrants are preferentially incorporated only into the depleted T-cell pool. *Proceedings of the National Academy of Sciences of the United States of America* 108: 5366-5371.

119. Berkley, A. M., D. W. Hendricks, K. B. Simmons, and P. J. Fink. 2013. Recent thymic emigrants and mature naive T cells exhibit differential DNA methylation at key cytokine loci. *Journal of immunology* 190: 6180-6186.

120. Houston, E. G., R. Nechanitzky, and P. J. Fink. 2008. Cutting Edge: Contact with Secondary Lymphoid Organs Drives Postthymic T Cell Maturation. *The Journal of Immunology* 181: 5213-5217.

121. Houston, E. G., Jr., and P. J. Fink. 2009. MHC drives TCR repertoire shaping, but not maturation, in recent thymic emigrants. *Journal of immunology* 183: 7244-7249.

122. Geenen, V., J. F. Poulin, M. L. Dion, H. Martens, E. Castermans, I. Hansenne, M. Moutschen, R. P. Sekaly, and R. Cheynier. 2003. Quantification of T cell receptor rearrangement excision circles to estimate thymic function: an important new tool for endocrine-immune physiology. *The Journal of endocrinology* 176: 305-311.

123. Scollay, R. C., W.; Shortman, K. 1984. The functional capabilities of cells leaving the thymus. *Journal of immunology* 132: 25-30.

124. Yu, W., H. Nagaoka, M. Jankovic, Z. Misulovin, H. Suh, A. Rolink, F. Melchers, E. Meffre, and M. C. Nussenzweig. 1999. Continued RAG expression in late stages of B cell development and no apparent re-induction after immunization. *Nature* 400: 682-687.

125. Li, O. Z., P.; Liu, Y. 2004. CD24 Expression on T cells is required for optimal T cell proliferation in lymphopenic host. *The Journal of experimental medicine* 200: 1083-1089.

126. Kelly, K. A. S., R. 1990. Analysis of recent thymic emigrants with subset- and maturity-related markers. *International Immunology* 2: 419-422.

127. Staton, T. L., A. Habtezion, M. M. Winslow, T. Sato, P. E. Love, and E. C. Butcher. 2006. CD8+ recent thymic emigrants home to and efficiently repopulate the small intestine epithelium. *Nature immunology* 7: 482-488.

128. Houston, E. G., Jr., T. E. Boursalian, and P. J. Fink. 2012. Homeostatic signals do not drive post-thymic T cell maturation. *Cellular immunology* 274: 39-45.

129. Priyadharshini, B. W., R. M.; Greiner, D. L.; Gerstein, R. M.; Brehm, M. A. 2010. Maturation-dependent licensing of naive T cells for rapid TNG production. *PloS one* 5: 1-15.

130. Makaroff, L. E. H., D. W.; Neic, R. E.; Fink, P. J. 2009. Postthymic maturation influences the CD8 T cell response to antigen. *Proceedings of the National Academy of Sciences of the United States of America* 106: 4799-4804.

131. Berkley, A. M., and P. J. Fink. 2014. Cutting edge: CD8+ recent thymic emigrants exhibit increased responses to low-affinity ligands and improved access to peripheral sites of inflammation. *Journal of immunology* 193: 3262-3266.

132. Hendricks, D. W., and P. J. Fink. 2011. Recent thymic emigrants are biased against the T-helper type 1 and toward the T-helper type 2 effector lineage. *Blood* 117: 1239-1249.

133. Clise-Dwyer, K., G. E. Huston, A. L. Buck, D. K. Duso, and S. L. Swain. 2007. Environmental and Intrinsic Factors Lead to Antigen Unresponsiveness in CD4+ Recent Thymic Emigrants from Aged Mice. *The Journal of Immunology* 178: 1321-1331.

134. Haynes, L., and S. L. Swain. 2012. Aged-related shifts in T cell homeostasis lead to intrinsic T cell defects. *Semin Immunol* 24: 350-355.

135. Klug, D. B., E. Crouch, C. Carter, L. Coghlan, C. J. Conti, and E. R. Richie. 2000. Transgenic Expression of Cyclin D1 in Thymic Epithelial Precursors Promotes Epithelial and T Cell Development. *The Journal of Immunology* 164: 1881-1888.

136. Robles, A. I. L., F.; Whalin, R.B.; Murillas, R.; Richie, E.; Gimenez-Conti, I.B.; Jorano, J.L.; Conti, C.J. 1996. Expression of cyclin D1 in epithelial tissues of transgenic mice results in epidermal hyperproliferation and severe thymic hyperplasia. *Proceedings of the National Academy of Sciences of the United States of America* 93: 7634-7638.

137. Fu, M., C. Wang, Z. Li, T. Sakamaki, and R. G. Pestell. 2004. Minireview: Cyclin D1: normal and abnormal functions. *Endocrinology* 145: 5439-5447.

138. Gray, D. H., A. L. Fletcher, M. Hammett, N. Seach, T. Ueno, L. F. Young, J. Barbuto, R. L. Boyd, and A. P. Chidgey. 2008. Unbiased analysis, enrichment and purification of thymic stromal cells. *Journal of immunological methods* 329: 56-66.

139. Seach, N., K. Wong, M. Hammett, R. L. Boyd, and A. P. Chidgey. 2012. Purified enzymes improve isolation and characterization of the adult thymic epithelium. *Journal of immunological methods* 385: 23-34.

140. Waterstrat, A., Y. Liang, C. F. Swiderski, B. J. Shelton, and G. Van Zant. 2010. Congenic interval of CD45/Ly-5 congenic mice contains multiple genes that may influence hematopoietic stem cell engraftment. *Blood* 115: 408-417.

141. Manley, N. R. R., E. R.; Blackburn, C. C.; Condie, B. G.; Sage, J. 2011. Structure and function of the thymic microenvironment. *Front Biosci* 16: 2461-2477.

142. Chinn, I. K., C. C. Blackburn, N. R. Manley, and G. D. Sempowski. 2012. Changes in primary lymphoid organs with aging. *Semin Immunol* 24: 309-320.

143. Robles, A. I. L., F.; Whalin, R. B.; Murillas, R.; Richie, E.; Gimenez-Conti, I. B.; Jorcano, J. L.; Conti, C. J. 1996. Expression of cyclin D1 in epithelial tissues of transgenic mice results in epidermal hyperproliferation and severe thyjmic hyperplasia. *Proceedings of the National Academy of Sciences of the United States of America* 93: 7634-7638.

144. Bolner, M. L. 2012. Effects of thymus size and involution on the contribution of recent thymic emigrants to the peripheral T cell pool. *UT GSBS Dissertations and Theses (Open Access)*: Paper 235.

145. Franckaert, D. S., S. M.; Heirman, N.; Gill, J.; Skogberg, G.; Ekwall, O.; Put, K.; Linterman, M. A.; Dooley, J.; Liston, A. 2015. Premature thymic involution is independent of structural plasticity of the thymic stroma. *European journal of immunology* 45: 1535-1547.

146. Nabarra, B. M., M.; Casanova M.; Godard, C.; London, J. 2001. Ultrastructural study of the FVB/N mouse thymus: presence of an immature epithelial cell in the medulla and premature involution. *Dev Comp Imm* 25: 231-243.

147. Li, L. H., H.; William, G. E.; Stockard, C. R.; Ho, K.; Lott, P.; Yang, P.; Zhang, H.; Mountz, J. 2003. Cellular mechanism of thymic involution. *Scand J Immunol*: 410-422.

148. Ortman, C. L. D., K.A.; Witte, P.L.; Le, P.T. 2002. Molecular characterization of the mosue involuted thymus: aberrations in expressions of transcription regulators in thymocyte and epithelial compartments. *International Immunology* 17: 813-822.

149. Min, H. M.-R., E.; Dorshkind, K. 2004. Reduction in the developmental potential of intrathymic T cell progenitors with age. *Journal of immunology* 173: 245-250.

150. Chen, W. 2004. The late stage of T cell development within mouse thymus. *Cellular & molecular immunology* 1: 3-11.

151. Moran, A. E., K. L. Holzapfel, Y. Xing, N. R. Cunningham, J. S. Maltzman, J. Punt, and K. A. Hogquist. 2011. T cell receptor signal strength in Treg and iNKT cell development demonstrated by a novel fluorescent reporter mouse. *The Journal of experimental medicine* 208: 1279-1289.

152. Garfin, P. M., D. Min, J. L. Bryson, T. Serwold, B. Edris, C. C. Blackburn, E. R. Richie, K. I. Weinberg, N. R. Manley, J. Sage, and P. Viatour. 2013. Inactivation of the RB family prevents thymus involution and promotes thymic function by direct control of Foxn1 expression. *The Journal of experimental medicine* 210: 1087-1097.

153. Thiault, N., J. Darrigues, V. Adoue, M. Gros, B. Binet, C. Perals, B. Leobon, N. Fazilleau, O. P. Joffre, E. A. Robey, J. P. van Meerwijk, and P. Romagnoli. 2015. Peripheral regulatory T lymphocytes recirculating to the thymus suppress the development of their precursors. *Nature immunology* 16: 628-634.

154. Appay, V., and D. Sauce. 2014. Naive T cells: the crux of cellular immune aging? *Experimental gerontology* 54: 90-93.

155. Tsukamoto, H., K. Clise-Dwyer, G. E. Huston, D. K. Duso, A. L. Buck, L. L. Johnson, L. Haynes, and S. L. Swain. 2009. Age-associated increase in lifespan of naive CD4 T cells contributes to T-cell homeostasis but facilitates development of functional defects. *Proceedings of the National Academy of Sciences of the United States of America* 106: 18333-18338.

156. Smithey, M. J., G. Li, V. Venturi, M. P. Davenport, and J. Nikolich-Zugich. 2012. Lifelong persistent viral infection alters the naive T cell pool, impairing CD8 T cell immunity in late life. *Journal of immunology* 189: 5356-5366.

157. Eaton, S. M., E. M. Burns, K. Kusser, T. D. Randall, and L. Haynes. 2004. Age-related defects in CD4 T cell cognate helper function lead to reductions in humoral responses. *The Journal of experimental medicine* 200: 1613-1622.

158. Berzins, S. P., D. I. Godfrey, J. F. Miller, and R. L. Boyd. 1999. A central role for thymic emigrants in peripheral T cell homeostasis. *Proceedings of the National Academy of Sciences of the United States of America* 96: 9787-9791.

159. Sprent, J., and C. D. Surh. 2011. Normal T cell homeostasis: the conversion of naive cells into memory-phenotype cells. *Nature immunology* 131: 478-484.

160. Sallusto, F., D. Lenig, R. Forster, M. Lipp, and A. Lanzavecchia. 1999. Two subsets of memory T lymphocytes with distinct homing potentials and effector functions. *Nature* 401: 708-712.

161. Pinchuk, L. M., and N. M. Filipov. 2008. Differential effects of age on circulating and splenic leukocyte populations in C57BL/6 and BALB/c male mice. *Immunity & ageing : I & A* 5: 1.

162. Decman, V., B. J. Laidlaw, T. A. Doering, J. Leng, H. C. Ertl, D. R. Goldstein, and E. J. Wherry. 2012. Defective CD8 T cell responses in aged mice are due to

quantitative and qualitative changes in virus-specific precursors. *Journal of immunology* 188: 1933-1941.

163. Forster, R., A. Schubel, D. Breitfeld, E. Kremmer, I. Renner-Muller, E. Wolf, and M. Lipp. 1999. CCR7 coordinates the primary immune response by establishing functional microenvironments in secondary lymphoid organs. *Cell* 99: 23-33.

164. Steeber, D. A., N. E. Green, S. Sato, and T. F. Tedder. 1996. Humoral immune responses in L-selectin-deficient mice. *Journal of immunology* 157: 4899-4907.

165. Swain, S. L., and J. Nikolich-Zugich. 2009. Key research opportunities in immune system aging. *The journals of gerontology. Series A, Biological sciences and medical sciences* 64: 183-186.

166. Zhang, W., V. Brahmakshatriya, and S. L. Swain. 2014. CD4 T cell defects in the aged: causes, consequences and strategies to circumvent. *Experimental gerontology* 54: 67-70.

167. Cheng, L., J. Guo, L. Sun, J. Fu, P. F. Barnes, D. Metzger, P. Chambon, R. G. Oshima, T. Amagai, and D. M. Su. 2010. Postnatal tissue-specific disruption of transcription factor FoxN1 triggers acute thymic atrophy. *The Journal of biological chemistry* 285: 5836-5847.

168. Heng, T. S., G. L. Goldberg, D. H. Gray, J. S. Sutherland, A. P. Chidgey, and R. L. Boyd. 2005. Effects of castration on thymocyte development in two different models of thymic involution. *Journal of immunology* 175: 2982-2993.

169. Bankovich, A. J., L. R. Shiow, and J. G. Cyster. 2010. CD69 suppresses sphingosine 1-phosophate receptor-1 (S1P1) function through interaction with membrane helix 4. *The Journal of biological chemistry* 285: 22328-22337.

170. Matloubian, M., C. G. Lo, G. Cinamon, M. J. Lesneski, Y. Xu, V. Brinkmann, M. L. Allende, R. L. Proia, and J. G. Cyster. 2004. Lymphocyte egress from thymus and peripheral lymphoid organs is dependent on S1P receptor 1. *Nature* 427: 355-360.

171. Laan, M., K. Kisand, V. Kont, K. Moll, L. Tserel, H. S. Scott, and P. Peterson. 2009. Autoimmune regulator deficiency results in decreased expression of CCR4 and CCR7 ligands and in delayed migration of CD4+ thymocytes. *Journal of immunology* 183: 7682-7691.

172. Ilangumaran, S., J. Gagnon, C. Leblanc, P. Poussier, and S. Ramanathan. 2010. Increased generation of CD8 single positive cells in SOCS1-deficient thymus does not proportionately increase their export. *Immunology letters* 132: 12-17.

173. Konkel, J. E., W. Jin, B. Abbatiello, J. R. Grainger, and W. Chen. 2014. Thymocyte apoptosis drives the intrathymic generation of regulatory T cells. *Proceedings of the National Academy of Sciences of the United States of America* 111: E465-473.

174. Surh, C. D., and J. Sprent. 2002. Regulation of naive and memory T-cell homeostasis. *Microbes and infection / Institut Pasteur* 4: 51-56.

175. Sprent, J., and C. D. Surh. 2012. Interleukin 7, maestro of the immune system. *Semin Immunol* 24: 149-150.

176. Shanley, D. P., D. Aw, N. R. Manley, and D. B. Palmer. 2009. An evolutionary perspective on the mechanisms of immunosenescence. *Trends in immunology* 30: 374-381.

177. Griffith, A. V., M. Fallahi, T. Venables, and H. T. Petrie. 2012. Persistent degenerative changes in thymic organ function revealed by an inducible model of organ regrowth. *Aging cell* 11: 169-177.

## Vita

Michelle Lynn Bolner was born in Del Rio, Texas on February 26, 1986, the daughter of Tammy Brightwell Bolner and Michael Lynn Bolner. After completing her degree at Canutillo High School, Canutillo, Texas in 2004, she entered Baylor University in Waco, Texas. She received the degree of Bachelor of Science with a major in biology from Baylor in May 2008. In September of 2008 she entered The University of Texas Graduate School of Biomedical Sciences at Houston and received the degree of Masters of Biomedical Sciences in May 2012.

Permanent address:

1008 Olympic Drive

Pflugerville, Texas 78660